

**Chair of Hydrology**  
University of Freiburg

Julia Schütze

---

**Quantifying the impact of soil organic carbon on the  
water balance in agricultural carbon sequestration projects**  
Application of a modeling approach to the case of Rwanda

---

First supervisor: Jun.-Prof. Dr. **Andreas Hartmann**

Second supervisor: Dr. **Till Pistorius**

Master thesis under the supervision of Jun.-Prof. Dr. **Andreas Hartmann**

Freiburg i.Br., May 2021



# Acknowledgements

At this point, I would like to thank all those who supported me in the course of my master thesis.

My special thanks goes to Jun.-Prof. Dr. Andreas Hartmann for being a fantastic first supervisor. His very competent and cordial guidance, as well as his constant encouragement to ask questions, allowed me to learn a great deal from the thesis writing process.

It also goes to my second supervisor Dr. Till Pistorius for his experienced tips and tricks, as well as for his enthusiasm and positivity.

I would further like to thank my proofreaders, friends and family for their constant support.

Finally, my thanks goes to my housemates for creating such a warm home that allowed me to have a beautiful place to work.

# Table of contents

|  |      |
|--|------|
| Acknowledgements.....  | I    |
| List of figures .....  | IV   |
| List of tables .....   | V    |
| List of abbreviations and symbols .....  | VI   |
| Abstract.....  | VII  |
| Keywords .....   | VII  |
| Zusammenfassung.....   | VIII |
| Stichworte.....  | IX   |
| 1 Introduction.....  | 1    |
| 1.1 Context and motivation for the thesis .....                                  | 1    |
| 1.2 Conceptual overview .....  | 3    |
| 1.2.1 Soil quality .....   | 3    |
| 1.2.2 Soil water balance.....  | 5    |
| 1.2.3 Drought.....   | 7    |
| 1.2.4 Heavy rain and soil erosion .....  | 9    |
| 1.2.5 Soils in agricultural carbon sequestration projects and the case of Rwanda | 10   |
| 1.3 State of science .....   | 12   |
| 1.3.1 The effect of soil organic carbon on soil hydrology .....                  | 12   |
| 1.3.2 Pedotransfer functions .....   | 14   |
| 2 Problem statement, aim and research questions .....                            | 16   |
| 3 Methodology.....   | 17   |
| 3.1 Development and validation of the modeling approach.....                     | 18   |
| 3.1.1 Hydrus-1D as a core component .....  | 18   |
| 3.1.2 Preselection of pedotransfer functions .....                               | 20   |
| 3.1.3 Scenarios and final selection of the pedotransfer function.....            | 22   |
| 3.1.4 The pedotransfer function of choice (eupthv2) .....                        | 26   |
| 3.2 Application of the modeling approach .....                                   | 27   |
| 3.2.1 Data generation .....  | 27   |
| 3.2.2 Modeling the Rwanda carbon project .....                                   | 33   |

|       |   |    |
|-------|---|----|
| 4     | Results.....  | 35 |
| 4.1   | Evaluation of the modeling approach.....  | 35 |
| 4.1.1 | Preselection of pedotransfer functions .....                                    | 35 |
| 4.1.2 | Scenarios for testing and justifying pedotransfer functions.....                | 36 |
| 4.1.3 | Evaluating the use of Hydrus-1D.....  | 37 |
| 4.2   | Application of the modeling approach .....                                      | 37 |
| 4.2.1 | Water retention .....   | 38 |
| 4.2.2 | Saturated hydraulic conductivity and runoff.....                                | 42 |
| 4.2.3 | Actual transpiration.....   | 44 |
| 4.2.4 | The Rwanda carbon project .....   | 46 |
| 5     | Discussion.....   | 48 |
| 5.1   | Extent of model applicability and reliability.....                              | 48 |
| 5.1.1 | The modeling approach: functionality and assumptions.....                       | 48 |
| 5.1.2 | The pedotransfer function of choice and tropical soils.....                     | 51 |
| 5.2   | The controlling factors of the benefits of soil organic carbon .....            | 55 |
| 5.2.1 | The quantity of sequestered organic carbon.....                                 | 55 |
| 5.2.2 | Soil texture.....   | 56 |
| 5.2.3 | The role of precipitation regimes.....  | 57 |
| 5.2.4 | Factors controlling plant water availability, transpiration and crop yield..... | 57 |
| 5.3   | Temporal and spatial transferability .....                                      | 58 |
| 5.3.1 | Temporal transferability .....  | 59 |
| 5.3.2 | Spatial transferability .....   | 60 |
| 6     | Conclusion and outlook.....   | 61 |
| 7     | References .....  | 63 |
|       | Appendix .....  | X  |
|       | Declaration of honor.....   | XX |

## List of figures

|           |   |    |
|-----------|---|----|
| Figure 1  | Conceptual overview: stocks and flows of soil water in soils.....         | 3  |
| Figure 2  | Soil classes by clay, silt and sand composition as used by the USDA ..... | 5  |
| Figure 3  | Overview of the SWB components considered in this thesis .....            | 6  |
| Figure 4  | Four types of drought and their causes.....                               | 8  |
| Figure 5  | Map of Rwanda showing the carbon project regions.....                     | 11 |
| Figure 6  | Flow chart showing the modeling approach as a methodological core .....   | 17 |
| Figure 7  | Flow chart showing different types of PTFs.....                           | 20 |
| Figure 8  | Interplay of components forming the proposed modeling approach.....       | 28 |
| Figure 9  | Extract from the H1D GUI profile information window .....                 | 30 |
| Figure 10 | Set of model runs with in- and outputs and processing steps.....          | 32 |
| Figure 11 | Difference of $Q_s$ and $Q_r$ as influenced by the SOC content.....       | 38 |
| Figure 12 | Theta under rain conditions as influenced by SOC content .....            | 39 |
| Figure 13 | Theta, $Q_s$ and $Q_r$ in sandy clay under rain conditions .....          | 40 |
| Figure 14 | Difference of theta and $Q_r$ as influenced by SOC content.....           | 41 |
| Figure 15 | Difference of $Q_s$ and theta as influenced by SOC content.....           | 41 |
| Figure 16 | $K_s$ of analyzed soils and its dependence on SOC content.....            | 43 |
| Figure 17 | Runoff and $K_s$ in loamy sand as influenced by SOC content .....         | 44 |
| Figure 18 | Actual plant transpiration under heavy rain.....                          | 45 |
| Figure 19 | Actual plant transpiration under extreme drought.....                     | 45 |
| Figure 20 | Map of Rwanda showing all soil types present in the project areas.....    | 46 |
| Figure 21 | Relative importance of predictors in euptfv2 .....                        | 52 |
| Figure 22 | Clay contents in temperate soils and in tropical soils .....              | 53 |

## List of tables

|         |   |    |
|---------|---|----|
| Table 1 | Obligatory and optional criteria for choosing a PTF .....                   | 21 |
| Table 2 | Control and SOC-amended scenarios from the literature .....                 | 24 |
| Table 3 | Classification of effect magnitudes into effect classes .....               | 25 |
| Table 4 | Results for Ks, Qr and Qs from the literature as compared to quantiles..... | 26 |
| Table 5 | Parametrization of precipitation types.....                                 | 31 |
| Table 6 | Soil types in the project regions and their soil hydrology .....            | 47 |

## List of abbreviations and symbols

|                             |  |
|-----------------------------|--|
| $\alpha$                    | Reciprocal of the air entry value  |
| AMO                         | Atlantic Multidecadal Oscillation  |
| ARCOS                       | Albertine Rift Conservation Society  |
| BD                          | Bulk density   |
| CO <sub>2</sub>             | Carbon dioxide   |
| d                           | Soil depth   |
| dt                          | Time step  |
| ENSO                        | El Niño Southern Oscillation   |
| eupthv2                     | 2 <sup>nd</sup> version of the European pedotransfer function by Szabó et al. (2020) |
| GUI                         | Graphic user interface   |
| h                           | Hydraulic potential  |
| HWSD                        | Harmonized world soil database   |
| H1D                         | Hydrus-1D modeling software  |
| IPCC                        | Intergovernmental Panel on Climate Change  |
| IOD                         | Indian Ocean Dipole  |
| K(h)                        | Hydraulic conductivity   |
| K <sub>s</sub>              | Saturated hydraulic conductivity   |
| K <sub>0</sub>              | Hydraulic conductivity acting as a matching point at saturation                      |
| l                           | Empiric pore connectivity parameter  |
| MRV                         | Measurement, reporting and verification  |
| MVG                         | Mualem-van Genuchten   |
| n                           | shape parameter of the retention curve   |
| OC                          | Organic carbon   |
| OM                          | Organic matter   |
| PET                         | Potential evapotranspiration   |
| PSD                         | Particle size distribution   |
| Q <sub>r</sub> / $\theta_r$ | Residual water content   |
| Q <sub>s</sub> / $\theta_s$ | Saturated water content  |
| RMSE                        | Root-mean-square error   |
| RQ                          | Research question  |
| SALM                        | Sustainable agricultural land management   |
| Se                          | Relative soil saturation   |
| SHP                         | Soil hydrological parameter  |
| SOC                         | Soil organic carbon  |
| SWB                         | Soil water balance   |
| theta/ $\theta$             | Actual water content   |
| USDA                        | United States Department of Agriculture  |



## Abstract

Soil organic carbon (SOC) is a key indicator of soil quality and an important lever in combating climate change. Due to the high carbon sequestration potential of soils, an important climate mitigation function is attributed to agricultural carbon sequestration projects. So far, systematic data on the influence of intentionally sequestered organic carbon on soil characteristics such as soil hydrology is scarce. Insights are however valuable for more informed planning of carbon projects and the quantification of carbon sequestration benefits.

In this thesis, the influence of intentionally enhanced SOC on the soil water balance (SWB) was analyzed, in combination with the main controlling factors of this relation. A proposed modeling approach consisting of a pedotransfer function (PTF) and the water flow model Hydrus-1D (H1D) was developed, tested and applied in order to systematically generate data. For the development, climatic boundary conditions from the Rwanda carbon project were used as a basis. Further, a selection process was performed to determine the most suitable PTF, which resulted in the use of the European PTF "eupthv2". The performance of eupthv2, as well as its interplay with H1D was tested and validated by a method of comparison with results extracted from the literature. Subsequently, the proposed modeling approach was used for data generation in virtual experiments. First, SWB data was generated for combinations of incrementally elevated SOC levels (0-9 mass %), six tropical soil textures, and four climatic conditions typical of the Rwandan project regions. Second, data was generated specifically for the conditions prevailing in the Rwanda carbon project to model the project's SWB before and after a 20-year project period.

Analysis showed that the modeling approach, under certain conditions, was suitable for systematically generating insights into the effect of SOC on SWB. It was additionally found that intentionally enhanced SOC significantly increased water retention and thereby plant available water. Under extreme drought, related increases in actual plant transpiration could possibly lead to higher plant yields. Furthermore, increases in SOC up to a certain texture dependent percentage were found to positively influence the saturated hydraulic conductivity and thereby reduce potentially occurring surface runoff. For the Rwanda carbon project, slightly positive effects of SOC on the SWB resulted.

Overall, the results indicated that carbon sequestration in agricultural soils contributes not only to climate mitigation, but also to climate adaptation by attenuating potentially negative effects of hydrologically extreme weather events.

## Keywords

Soil organic carbon, soil water balance, carbon project, pedotransfer function, Hydrus-1D, modeling approach, sustainable agriculture, Rwanda, tropics and subtropics

## Zusammenfassung

Organischer Bodenkohlenstoff (SOC) ist ein Schlüsselindikator für die Bodenqualität und ein wichtiger Beitrag zur Bekämpfung des Klimawandels. Aufgrund des hohen Kohlenstoffbindungspotenzials von Böden wird landwirtschaftlichen Kohlenstoffprojekten eine wichtige Klimaschutzfunktion zugeschrieben. Bislang gibt es kaum systematisch erhobene Daten zum Einfluss von gezielt gespeichertem organischem Kohlenstoff auf Bodeneigenschaften wie die Bodenhydrologie. Entsprechende Erkenntnisse sind jedoch wertvoll für eine fundierte Planung von Kohlenstoffprojekten und die Quantifizierung des Nutzens der Kohlenstoffspeicherung.

In dieser Arbeit wurde die Auswirkung von gezielt erhöhtem SOC auf den Bodenwasserhaushalt (SWB) und die wichtigsten Kontrollfaktoren dieses Einflusses analysiert. Ein Modellierungsansatz, bestehend aus einer Pedotransferfunktion (PTF) und dem Wasserflussmodell Hydrus-1D (H1D), wurde entwickelt, getestet und angewendet, um systematisch Daten zu generieren. Für die Entwicklung wurden klimatische Rahmenbedingungen aus dem Ruanda-Kohlenstoffprojekt als Grundlage verwendet. Des Weiteren wurde ein Auswahlprozess durchgeführt, um die am besten geeignete PTF zu bestimmen, was zur Verwendung der europäischen PTF "eupthv2" führte. Die Zuverlässigkeit von eupthv2, sowie das Zusammenspiel mit H1D wurde durch eine Vergleichsmethode mit Ergebnissen aus der Literatur getestet und validiert. Anschließend wurde der vorgeschlagene Modellierungsansatz verwendet, um mithilfe von virtuellen Experimenten Daten zu generieren. Zunächst wurden SWB-Daten für Kombinationen von schrittweise erhöhten SOC-Gehalten (0-9 Masse-%), sechs tropischen Bodentexturen und vier für die ruandischen Projektregionen typischen klimatischen Rahmenbedingungen generiert. Anschließend wurden Daten speziell für die im ruandischen Kohlenstoffprojekt vorherrschenden Bedingungen erzeugt, um den SWB des Projekts vor und nach einem 20-jährigen Projektzeitraum zu modellieren.

Die Analyse zeigte, dass der Modellierungsansatz unter bestimmten Bedingungen geeignet war, um systematisch Daten zur Wirkung des SOC auf den SWB zu generieren. Darüber hinaus wurde festgestellt, dass ein gezielt erhöhter SOC das Wasserrückhaltevermögen und damit das pflanzenverfügbare Wasser signifikant erhöht. Unter extremer Trockenheit könnten die damit verbundenen Erhöhungen der tatsächlichen Pflanzentranspiration möglicherweise zu höheren Pflanzenerträgen führen. Weiterhin wurde festgestellt, dass Erhöhungen des SOC bis zu einem bestimmten texturabhängigen Prozentsatz die gesättigte hydraulische Leitfähigkeit positiv beeinflussen und dadurch potentiell auftretenden Oberflächenabfluss reduzieren. Für das Kohlenstoffprojekt in Ruanda ergaben sich leicht positive Effekte des SOC auf den SWB.

Insgesamt deuten die Ergebnisse darauf hin, dass die Kohlenstoffspeicherung in landwirtschaftlichen Böden nicht nur zum Klimaschutz, sondern auch zur Klimaanpassung beiträgt, indem sie potenziell negative Auswirkungen hydrologischer Extremwetterereignisse abschwächt.

## Stichworte

Organischer Bodenkohlenstoff, Bodenwasserhaushalt, Kohlenstoffprojekt, Pedotransferfunktion, Hydrus-1D, Modellierungsansatz, nachhaltige Landwirtschaft, Ruanda, Tropen und Subtropen



# 1 Introduction

## 1.1 Context and motivation for the thesis

Climate change is one of the most pressing issues of our century. In 2015, the Paris Agreement, a legally binding international treaty on climate change, was adopted by 196 parties. It contains the goal to limit global warming to a maximum increase of 2°C compared to pre-industrial levels (United Nations, 2015). Policy makers and environmental programs focus on climate mitigation to meet this challenge, while also addressing climate adaptation to avoid climate-induced damages (Di Gregorio et al., 2017; Intergovernmental Panel on Climate Change, 2019). Due to their great potential to emit, as well as to store carbon, soils play a crucial role in these efforts (Intergovernmental Panel on Climate Change, 2019).

The application of compost and organic residues to agriculturally used soils has been practiced for many years worldwide in order to maintain the fertility of cultivated soils. Nonetheless, in many cases these circular practices of returning residues to the fields were lost, often due to the advent of mineral fertilizers which made the use of compost, as a nutrient supply source, obsolete (Melillo, 2012). Widespread and rather linear agricultural approaches consist of mineral fertilizer application before the growing season and the removal or burning of residues after the growing season. The effects of such practices are diverse, several negative on-site and off-site effects are known (Lehtinen et al., 2017; Reynolds et al., 2015). One important negative on-site effect stands out due to its various implications for soil structure, quality and health: the depletion of soil organic carbon (SOC, Zdruli et al., 2016).

Given that CO<sub>2</sub> accumulation in the atmosphere is widely recognized as being a severe global problem, the practice of compost use is returning to the fields in a new shape. The benefit for farmers is still the improved soil quality, but with a new driver: a new awareness mechanism of the climate change problematic and, as a consequence, the need to sequester or leave more SOC in soils. In related discussions around reaching climate goals increasing attention is being paid to the possibilities of sequestering carbon from the atmosphere (Intergovernmental Panel on Climate Change, 2019). One SOC sequestration method is the intentional increase of organic carbon (OC) contents in soils by applying (composted) organic residues to the fields. When the intentional and systematic storing of SOC in agricultural fields is done, within the framework of a project, the term agricultural carbon sequestration project (or short: carbon project) is used. These projects are mainly conducted in tropical and subtropical regions (VERRA, 2021a). However, in the context of carbon projects, the original focus of compost as a soil amendment is rather shifted to the background, especially in terms of scientific studies and the quantification of its benefits.

Nonetheless, various case studies found OC-rich soils to present not only improved biological but also amended physical properties as compared to OC-depleted soils. This is mainly due to an altered soil structure, which, under certain conditions and among other

effects, can improve a soils ability to absorb and store water (Brown & Cotton, 2011; Chen et al., 2014; Gülser & Candemir, 2015; Reynolds et al., 2015). With continuing climate change, extreme weather events, including drought and heavy rain, are likely to become more frequent worldwide and knowledge on these soil hydrological parameters (SHPs) is becoming increasingly critical. So far, changes in soil hydrology have been addressed in a number of case and laboratory studies, but no attempts of systematic quantification in carbon projects have been made (Razzaghi et al., 2020).

This master thesis aims to fill that knowledge gap by looking at the practice of OC sequestration by compost application in the context of carbon projects and trying to quantify its impact on the soil water balance (SWB). A modeling approach was proposed for the purpose of systematic quantification. The Rwanda carbon project served both as a basis for developing the approach and as a model test run. The motivation of this thesis is thus to determine whether, to what extent and under which conditions, the practice of OC sequestration in carbon projects can contribute to two pressing issues at once: the adaptation to extreme hydrological events and the mitigation of excess atmospheric CO<sub>2</sub>.

Corresponding concise research questions (RQs) of this thesis will be defined in chapter 2, derived from research gaps in the state of science.

## 1.2 Conceptual overview

This chapter provides an overview of the basic concepts, processes and definitions used in the course of this thesis. It addresses the topic of soil quality and the aspects that will play a role. The influence of SOC plays a central role here.

Further, the chapter covers the central issue of SWB and, related to it, explains the concepts of drought, heavy rain and erosion. Finally, it briefly presents the case of the Rwanda agricultural carbon sequestration project that serves as an example and as a data source in this thesis. Region specific boundary conditions required for calculations and analyses will be extracted from this project's database.

Figure 1 schematizes the natural system under consideration. It depicts the project-induced changes in soil carbon and the stocks and flows of soil water under two exemplary types of climatic boundary conditions. Changes between flows 1 and flows 2 (left and right side of the dashed lines, low and high SOC contents) are the main interest of this thesis.

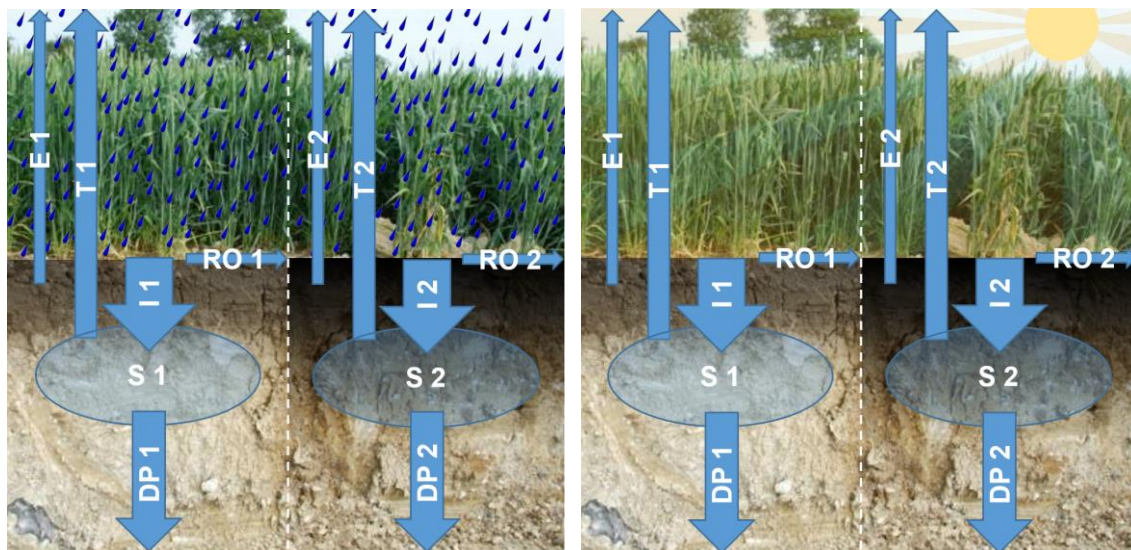


**Figure 1** Conceptual overview: stocks and flows of soil water in soils with low (light shade) and high (dark shade) SOC contents. Two exemplary types of climatic boundary conditions are shown with wet conditions in the left picture and dry conditions in the right picture. SWB type 1 and type 2 (different SOC contents) will be compared in this thesis. E = evaporation, T = transpiration, I = infiltration, RO = surface runoff, S = soil storage, DP = deep percolation.

### 1.2.1 Soil quality

Fertile and stable soil is a resource essential to human life. Rates of degeneration can be very fast whereas processes of regeneration and formation are extremely slow. The speed of soil formation depends on the bedrock, but always takes place beyond human time scales, which makes soil a non-renewable resource (Amelung et al., 2018; van Camp et al., 2004). Soil fertility is defined by Abbott and Murphy (2007) as “the capacity of a soil to satisfy

physical, chemical and biological requirements for the growth of plants in order to guarantee productivity, reproduction and quality according to plant type, soil type, land use and climatic conditions". In this thesis, the focus lies on the physical requirements, since these have the capacity to influence the stocks and flows of soil water. Reynolds et al. (2015) present in their study a list of the most important soil physical quality parameters including dry bulk density, SOC content, air capacity, plant available water capacity, relative field capacity and saturated hydraulic conductivity. The original table with descriptions and optimal ranges can be found in Appendix 1. Among these parameters, SOC is of special importance, as it influences, to different degrees, all other parameters, with the exact effect depending on a variety of determining factors (Brown & Cotton, 2011; Reynolds et al., 2015). The optimal range of SOC was found to average between 30 and 50 g/ kg (3 to 5 mass % SOC). Upper and lower critical limits are first reached in fine-textured soils, where soil structure loss and compaction occur, respectively (Reynolds et al., 2015).

While excessive levels of SOC are rarely found to be an issue, a worldwide SOC decline tendency is a serious problem, especially in agriculturally used soils. It is a major process of soil degradation, as OC-depleted soils cannot maintain sustainable production (Diacono & Montemurro, 2011). However, the production of OC-rich organic wastes in urban, as well as in rural contexts, is high, in form of food waste and industrial and agricultural residues. These organic residues can be returned to fields, either in composted form or as mulch, thus closing the cycle of OC and thereby augmenting SOC contents (Diacono & Montemurro, 2011; Larney & Angers, 2012). It shall be noted in this context that the maintenance of SOC, and thereby soil quality, is an important aspect of organic farming (Diacono & Montemurro, 2011). Organic farming is in turn, according to the European Union Council (2007), the only legally defined sustainable form of agriculture. Compared to alternative mineral fertilizers, such organic amendments are cheaper, more effective in the long-term and, due to increasing the SOC content, influence soil physical parameters in a positive way (Lehtinen et al., 2017; Reynolds et al., 2015). All of these advantages play a role in the context of carbon projects, with the final one being of special interest for this thesis. It is important to note that for a long-term effect on soil physical parameters, OC must be stabilized in the soil in order for it not to be mineralized to CO<sub>2</sub>.

OC sequestration can thus be defined as "the process of transferring CO<sub>2</sub> from the atmosphere into the soil of a land unit through plant residues and other organic materials which are stored or retained in the unit as a part of the SOC with a long mean residence time so that it is not re-emitted back into the atmosphere" (Olson et al., 2014). According to various studies such as the one by Diacono and Montemurro (2011), stabilized SOC increases significantly with the application of organic matter (OM) and compost. Further, the more compost or OM is applied to the surface, the more the SOC content increases (Brown & Cotton, 2011; Sciubba et al., 2014). Based on relevant literature, this thesis refers to different practices such as compost application (composting), mulching, OM or OC application,



and plant residue application, but always refers to OC application and thus increased SOC levels.

In addition, soil texture plays an important role in both soil quality and other soil-related research areas. Also called particle size distribution (PSD), it describes the proportions of clay ( $< 2 \mu\text{m}$ ), silt ( $2 \mu\text{m} - 63 \mu\text{m}$ ) and sand ( $63 \mu\text{m} - 2 \text{mm}$ ) in a soil according to their weight percentages (Amelung et al., 2018). Figure 2 shows the classification of PSDs into soil classes as defined by the United States Department of Agriculture (USDA).

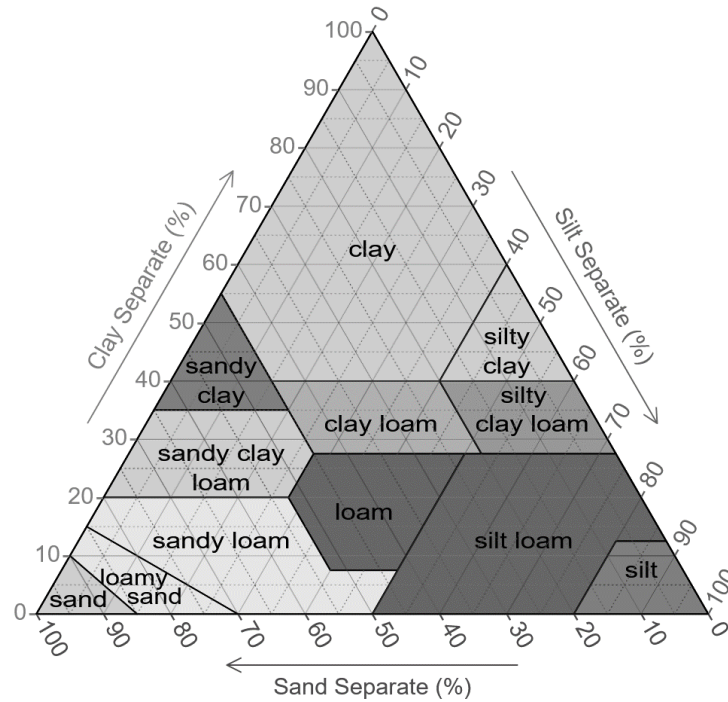


**Figure 2** Soil classes by clay, silt and sand composition as used by the USDA; taken from Vittucci (2015), courtesy of USDA.

### 1.2.2 Soil water balance

The water balance in general describes the water in- and outflows of a system. In this thesis, the system is the soil in an agricultural carbon project. Figure 3 shows an overview of the SWB components considered. In a system in equilibrium, as it shall be studied in this thesis, the in- and outflows are equal when averaged over a long period of time. Under this so-called steady state, changes in soil storage are levelling off. Although the occurrence of surface inflow, as well as other forms of additional water input to the soil system, are possible in the realm of carbon projects, the only input considered here is precipitation. This input is either added to the soil storage, or contributing to flows of deep percolation, transpiration or evaporation (together: evapotranspiration), or runs off superficially (surface runoff). In this context, deep percolation is the flow of water out of the soil system under consideration, which is then no longer available to plant roots.

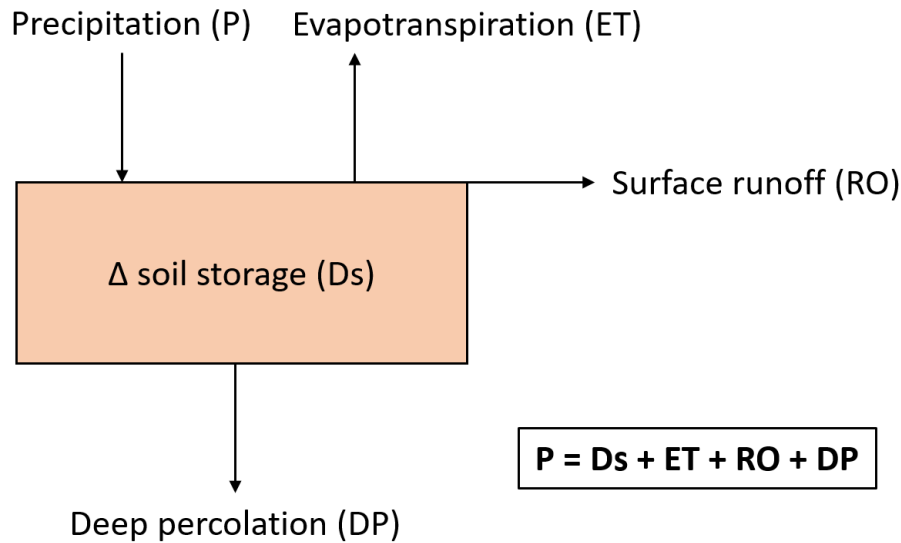


**Figure 3** Overview of the SWB components considered in this thesis and the resulting water balance equation. Figure adapted from Vittucci (2015).

The way rain water is divided among the four SWB components evapotranspiration, surface runoff, change in soil storage and deep percolation is defined by SHPs (Tóth et al., 2015). In this thesis, SWB and SHPs are together referred to as soil hydrology.

SHPs refer to specific physical properties of the soil that are independent from actual water in- and outputs. They are directly influenced by changes in soil structure, for example by amended SOC contents, and translate into SWB components through external influences such as meteorological or topographic boundary conditions (Šimůnek et al., 2013). The main determining SHPs are described by van Genuchten (1980) as saturated water content ( $Q_s$ ), residual water content ( $Q_r$ ) and saturated hydraulic conductivity ( $K_s$ ).  $Q_s$  describes the volume of water that a soil can absorb until saturation. It thereby theoretically corresponds to the soil's porosity but is often about 10-25% less due to dissolved or entrapped air (van Genuchten, 1980).  $Q_r$  is the volumetric water content beyond which further suction only leads to a marginal decrease in soil water. It can be set equal to the wilting point used in the context of plant growth. The wilting point quantifies the minimum soil water content that is still available to plants through root suction. Water that is potentially available to plants is thus equal to the difference between  $Q_s$  and  $Q_r$  (Amelung et al., 2018). The parameter  $K_s$  defines how fast water can flow through a fully saturated soil. As long as a soil is unsaturated, infiltration rates are variable, but once saturation sets in,  $K_s$  is the limiting factor for further infiltration. All water that is added to a saturated soil at rates that surpass  $K_s$  therefore either ponds up to a certain height or runs off superficially (Ferré & Warrick, 2005).

Various models of environmental processes and decision support systems, related to land surface processes, depend on accurate and high-resolution quantitative information on state and flux of water in the critical zone of soils. Simulating these fluxes is possible

either with the help of simple modeling approaches, requiring only few direct measurements, or with the Richards equation (Szabó et al., 2020; Vereecken et al., 2015). The latter opens up a broad field of applications but also requires knowledge about the SHPs over the full moisture range. One of the most common approaches to describe Ks and water retention curves, that are required to solve the Richards equation, is the Mualem-van Genuchten (MVG) model (Mualem, 1976; van Genuchten, 1980; Weber et al., 2019). Soil hydraulic measurements however, that would be necessary to obtain the required SHPs for this model, are often difficult, time consuming and expensive.

This is why indirect methods using easily available surrogate data have been developed to estimate the required parameters described above. Under the term of pedotransfer functions (PTFs), a large number of approaches exists to date with different combinations of input and output parameters (van Looy et al., 2017). Constructing a PTF requires three elements: predictor variables, predicted variables (property of interest) and a transfer method between both (Szabó et al., 2020). The PTFs of interest in this thesis translate soil properties such as texture and SOC content to the MVG parameters. A more detailed overview of PTF properties required for this thesis will be given in chapter 3.1.2.

Dry and rainy seasons can often be distinguished in tropical climates with their difference being more or less pronounced depending on the location (Glaser et al., 2016). The SWB is strongly influenced by this seasonality, and particularly in the agricultural context, it is important to mitigate related extremes of drought and heavy rain (Diacono & Montemurro, 2011).

### 1.2.3 Drought

Droughts are described by van Loon (2015) as the “creeping disaster” as their impacts are slower, more indirect than extreme flood events and they therefore often receive less attention. Drought can be defined as “a sustained period of below-normal water availability” (Tallaksen & van Lanen), implying that the use of the term drought is also closely linked to geographical location and its prevailing water availability. The notion of drought has thus a spatial and a temporal component.

Regarding agricultural carbon projects, droughts pose problems when negative deviations from the mean seasonal precipitation are the limiting factor for plant growth (Amelung et al., 2018). This is especially the case during dry season and a main issue for rural households in the tropics. They often rely solely on crop production and cannot easily fall back on supplementing income via other products such as timber. Incomes of the poorest are often directly dependent on crop yields which fluctuate with seasons and weather extremes (Noack et al., 2019). Furthermore, when plants do not grow due to a lack of soil water contents, very little to no carbon is being sequestered and the functioning logic behind agricultural carbon sequestration projects is impaired.

According to van Loon (2015), four types of drought and their successive development steps can be distinguished. An overview is given in Figure 4. Meteorological drought is the one stemming directly from an anomaly in precipitation. It translates into a soil moisture drought which is enhanced by anomalies in temperature. A soil moisture drought thus has its origin in a specific meteorological situation. It is often called agricultural drought as mainly the root zone is affected, thus linking this type of drought to crop failure. In line with the agricultural focus of this thesis, the use of the term drought will refer to an agricultural drought.

Soil moisture drought further translates to a hydrological drought when the low soil moisture and continued high temperatures lead to water bodies and ground water being affected. The low discharge of running waters and decreased ground water storage volume, together with low soil moisture and continued high temperatures, leads to what is called a socio-economic drought. This type of drought implies persons being affected. While this is also the case during soil moisture drought, whereby rural households and carbon projects may be affected, the effects of a socio-economic drought are at country scale and affect the whole society (van Loon, 2015).

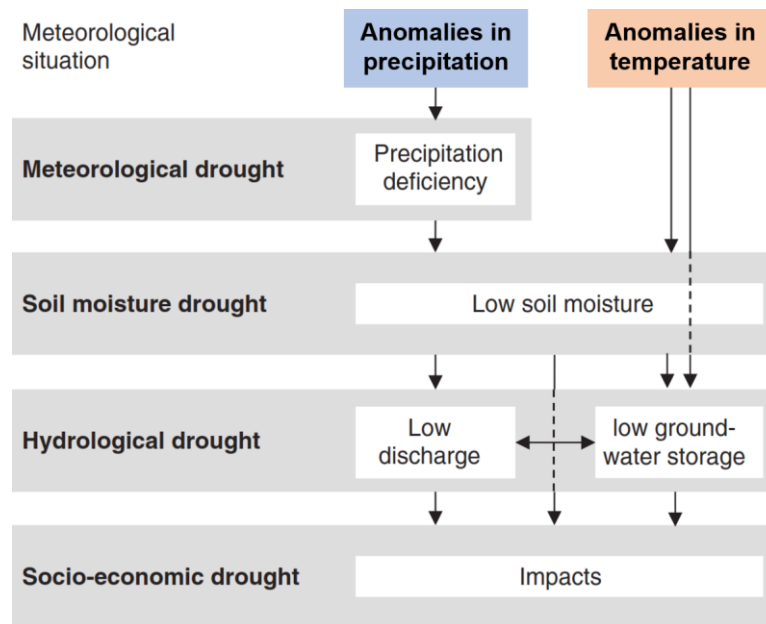


**Figure 4** Four types of drought and their causes according to and taken from van Loon (2015).

The emergence of tropical and subtropical drought events worldwide is influenced by various macroclimatic factors. It is particularly tied to changes in convergence zones and monsoons with an important role being attributed to sea surface temperatures (Brando et al., 2019). The El Niño Southern Oscillation (ENSO) phenomenon in the tropical Pacific is an example of such changes and provokes less precipitation and higher temperatures in Indonesia and northern South America while bringing more rainfall to southeastern South

America and eastern Africa (Brando et al., 2019). In addition, the Indian Ocean Dipole (IOD) causes warmer conditions in the western Indian Ocean, leading to deficits in precipitation in Southeast Asia. Furthermore, the Atlantic Multidecadal Oscillation (AMO) brings, in its warm phase, increased precipitation over the Sahel, India and South America while in its cold phase the contrary occurs (Brando et al., 2019; Shanahan et al., 2009).

According to predictions of the Intergovernmental Panel on Climate Change (2014) and Cai et al. (2014), the ENSO, as well as the IOD are, with the forecasted course of climate change, likely to become extremers and thereby cause more severe droughts. For South America, and especially southern Amazonia, climate models generally project a very likely increase in temperatures (Intergovernmental Panel on Climate Change, 2014). They further agree on dryer conditions in the Amazon, especially in the east and during the dry season, with increasing numbers of consecutive dry days and decreasing soil moisture. For Africa, no clear general predictions are available, which is mainly due to limited observational record and related low confidence levels (Brando et al., 2019). Trends towards the extremes are however visible in individual national prognostics as for example in Rwanda (Asumadu-Sarkodie et al., 2015). In Southeast Asia, due to mesoscale and sub-mesoscale systems in a complex topography, no high confidence levels of climate projections are available either (Brando et al., 2019).

#### 1.2.4 Heavy rain and soil erosion

Soil erosion can be defined as a displacement of the upper layer of soil and is thus a form of soil degradation. It is classified according to the eroding agents which can be water, ice (glaciers), air (wind), plants, animals and humans (Amelung et al., 2018). In the framework of this thesis, the term erosion refers to water erosion caused by surface runoff of rainwater. Although it is overall a natural phenomenon with (extreme) precipitation as its main cause, water erosion is greatly enhanced by human activity, especially by land use change and certain destabilizing agricultural practices (Amelung et al., 2018).

The maximum potential erosion is however determined by the natural erosivity factor which is directly linked to the rainfall quantity and intensity causing the surface runoff (Panagos et al., 2015). Runoff and erosion are thus closely interlinked and are impacted in similar ways. According to Nearing et al. (2005) erosion is impacted disproportionately more by increased rainfall intensity than by runoff, meaning that erosion is more sensitive to increased concentration in precipitation.

In the course of climate change, more concentrated forms of rainfall are predicted for large parts of tropical and subtropical areas. The ENSO and IOD are likely to shift towards the extremes, as outlined above, which also brings more intense rainfall events to the respective areas. The Intergovernmental Panel on Climate Change (IPCC) further predicts an extension of the monsoon area causing more regions to be affected by extreme monsoon

rain than previously. Additionally, climate models agree on an increase in extreme precipitation over South America (Intergovernmental Panel on Climate Change, 2014). However, this must be seen before the background of higher uncertainty for wet season changes than for drought periods, as some models project overall higher and some overall lower precipitations (Intergovernmental Panel on Climate Change, 2014). For the African tropical and subtropical regions, as well as for vast areas of Southeast Asia, the uncertainties described in chapters 1.2.3 and 1.2.4 apply and no clear predictions have been made thus far.

### 1.2.5 Soils in agricultural carbon sequestration projects and the case of Rwanda

As mentioned above, agricultural carbon sequestration projects are motivated by two main objectives: climate adaptation and climate mitigation.

Climate adaptation takes place by making soils more resilient to climatic extremes. In carbon projects this is achieved by a set of common practices such as the inclusion of trees on fields (agroforestry), intercropping, composting, mulching and many more, depending on the local conditions and priorities (VERRA, 2021b). In this thesis, the focus lies on the effect of OC application, which limits the consideration to the practices of composting and mulching. Although only the quantity of OC is considered for the analyses, it shall be noted here that for the influence on soils the quality of amendments also plays a not negligible role. As indicated by various studies, especially the C:N ratio is crucial for the beneficial climate adaptation and mitigation effects of OC applications (Farrick et al., 2018; Gülser & Candemir, 2015; Mbagwu, 1989; Reynolds et al., 2015). For this thesis, it is assumed that the predominant share of OC applications is made up of plant residues (high C:N ratio) instead of manure (low C:N ratio, risk of surface clogging, Cherobim et al., 2018).

Climate mitigation is strived for in carbon projects by withdrawing CO<sub>2</sub> from the atmosphere. According to global estimates, soils contain between  $1,206 \cdot 10^9$  t and  $1,550 \cdot 10^9$  t SOC within one meter depth. While the figure of  $1,550 \cdot 10^9$  t C is already twice the carbon content of the atmosphere, soils would, according to Zdruli et al. (2016) have the capacity to store up to five times of today's atmospheric carbon content. However,  $78 \pm 12 \cdot 10^9$  t of total atmospheric carbon emissions could, already in 1999, be attributed to depletion of SOC, mainly due to land use change (Lal, 2003). Today, emissions from land use change and, related to it, loss of biomass and SOC are estimated to make up 20 % of atmospheric CO<sub>2</sub> (Zdruli et al., 2016). Due to the importance of soils, in terms of quantities of stored SOC, small changes in this stock could result in significant impacts on atmospheric stocks (Lal et al., 2018; Stockmann et al., 2013). The most effective agricultural management practices were found to have the ability to restore parts of the SOC that had been lost during previous agricultural use (Lal et al., 2018). A systematic review by Fuss et al. (2018) suggests that overall the global OC sequestration potential is at  $2 \cdot 10^9$  to  $5 \cdot 10^9$  t CO<sub>2</sub>/ year ( $\pm 0.55 \cdot 10^9$  to  $1.36 \cdot 10^9$  t C/ year).

Based on such findings, research and investment in the area of OC sequestration are gaining momentum. Measurement, reporting and verification (MRV) schemes have been developed to quantify and validate agriculturally sequestered carbon and thereby pave the way for investment. The VERRA Verified Carbon Standard that certifies the Rwanda agricultural carbon project is one of these MRV schemes and defines the Rwanda project more narrowly as a “sustainable agricultural land management” (SALM) project (VERRA, 2021c). This thesis, however, will continue to use the broader term agricultural carbon sequestration project, or carbon project for short.

The Rwanda carbon project is used as an example in this thesis as well as a source of data. It is funded by the Livelihoods Funds, developed by the non-government organization Albertine Rift Conservation Society (ARCOS) and implemented by UNIQUE forestry and land use (ARCOS network, 2021; Livelihoods Funds, 2021; UNIQUE forestry and land use, 2021). Throughout the country, more than 80% of the workforce lives in rural areas and is engaged in agriculture (Livelihoods Funds, 2021; Muhire & Ahmed, 2015). The project is being implemented in the districts of Rulindo and Bugesera, as indicated in Figure 5. It aims to sequester a total of  $2.3 \cdot 10^6$  to  $3.5 \cdot 10^6$  t CO<sub>2</sub> ( $\pm 0.63 \cdot 10^6$  to  $0.95 \cdot 10^6$  t C) over 20 years and on a project area of 15,200 ha (Livelihoods Funds, 2021; UNIQUE forestry and land use, 2021).

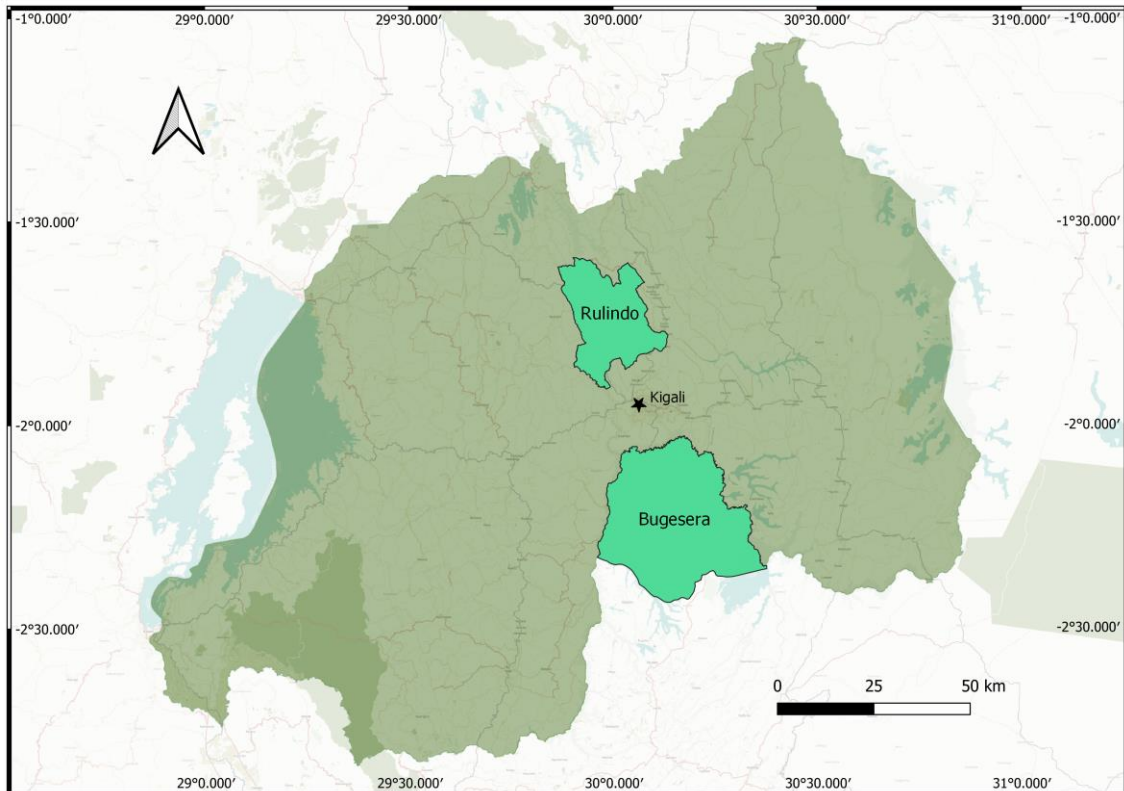


**Figure 5** Map of Rwanda showing the carbon project regions Rulindo and Bugesera, as well as the Capital Kigali.

## 1.3 State of science

In this chapter, an overview of recently published literature related to this thesis is given. In the first part, central studies addressing the research field of SOC effects on soil hydrology are presented, while in a second part, recent developments in PTFs are outlined.

### 1.3.1 The effect of soil organic carbon on soil hydrology

A variety of studies has thus far addressed the effect of SOC on SWB components, SHPs or both. Predominantly positive effects were found in recent publications and are in line with older findings. A new development in the realm of the research field is the increasing interest in biochar due to its high OC content and long residence time in soils. Although this thesis focuses on compost use, as practiced in carbon projects, most important findings on biochar are also included here due to their recent gain in scientific importance.

With regards to the general attention to OC sequestration, it can be noted that Amelung et al. (2020) reemphasized the great global potential of carbon sequestration in agricultural soils, especially those severely degraded or with very low yields. The enhancement of SOC in the root zone as an adaption to increasing food requirements is attributed as being a vital factor and therein supported by earlier literature, among others by Lal (2006) and Diacono and Montemurro (2011).

Filipović et al. (2020) conducted a study that, for this thesis, is of exceptional interest. In their study the effect of compost and biochar on SHPs (measured) and SWB (modeled with the water flow model Hydrus-1D, H1D) is examined in rendzina and terra rossa soils. They mainly found improved water retention related to higher  $Q_s$ , higher field capacity and increased available water content. However, they concluded a strong soil dependency, with positive effects on soil water retention being highest in coarser textured soils. This is in line with earlier findings from a tropical study by Bass et al. (2016) stating that improvements in soil water retention were highest in coarse textured soils, and could not be detected in clayey soils.

Kranz et al. (2020) focused on the use of compost and its effect on soil physical properties in urban soils. In their review including relevant literature from the last decade, they concluded that compost application has a positive effect on infiltration rates,  $K_s$ , water retention and plant available water.

Besides these positive effects of SOC on soil hydrology, adverse effects of increased SOC contents were also discussed in recent literature. Increasing phosphorus mobility and related eutrophication of receiving waters, due to compost application, was studied by Filipović et al. (2020), but not found to be an issue. They instead attributed an important role to compost and biochar in acting as a soil fertilizer and erosion avoiding soil stabilizer, without being an environmental threat.



Water repellency has also been discussed as a possible negative result of SOC amendments. Farrick et al. (2018) conducted a study on this topic in the tropics. Their results mainly support prior findings stating that SOC content was not the key cause of water repellency. It depended much more on the type and the C:N ratio than on the quantity of organic amendment application. On the contrary, in their study, the application of composted organic residues, as proposed in this thesis, was found to rather act against the water repellency caused by manure application. Cherobim et al. (2018) added in this context the aspect of soil texture, stating that liquid manure could lead to surface sealing, especially on uncovered clayey soils without good aggregate formation. Otherwise, sandy soils were found to be more susceptible to water repellency. This was however not found to be the case for the application of composted plant residues.

Yet, Cherobim et al. (2018), as well as Farrick et al. (2018) concluded that soil water repellency and its causes are still not sufficiently understood and must be subject to further research. Since water repellency is thus far not fully grasped nor quantifiable, and additionally does not seem to be a primary issue in the context of compost use, water repellency is not considered any further in this thesis.

In the context of physical and hydrological improvements of soils through SOC, positive effects of biochar on soil structure have recently gained in scientific importance. Compared to compost, biochar could have similar but more pronounced effects on soil physical parameters due to its much higher OC content of up to over 60 %, depending on the production procedure (Filipović et al., 2020). Toková et al. (2020) found significant increases in soil porosity under biochar application with related improvements in SHPs. Villagra-Mendoza and Horn (2018) specified that especially wetting and drying cycles enhanced the structural stability in sandy soils amended with biochar. Filipović et al. (2020) supported these results, while Yu et al. (2019) pointed out that especially on poor soils these effects could lead to better plant growth. Razzaghi et al. (2020) reviewed literature on the effect of biochar on soil physical properties. From their findings, they added that the improvement in water retention variables were very much dependent on soil texture with much larger benefits in coarse textured soils. This is also in line with the above mentioned findings by Filipović et al. (2020) on the effect of compost and biochar. Additionally, Lal et al. (2018) attributed high rates of carbon sequestration, and thereby important climate change mitigation effects to this agricultural technology. They however stress that the production process, logistics and alternative uses of biomass must also be considered in this calculation.

In conclusion, for the fairly new area of biochar, Toková et al. (2020) point out further research needs to be conducted on different soil types, to gain broad evidence of beneficial effects, before the practice of biochar application can be generally recommended to farmers.

### 1.3.2 Pedotransfer functions

As mentioned in chapter 1.2.2, PTFs are central to soil sciences. As a result, a great variety of PTFs has been proposed in the last few decades. Recent developments in PTF research focus especially on more targeted prediction of specificities related to soil type and climatic region. The most attention, in this context, is given to the differences between tropical and temperate regions. The main issue in predicting tropical conditions with a temperate PTF, and vice versa, was found to be related to  $K_s$  which seems to be very region dependent (Ottoni et al., 2019; Reichert et al., 2020).

Ottoni et al. (2019) so far developed the most broadly calibrated, and therefore promising tropical set of PTFs, based on the Brazilian database HYBRAS that is described in Ottoni et al. (2018). This set also contains temperate PTFs that are, however, based on the older database HYPRES that was previously found to be less accurate than the newer and more comprehensive EU-HYDI (Tóth et al., 2015). Compared to the majority of PTFs published, the ones proposed by Ottoni et al. (2019) do not contain the common set of predictors including texture and SOC or bulk density (BD). Their main predictor is instead effective porosity, arbitrarily defined as the total porosity minus the volumetric content at suction 330 cm, which they found to be more appropriate for predicting tropical soils. Despite this major change in predictors, they also had difficulties in accurately predicting  $K_s$  in very fine textured soils due to higher structural complexity (Ottoni et al., 2019).

Szabó et al. (2020) published a revised version of their temperate set of PTFs, which had originally been developed in 2015. It is calibrated with the, to-date, broadest set of temperate soils and is therefore a promising development in the prediction of SHPs (Tóth et al., 2015). In the newer version, called euptfv2, is included the communication of uncertainties which can help in illuminating the reliability of predictions made by the PTFs. A detailed sensitivity analysis provided in the study of Szabó et al. (2020) further provides insight into the relative importance of predictors for the respective output parameter.

Macroporosity and soil aggregates are two phenomena that play important roles in recent studies on the modeling of soil water parameters. They are however not yet included in any of the common PTFs available in the literature. Especially regarding the positive influence of SOC on soil hydrology, an important role is being attributed to these effects and their power to cause deviations between PTF results and reality. The prediction of  $K_s$ , depending on climate and soil type, seems to be particularly affected by these deviations (Y. Zhang & Schaap, 2017). Under increased SOC contents, Filipović et al. (2020) found a higher number of macro and medium pores and thereby an increase in total porosity, which led to higher soil water retention,  $K_s$ , field capacity and available water. Kranz et al. (2020) additionally stress the importance of SOC not only for the size of macropores and aggregates, but also for aggregate stability. By linking SOC to erosion prevention they support earlier findings by Gülser and Candemir (2015). Macroporosity was additionally found to be climate sensitive and is, together with  $K_s$ , expected to decrease in the course of climate change

due to altered precipitation patterns (Hirmas et al., 2018). Yet, since such trends have not been studied well so far and macroporosity, as well as soil aggregates, are not included in commonly available PTFs, phenomena of macroporosity are not included in the modeling approach proposed in this thesis. The potential of macroporosity causing divergence between model and reality must however be kept in mind in the further course of this thesis.

## 2 Problem statement, aim and research questions

From the state of science, several research gaps can be deduced. Firstly, most studies analyze and quantify only either SHPs or the SWB but not both in their interdependence. Secondly, findings stem so far exclusively from case studies, which yield valuable knowledge for specific conditions, but can be generalized only to a limited extent. Thirdly, no attempt to design a model for making general predictions on the effect of SOC on SWB could be identified. Finally, in the studies considered, the OC was sequestered in soils always with the goal to achieve specific soil physical, chemical or biological properties. The type and quantity of OC was thus determined and studied with this focus. The effects of intentional maximization of sequestered SOC on soil hydrology in the context of agricultural carbon sequestration projects have not been studied so far.

Based on these gaps, the aim of this thesis is to study the impact of SOC on SHPs, as well as on the SWB components, under different conditions in the context of carbon sequestration projects.

To make the results comparable and increase their generalizability a modeling approach shall be proposed and validated to quantify these relationships. The proposed method will subsequently be used to generate data on the effects of a stepwise increase in SOC contents, and to make predictions for the agricultural carbon project in Rwanda.

The approach of this study is to conduct a meta-level analysis, as no model calibration in the classical sense can be done through field measurements. Instead, a remote modeling approach shall be proposed to estimate the magnitude of impacts in carbon sequestration projects.

These objectives can be formulated as succinct RQs as follows:

- RQ 1:** Is intentionally enhanced SOC beneficial to the SWB in the context of carbon sequestration projects? What are the main controlling factors to optimize the benefits?
- RQ 2:** How can the effect of SOC on the SWB be predicted by a physically based soil hydrology model?

### 3 Methodology

The development and testing of a modeling approach is the methodological core of this thesis and central to answering the RQs.

Consisting of a PTF plus H1D, the approach was, in a first and most important step, designed and evaluated in a thorough literature research. Via the comparison with scenarios from the literature, the approach was proven to yield qualitatively accurate results and was thereby validated (chapter 3.1).

In a second step, the proposed modeling approach was applied (chapter 3.2). On the one hand, the application took place in virtual experiments to generate data on the relation between gradually modified SOC contents and soil hydrology (chapter 3.2.1). On the other hand, the modeling approach was applied to compare the Rwanda carbon project soil hydrology before and after 20 years of compost application practice (chapter 3.2.2).

An overview of these steps, as well as of the outcomes is depicted in Figure 6. A detailed flow chart of the consecutive methodological steps can be found in Appendix 2 to 4.

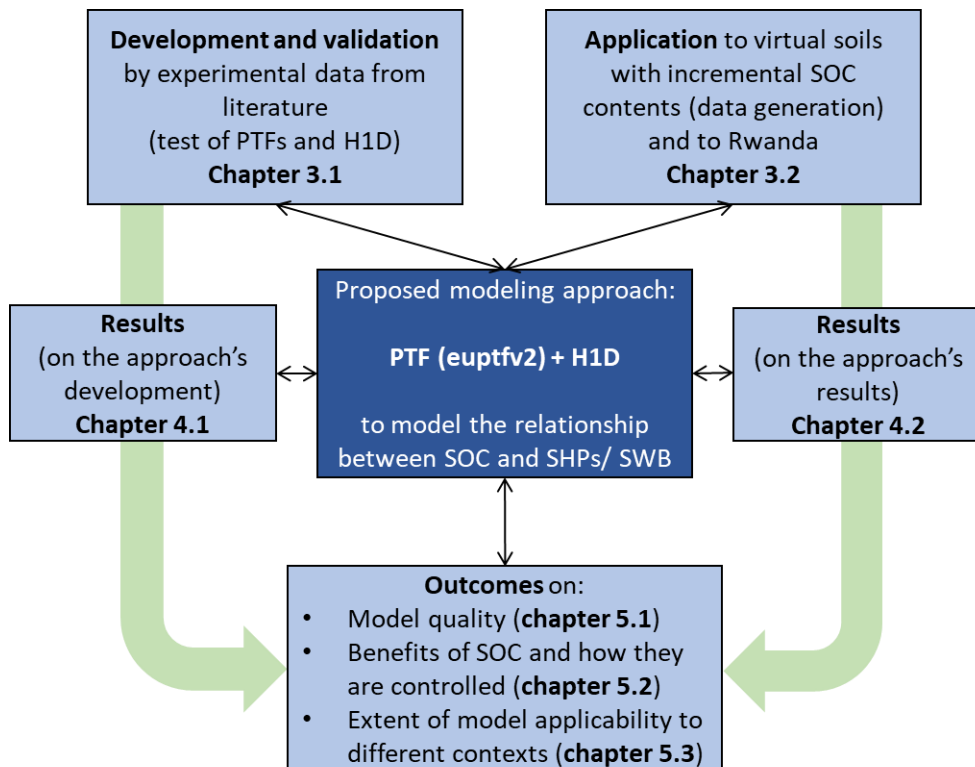


**Figure 6** Flow chart showing the modeling approach as a methodological core and its role in the methodology, results and discussion parts of this thesis.

### 3.1 Development and validation of the modeling approach

The design of the modeling approach was determined by the objective of determining whether, and under which controlling factors, OC application is beneficial to the SWB in carbon projects. Meeting this objective required a physically based model to yield quantitative results. Further, the approach was designed to fulfill the condition of being applicable to a preferably broad regional context (in terms of climate and soils), with a focus on the tropics to account for the way carbon projects are distributed globally (VERRA, 2021a). Possible controlling factors inherent to carbon projects such as soil texture, precipitation regime and soil depth, besides SOC content, must be independent inputs to the modeling approach.

#### 3.1.1 Hydrus-1D as a core component

##### Basic description

H1D was chosen as a basis for the modeling approach. It is a physically based model using a numeric solution method for the one-dimensional modeling of variably saturated soil water flow. The original Hydrus code was published in 1998 and has been subject to a great variety of additions and advancements ever since (Šimůnek et al., 2013). This thesis draws on its latest version Hydrus-1D 4.17.

The main criterion to choose H1D for the modeling approach was its reliability and accuracy. It is widely used, highly cited and has shown to yield accurate results of water movement in experiments similar to the ones in this thesis, also taking place in tropical and other pedogenetic regions (Da Pinho & Miranda, 2014; Filipović et al., 2020; Šimůnek et al., 2005; Taheri Soudejani et al., 2020; Ventrella et al., 2019; Wang et al., 2018; Whelan et al., 2013).

The most popular approach for determining variably saturated flow in soils is the Richards equation. H1D numerically solves this equation for saturated-unsaturated water flow (Šimůnek et al., 2013). To do so, the hydraulic conductivity ( $K(h)$  [cm/day]) at a given hydraulic potential ( $h$  [cm]) is determined with the use of the MVG approach (van Genuchten, 1980).

To do so, the relative soil saturation ( $Se$  [-]) is first described as a function of  $h$  and the empirical constants  $\alpha$ ,  $n$  and  $m$ ,

$$Se = \frac{\theta - \theta_r}{\theta_s - \theta_r} = [1 + (\alpha \cdot h)^n]^{-m} \quad (1)$$

with  $\theta$  [-] being the actual water content,  $\theta_r$  [-] the residual water content,  $\theta_s$  [-] the saturated water content,  $\alpha$  [1/L] the air entry value,  $n$  [-] a shape parameter of the retention curve and  $m = 1 - 1/n$ .

$K(h)$  [cm/day] can then be calculated as a function of the saturated hydraulic conductivity ( $K_s$  [cm/day]) and  $Se$  [-],

$$K(h) = K_s \cdot Se^l \left[ 1 - \left( 1 - Se^{\frac{1}{m}} \right)^m \right]^2 \quad (2)$$

where  $l$  [-] is an empiric pore connectivity parameter (Vereecken et al., 2010).

### **General model set up, boundary conditions and temporal and spatial discretization**

To develop and justify the modeling approach, H1D was excelled in its common version via the graphic user interface (GUI). Modeling parameters and conditions that are not described here were kept as default.

The main H1D modeling modules used for this thesis is the H1D water flow module together with a sink term to account for water uptake by plant roots (Šimůnek et al., 2013). The corresponding models chosen within the H1D realm were the well-established MVG single porosity hydraulic model with no hysteresis and the Feddes root water uptake model.

Time variable boundary conditions were specified in a way that the inclusion of specific precipitation patterns, as well as potential evapotranspiration (PET) values, is allowed. In addition to that, fix boundary conditions were specified as follows: as the upper boundary condition on the soil surface, an atmospheric boundary condition with surface runoff was chosen in order to get runoff as a result for any non-infiltrated water. It was thus assumed that, above the surface, water does not pond up to a certain height, but runs off directly. The lower boundary condition, which applies to the lower end of the soil depth was specified as free drainage to account for deep vertical percolation. This allowed deducing a proxy for potential ground water recharge.

For the temporal discretization in H1D, three values are needed: an initial time step ( $dt$ ), a minimum time step ( $dt_{\min}$ ) and a maximum time step ( $dt_{\max}$ ).  $Dt$  defines the time step that is used at the beginning of each model run. It is also used whenever a variable boundary condition (e.g. precipitation or meteorological condition) changes significantly. The time step is automatically modified to optimize computing times, but always ranges between  $dt_{\min}$  and  $dt_{\max}$  (Šimůnek et al., 2013). For the purposes of this thesis, time steps were set as follows:  $dt = 0.001$  days,  $dt_{\min} = 10^{-4}$  days and  $dt_{\max} = 5$  days. The definition of these time steps is crucial and will be analyzed with more detail in chapter 5.1.1.

The spatial discretization is specified by dividing the previously defined soil depth into a number of nodes. Here, the default number of 101 nodes was kept. For nodes that are defined as observation nodes, output data is generated by the model.

Further inputs to the model are the MVG water flow parameters  $Q_r$  [-],  $Q_s$  [-],  $\alpha$  [1/cm],  $n$  [-],  $K_s$  [cm/day] and  $l$  [-]. In case these inputs are not available, it is possible

to draw upon a soil catalog and indicate a soil texture or specific PSD. Based on this information MVG parameters are calculated through the integrated PTF Rosetta (Schaap et al., 2001). However, Rosetta does not include SOC content as a predictor and does thus not serve the purpose of this thesis. Therefore, it was necessary to find another PTF to substitute Rosetta and enter its resulting MVG parameters directly into H1D. This alternative PTF including SOC as a predictor can then be used as a pre-step before the modeling with H1D.

It shall be noted here, that in some cases, issues of non-convergence occurred in the execution of H1D. This means that certain combinations of parameter inputs did not yield model results because the respective equation could numerically not be solved. Further information on convergence can be found in the H1D technical manual (Šimůnek et al., 2013). Its relevance to this thesis is analyzed in chapter 5.1.1.

### 3.1.2 Preselection of pedotransfer functions

The PTF to substitute Rosetta needed to be, similar to the latter, a continuous one to generate outputs from continuous inputs. It was further required to be parametric and yield the MVG parameters in the outputs. The flow chart in Figure 7 depicts the interconnections of these requirements.

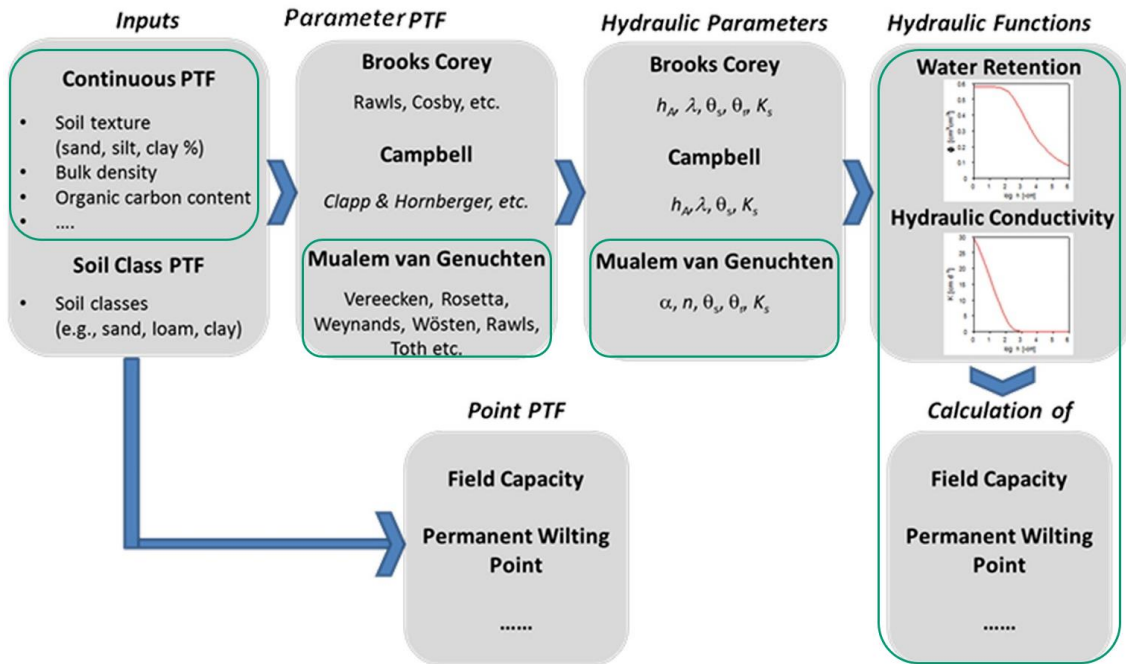


**Figure 7** Flow chart modified from van Looy et al. (2017) showing different types of PTFs. The green markings correspond to the basic PTF requirements of this work.

$\theta_s$  [-] = saturated water content;  $\theta_r$  [-] = residual water content;  $K_s$  [cm/day] = saturated hydraulic conductivity;  $\alpha$  [1/cm] = reciprocal of the air entrance value for MVG;  $n$  [-] = shape parameter for MVG



Due to a great variety of PTFs available, a set of criteria was elaborated to find the best PTF for this thesis. Criteria were defined as shown in Table 1. See Appendix 7 for a non-exhaustive list of PTFs considered.

**Table 1** Obligatory and optional criteria for choosing a PTF as part of the modeling approach.

| Obligatory criteria   | Optional criteria   |
|---|---|
| <ul style="list-style-type: none"> <li>• Continuous and parametric PTF</li> <li>• Minimum predictors: soil texture plus OC or OM content</li> <li>• Minimum output: full set of MVG parameters</li> <li>• Recentness: based on a dataset that was developed or reviewed after the year 2000</li> <li>• Generalizability: geographically broad range of application</li> </ul> | <ul style="list-style-type: none"> <li>• GUI published</li> <li>• Tropical: specifically developed for tropical regions (low RMSE for tropical soils)</li> <li>• Error margins included in results</li> </ul> |

The inclusion of SOC as a predictor was often the decisive limiting factor in the choice against a certain PTF. However, including SOC is justified also beyond the necessity of inclusion in this thesis: According to a review of van Looy et al. (2017), the most accurate PTFs could be obtained when either OM or SOC was included in the set of predictors, in addition to texture and BD. The latter however was found to be a very dynamic soil property as it is strongly influenced by land use practices, weathering, drainage and biological activities. It was therefore not taken into account as a predictor in this thesis.

Although the greater share of agricultural carbon projects is conducted in tropical regions, the criterion of the PTF being specifically developed for tropical soils was only classified as optional. Many tropical PTFs do not include Ks as output or include very specific inputs that are not easily available (Hodnett & Tomasella, 2002; Reichert et al., 2020). Additionally, most tropical PTFs are developed based on Brazilian soil databases and may be limited to very specific regions (Oliveira et al., 2002; Ottoni et al., 2018). Although from personal comments and from the literature it was clear that regionally appropriate PTFs could most probably yield more accurate results, the criterion of being developed in the tropics was therefore not classified as obligatory (Botula et al., 2012; Hodnett & Tomasella, 2002; Ottoni et al., 2019). This decision was also supported by findings from the literature stating that in spite of drawbacks, good PTFs from temperate regions were able to perform sufficiently well in the tropics (Botula et al., 2012; Minasny & Hartemink, 2011).

Following this criteria driven procedure of exclusion two PTFs, based on temperate soil data, remained (see chapter 4.1.1 for the reason of exclusion of other popular PTFs). As had been the case in various previous studies, also became the case for this thesis: the use of purely temperate PTFs prevailed although they were regionally not fully appropriate (Ottoni et al., 2018).

The two remaining candidate PTFs were the very recent euptfv2 (Szabó et al., 2020), based on its previous version euptfv1 by Tóth et al. (2015); and SPAW, a highly cited PTF by Singh and Frevert (2006). The subsequent step was to perform a testing procedure to identify the one PTF among them that provides the better results in the context of this thesis and to justify its further use.

### 3.1.3 Scenarios and final selection of the pedotransfer function

The usual approach of validating a model would be to compare model results to results from field measurements. This however goes beyond the scope of this thesis. In order to enable solid remote estimations without such studies, the method of validation by scenarios from the literature was applied. This means that data on soil texture, as well as SOC content, were taken from the literature and used as inputs for the proposed modeling approach. Modeled results were subsequently compared to literature results. This was done in a first step for the two PTFs to compare them and then for the PTF of choice plus H1D. Only Ks, Qr and Qs were taken into consideration since no sufficient information was provided on the remaining MVG parameters in the literature.

#### **Determining suitable literature**

To determine the studies to be chosen as a basis of comparison, a literature review was conducted on Google Scholar and Research Gate. The main intention of this review was to identify studies that examined the effect of SOC, OM or compost soil amendments on soil hydrology. In addition, the inclusion of tropical climates, as well as the representation of a maximum of different OC application quantities and soil textures, was sought out in order to fully represent the range of the intended model application.

After conducting a comprehensive literature research based on these criteria, the resulting papers were examined more closely to determine whether they included quantitative data on the following parameters: PSD/ soil texture, SOC content before and after the experiment, MVG parameters before and after the experiment (at least Ks, Qr and Qs) and soil depth influenced by the experiment. In the case of incomplete information provision, either the paper was excluded or, if possible, an additional calculation was done to find the missing SOC values. The following formula was applied whenever the SOC content [mass %] after the experiment, and thus the quantitative impact of the measure, was not given in a paper:

$$SOC = \frac{\left(\frac{OCC}{100}\right) \cdot CR}{\left(\left(\frac{OCC}{100}\right) \cdot CR\right) + (BD \cdot d \cdot 10000)} \cdot 100 \quad (3)$$

Where  $BD$  [ $t/m^3$  or  $g/cm^3$ ] is soil bulk density,  $CR$  [ $t/ha$ ] is compost rate,  $OCC$  [mass %] is OC in compost and  $d$  [m] is amended soil depth. The resulting SOC content was subsequently added to the baseline SOC content.

Further, when only application quantities of composted municipal solid waste were given, a  $BD$  of  $0.67 \text{ g/cm}^3$  was assumed, as found by Mandal et al. (2014) and used as an input to formula 3.

For the sake of calculation simplicity, and due to largely missing information, it was assumed that all input parameters, apart from SOC content, remained the same over the duration of the experiments. Additional information on  $BD$  and  $pH$ , in spite of the possibility of inclusion in euptfv2, was not included in the scenario testing procedure in order to obtain comparable results and mimic the limited data situation in carbon projects as closely as possible.

Table 2 shows the resulting literature scenarios in their control and amended version, as well as the predictions by euptfv2 and SPAW, based on their input data. The color-coding is explained below while the results in terms of color-coding and steps of deviation will further be described in chapter 4.1.2 in the results section.

**Table 2** Control and SOC-amended scenarios with their measured values from the literature and modeled values from euptfv2 and SPAW. The color coding and resulting steps of deviation from the original literature scenarios serve as a basis to choose and justify a PTF.

| Paper                         | SOC<br>[mass %]                           | Scenario | Soil type       | Ks<br>[cm/day]                     | Qr<br>[-] | Qs<br>[-] | Steps of<br>deviation |
|-------------------------------|---|----------|-----------------|------------------------------------|-----------|-----------|-----------------------|
| Taheri Soudejani et al., 2020 | 1.03                                      | control  | loamy sand      | 95.900                             | NA        | NA        |                       |
| Taheri Soudejani et al., 2020 | 1.45                                      | amended  | loamy sand      | 77.800                             | NA        | NA        |                       |
| euptfv2                       |   | control  |                 | 51.719                             | 0.043     | 0.391     | 3 + / + /             |
| euptfv2                       |   | amended  |                 | 55.824                             | 0.037     | 0.394     |                       |
| SPAW                          |   | control  |                 | 202.608                            | 0.041     | 0.422     | 3 + / + /             |
| SPAW                          |   | amended  |                 | 207.408                            | 0.046     | 0.433     |                       |
| Filipovic et al., 2020        | 0.54                                      | control  | silty clay loam | 6.810                              | 0.093     | 0.450     |                       |
| Filipovic et al., 2020        | 1.40                                      | amended  | silty clay loam | 6.940                              | 0.158     | 0.510     |                       |
| euptfv2                       |   | control  |                 | 41.616                             | 0.037     | 0.468     | 1 + 1 + 1             |
| euptfv2                       |   | amended  |                 | 55.501                             | 0.042     | 0.484     |                       |
| SPAW                          |   | control  |                 | 5.424                              | 0.216     | 0.476     | 1 + 1 + 1             |
| SPAW                          |   | amended  |                 | 8.544                              | 0.218     | 0.495     |                       |
| Filipovic et al., 2020        | 6.11                                      | control  | silty clay      | 6.940                              | 0.005     | 0.346     |                       |
| Filipovic et al., 2020        | 7.06                                      | amended  | silty clay      | 7.070                              | 0.019     | 0.418     |                       |
| euptfv2                       |   | control  |                 | 16.787                             | 0.055     | 0.647     | 0 + 2 + 1             |
| euptfv2                       |   | amended  |                 | 17.418                             | 0.060     | 0.657     |                       |
| SPAW                          |   | control  |                 | 29.448                             | 0.277     | 0.583     | 1 + 2 + 1             |
| SPAW                          |   | amended  |                 | 36.912                             | 0.277     | 0.595     |                       |
| Mbagwu et al., 1989           | 1.65                                      | control  | sandy clay loam | 61.920                             | 0.060     | 0.108     |                       |
| Mbagwu et al., 1989           | 2.63                                      | amended  | sandy clay loam | 168.480                            | 0.071     | 0.206     |                       |
| euptfv2                       |   | control  |                 | 44.891                             | 0.080     | 0.393     | 1 + 1 + 1             |
| euptfv2                       |   | amended  |                 | 50.359                             | 0.084     | 0.475     |                       |
| SPAW                          |   | control  |                 | 15.480                             | 0.184     | 0.409     | 2 + 2 + 2             |
| SPAW                          |   | amended  |                 | 16.416                             | 0.190     | 0.421     |                       |
| Reynolds et al., 2015         | 0.23                                      | control  | clay loam       | 1,235.520                          | 0.370     | 0.490     |                       |
| Reynolds et al., 2015         | 0.43                                      | amended  | clay loam       | 3,248.640                          | 0.370     | 0.540     |                       |
| euptfv2                       |   | control  |                 | 125.708                            | 0.063     | 0.462     | 1 + 2 + 1             |
| euptfv2                       |   | amended  |                 | 183.027                            | 0.062     | 0.470     |                       |
| SPAW                          |   | control  |                 | 3.912                              | 0.227     | 0.449     | 1 + 1 + 1             |
| SPAW                          |   | amended  |                 | 4.200                              | 0.228     | 0.452     |                       |
| Whelan et al., 2013           | 1.00                                      | control  | sandy loam      | 44.000                             | 0.160     | 0.429     |                       |
| Whelan et al., 2013           | 7.98                                      | amended  | sandy loam      | 102.000                            | 0.161     | 0.460     |                       |
| euptfv2                       |   | control  |                 | 27.710                             | 0.051     | 0.421     | 0 + 1 + 0             |
| euptfv2                       |   | amended  |                 | 49.963                             | 0.069     | 0.581     |                       |
| SPAW                          |   | control  |                 | 80.832                             | 0.069     | 0.410     | 0 + 2 + 1             |
| SPAW                          |   | amended  |                 | 219.192                            | 0.127     | 0.619     |                       |
| Whelan et al., 2013           | 0.00                                      | control  | clay loam       | 8.000                              | 0.223     | 0.566     |                       |
| Whelan et al., 2013           | 6.37                                      | amended  | clay loam       | 122.000                            | 0.319     | 0.654     |                       |
| euptfv2                       |   | control  |                 | 80.292                             | 0.082     | 0.438     | 1 + 2 + 0             |
| euptfv2                       |   | amended  |                 | 99.186                             | 0.069     | 0.609     |                       |
| SPAW                          |   | control  |                 | 5.160                              | 0.204     | 0.429     | 0 + 1 + 0             |
| SPAW                          |   | amended  |                 | 26.496                             | 0.227     | 0.538     |                       |
| > +50%                        | very positive effect of SOC amendment     |          |                 | Sum of deviation steps SPAW: 23    |           |           |                       |
| +50% to +5%                   | positive effect of SOC amendment          |          |                 | Sum of deviation steps euptfv2: 20 |           |           |                       |
| +5% to 0%                     | slightly positive effect of SOC amendment |          |                 |                                    |           |           |                       |
| 0% to -5%                     | slightly negative effect of SOC amendment |          |                 |                                    |           |           |                       |
| -5% to -50%                   | negative effect of SOC amendment          |          |                 |                                    |           |           |                       |
| < -50%                        | very negative effect of SOC amendment     |          |                 |                                    |           |           |                       |

### Comparing PTFs by classifying their results

Seven experiments resulted from the literature review and were used as a basis of comparison. Results from the literature and from the PTFs were required to be qualitatively and semi-quantitatively in line. To be qualitatively in line meant that a change in model inputs (OC amendment) resulted in the qualitative same reaction of the output parameters as described in the paper from which the inputs were extracted. Semi-quantitatively meant, in this context, that the effect of increased SOC on output parameters was evaluated and color-coded for the paper results and the modeling results in order to compare the magnitude of the effects. Effect magnitudes were grouped into six classes as shown in Table 3.

**Table 3** Classification of effect magnitudes into effect classes.

| Effect magnitude | Effect class                              |
|------------------|---|
| > +50%           | very positive effect of SOC amendment     |
| +50% to +5%      | positive effect of SOC amendment          |
| +5% to 0%        | slightly positive effect of SOC amendment |
| 0% to -5%        | slightly negative effect of SOC amendment |
| -5% to -50%      | negative effect of SOC amendment          |
| < -50%           | very negative effect of SOC amendment     |

The qualitative evaluation method was thereby amended by a semi-quantitative element to form a more meaningful basis of comparison and validation. Due to very diverse experimental setups in literature and non-reproducible random effects from real world studies affecting the effect size of SOC, an evaluation based on a purely quantitative method was not applicable.

The accuracy of modeling results from the two PTFs was determined by comparing steps of color-coding. These steps were defined by the six effect classes shown in Table 3. The PTF showing overall fewer deviations from the original results in the literature scenario in terms of color-coding steps was defined as the more accurate one to proceed.

The semi-quantitative color-coding approach (see Table 2) was applied first to compare the two candidate PTFs SPAW and euptfv2, with euptfv2 found to be the most accurate. Due to the option of including quantiles in the output of euptfv2, an additional step of justification was added for this PTF: to ensure that euptfv2 actually yielded realistic results, its results from the scenarios were additionally required to be qualitatively in line with the majority of paper results. A threshold of at least 80 % accordance was stated to justify the PTF's use in the further course of this thesis. To confirm this level of accordance, it was verified whether the paper results for Ks, Qr and Qs were lying within the range between the 5<sup>th</sup> and the 95<sup>th</sup> quantile of euptfv2 outputs (see Table 4). Results from this step are described in chapter 4.1.2.

**Table 4** Results for Ks, Qr and Qs from the literature, as well as for the 5<sup>th</sup> (q = 0.05) and the 95<sup>th</sup> (q = 0.95) quantile modeled by euptfv2 based on inputs from the literature.

| Paper                         | SOC<br>[%] | Ks                 |                   |                    | Qr            |              |               | Qs            |              |               |
|-------------------------------|------------|--------------------|-------------------|--------------------|---------------|--------------|---------------|---------------|--------------|---------------|
|                               |            | [cm/day]<br>q=0.05 | [cm/day]<br>paper | [cm/day]<br>q=0.95 | [-]<br>q=0.05 | [-]<br>paper | [-]<br>q=0.95 | [-]<br>q=0.05 | [-]<br>paper | [-]<br>q=0.95 |
| Taheri Soudejani et al., 2020 | 1.03       | 0.66               | 95.90             | 531.13             | 0.00          | NA           | 0.14          | 0.34          | NA           | 0.52          |
| Taheri Soudejani et al., 2020 | 1.45       | 0.66               | 77.80             | 531.13             | 0.00          | NA           | 0.13          | 0.34          | NA           | 0.52          |
| Filipovic et al., 2020        | 0.54       | 0.17               | 6.81              | 2051.08            | 0.00          | 0.09         | 0.23          | 0.39          | 0.45         | 0.56          |
| Filipovic et al., 2020        | 1.40       | 0.41               | 6.94              | 2051.08            | 0.00          | 0.16         | 0.22          | 0.39          | 0.51         | 0.56          |
| Filipovic et al., 2020        | 6.11       | 0.17               | 6.94              | 5495.14            | 0.00          | 0.01         | 0.36          | 0.52          | 0.35         | 0.80          |
| Filipovic et al., 2020        | 7.06       | 0.17               | 7.07              | 5495.14            | 0.00          | 0.02         | 0.36          | 0.53          | 0.42         | 0.80          |
| Mbagwu et al., 1989           | 1.65       | 1.48               | 61.92             | 4048.48            | 0.00          | 0.06         | 0.16          | 0.22          | 0.11         | 0.58          |
| Mbagwu et al., 1989           | 2.63       | 1.48               | 168.48            | 10000.00           | 0.00          | 0.07         | 0.18          | 0.23          | 0.21         | 0.58          |
| Reynolds et al., 2015         | 0.23       | 0.17               | 1235.52           | 6993.51            | 0.00          | 0.37         | 0.27          | 0.37          | 0.49         | 0.55          |
| Reynolds et al., 2015         | 0.43       | 0.29               | 3248.64           | 6993.51            | 0.00          | 0.37         | 0.24          | 0.37          | 0.54         | 0.55          |
| Whelan et al., 2013           | 1.00       | 2.17               | 44.00             | 697.77             | 0.00          | 0.16         | 0.15          | 0.31          | 0.43         | 0.50          |
| Whelan et al., 2013           | 7.98       | 0.25               | 102.00            | 5495.14            | 0.00          | 0.16         | 0.36          | 0.37          | 0.46         | 0.80          |
| Whelan et al., 2013           | 0.00       | 0.52               | 8.00              | 6863.11            | 0.00          | 0.22         | 0.24          | 0.35          | 0.55         | 0.55          |
| Whelan et al., 2013           | 6.37       | 0.34               | 122.00            | 10000.00           | 0.00          | 0.32         | 0.36          | 0.46          | 0.65         | 0.80          |

### The combination with H1D

Next, the method of comparison with scenarios from the literature was applied to evaluate the combination of euptfv2 and H1D. This second step, however, did not need to be tested as thoroughly as the PTF alone due to the confirmed reliability of H1D in related studies (Caiqiong & Jun, 2016; Filipović et al., 2020; Ventrella et al., 2019). One out of the seven scenarios considered (Whelan et al., 2013) included SWB output parameters that could be compared to results from the entire modeling approach consisting of the chosen PTF (SHP results) plus H1D (SWB results). Information from this paper was used as an input in addition to the MVG parameters, while remaining details were left as default in H1D. As above, the effect magnitudes of OC application on paper results and modeling approach results were compared and checked for qualitative accordance.

#### 3.1.4 The pedotransfer function of choice (euptfv2)

The PTF resulting from the final selection process was the euptfv2 by Szabó et al. (2020). It complies with all criteria formulated above except the optional criterion of being developed in the tropics. In comparison to its predecessor, euptfv2 includes new features such as the disclosure of quantiles for each output parameter, 32 instead of five predictor variable combinations and a significantly higher accuracy (Szabó et al., 2020; Tóth et al., 2015). Further, a GUI is provided online which allows for very fast and simple handling (Szabó et al., 2019).

Euptfv2 is based on and trained with a large pan-European soil dataset named “European Hydropedological Data Inventory” (EU-HYDI). This dataset is representative for European soils and holds the most comprehensive geographical and thematic coverage of

hydro-pedological data in Europe (Tóth et al., 2015). This makes the euptfv2 reliable and applicable to a broad range of soils and input parameters at continental scale. In a review by van Looy et al. (2017), it was found to be one out of very few large scale PTFs worldwide, with a calibration database holding a very high number of soils samples (4,749), in comparison to other highly cited PTFs, such as Rosetta with 2,134 samples (Ottoni et al., 2018). According to the authors, already the first version euptfv1 was more accurate and more broadly applicable than any previous well-known PTFs such as Børgesen and Schaap (2005), Vereecken et al. (1989) or Weynants et al. (2009).

The PTF euptfv2 was therefore taken as a good option to complement H1D for thesis calculations. To test its reliability in the tropics, euptfv2 was used to make predictions for Ks, Qr and Qs based on the tropical soil database HYBRAS described in Ottoni et al. (2018). PTF results were subsequently compared to SHPs from the database and the overall deviations were found to be in the acceptable range (see Appendix 5 for a complete overview of deviations).

## 3.2 Application of the modeling approach

The modeling approach developed in chapter 3.1 was applied in a next step for automated data generation and modeling of the Rwanda carbon project. Figure 8 depicts the interplay of its components.

### 3.2.1 Data generation

The objective of data generation with the proposed modeling approach of euptfv2 plus H1D was to gain quantitative insights into the interrelation between predictors and the resulting SWB components. It is based on the method of virtual experiments, as described by Sarrazin et al. (2018). Such experiments are conducted in a virtual experimental setup with well-defined inputs and modeled outputs. Virtual experiments permit full control of experimental conditions which allows changes in model outputs unequivocally to be attributed to changes in model inputs (Sarrazin et al., 2018). For the use of data generation in this thesis, systematically modified input data was fed into the proposed modeling approach and the model outputs subsequently analyzed and evaluated in relation to respective inputs.

For two reasons, a focus was put on automating the process of data generation. First, as it was not previously clear what results could be expected, it was important to be able to replace certain elements, probe the data and have a closer look at interesting aspects. Second, as stated above, euptfv2 is not developed for tropical soils, but was, at the time of experimentation, the best alternative available.

An automated way of data generation keeps the process dynamic, and the PTF, as well as any other component or input, can easily be replaced whereby the approach can be used for further research and improvements later on.

## (SEMI-)VARIABLE MODEL INPUTS

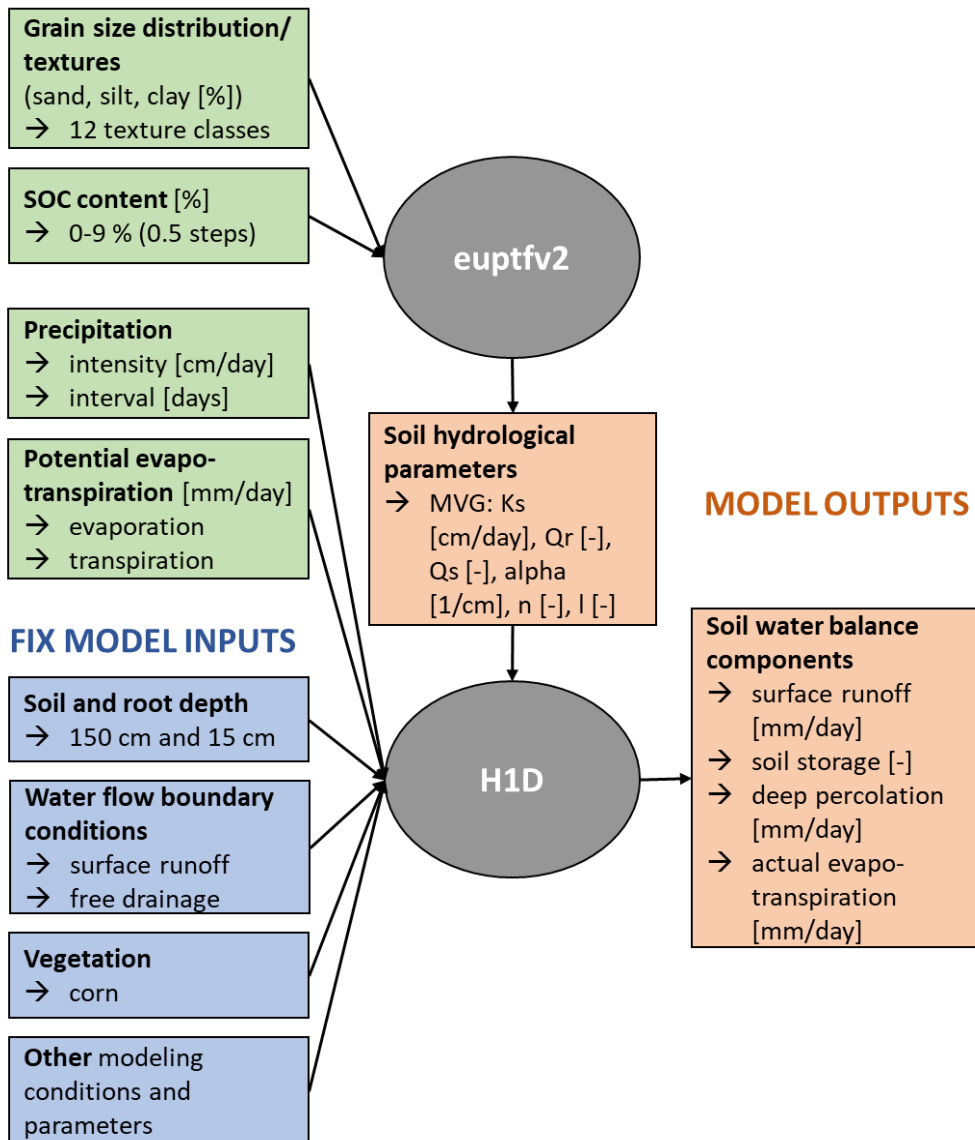


**Figure 8** Interplay of components forming the proposed modeling approach.

### Running euptfv2

As a first step, an euptfv2 input file was compiled containing all USDA texture classes, in combination with SOC percentages, from zero to nine in steps of 0.5 %. Sample IDs and a soil depth of 0.15 m were added to the file. Texture classes and SOC percentages are variable inputs to the modeling approach, since their values change for every model run.

Using the resulting document as an input, in a next step MVG parameters were calculated for all texture-SOC combinations with the help of the online GUI of euptfv2 (Szabó et al., 2019). The MVG parameter set that can be chosen as an output contained K0 instead of Ks, which, in comparison to Ks, does not account for macropores yet. However, K0 as part of the MVG parameter set was preferred before the point prediction of Ks. This was done



primarily because it proved to be more accurate during the literature scenarios testing phase. Furthermore, a coherent MVG parameter set was required as an input for H1D. The exclusion of macropores in K0 was in addition considered to be representative for plowed or worked agricultural soils. In the further course of the thesis, this MVG component will commonly be referred to as Ks.

The option of including quantiles in the euptfv2 outputs was not used for data generation since this would have proliferated into too broad ranges of insecurity. The results from data generation are thus based on mean values of euptfv2 MGV outputs.

### **Running H1D**

MVG output parameters were subsequently copied into an H1D input file, together with values for precipitation, potential evaporation and potential transpiration (H1D input 1). Four different versions of H1D input 1 were generated according to four different climatic conditions, as defined in Table 5.

H1D further requires for its execution a template folder containing specifically formatted input files (H1D input 2). This folder is automatically generated and modified when using the GUI. Its access and manipulation also needed to be included in automated model runs. As input information, it includes two “.dat” files, containing general information (fix inputs), and two “.in” files with atmospheric boundary conditions such as precipitation, potential evaporation and potential transpiration rates (“atmosph.in”) and information on the use of sub-models and modeling conditions (“selector.in”). These input files are different for each set of model runs and their inputs therefore called semi-variable. They were generated with the use of the H1D GUI and saved to the input template folder H1D input 2. The remaining files in the template folder are “.out” files that are populated with results as soon as the H1D software is run. In case the model does not converge, an additional error file is produced.

In order to generate data for statistical and analytical purposes, various sets of model runs were conducted. One model run consisted of fix and (semi-)variable inputs (see Figure 8 and Figure 10).

### **Fix H1D inputs**

Fix inputs and modeling choices remain consistent for every experiment as described in chapter 3.1.1. They are specified in the “.dat” files in H1D input 2. In addition to previously defined parameters, print times were defined to be eight times per day (every three hours) and length units were set to cm in order to be consistent with eutpfv2 outputs. Especially the latter must be kept in mind as it resulted in H1D outputs being displayed in cm instead of the more commonly used mm. Soil depth and vegetation cover were also included as fix model inputs in order to respect less degrees of freedom.

Root depth was assumed equal to the mean rooting depth of common crops, since that is the depth of interest for this thesis' considerations. According to Fan et al. (2016), 95 % of crop roots can be found within 100 cm depth. It is unlikely however that in a common carbon project soil carbon amendments will reach this depth. This is why only the upper 50 % of crop roots were considered, which leads to a root depth of 15 cm (Fan et al., 2016). Root concentration was kept constant over the whole root depth since steep negative gradients of root concentration were assumed to develop mostly below 15 cm. Soil depth was defined as 150 cm, a depth that permits to run H1D for almost all soils without causing issues of non-convergence. For the spatial resolution, it was divided into the default 101 observation nodes. An observation node was inserted at node five, which corresponds to a soil depth of 7.5 cm and thus half of the root zone (see Figure 9). Vegetation cover was set to be corn, which is a common crop in many carbon projects (VERRA, 2021a).

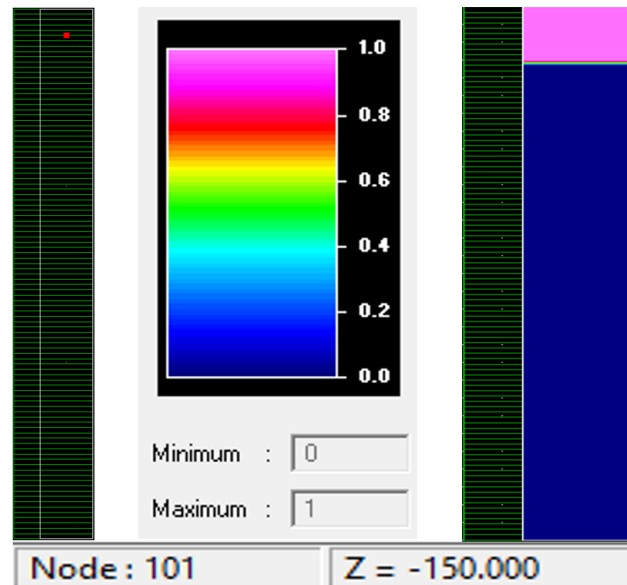


**Figure 9** Extract from the H1D GUI profile information window. A compilation of elements from the observation points and the root distribution tabs is shown to illustrate the point of observation (red point, left), the distribution of roots (right) and its legend (middle). The soil is modeled down to a depth of -150 cm and partitioned into 101 nodes (green subdivisions).

### Semi-variable H1D inputs

Atmospheric boundary conditions were defined as semi-variable inputs. They were kept constant over one set of model runs since climatic conditions do only change when either place (different project location) or time (time of the year or future effects of climate change) is varied.

For each set of model runs, precipitation was parametrized by a procedure that Sarrazin et al. (2018) proposed in the context of their method of virtual experiments. It consists of precipitation intensity [mm/day] and the interval between two wet days [days].

Both parameters can be calculated from readily available information on average monthly rainfall and average number of rainy days per month. Such synthetic precipitation time series can be used to analyze the impact of specific precipitation characteristics (certain spatial/ temporal distributions) such as rainfall frequency and intensity, storminess and seasonality (Sarrazin et al., 2018).

Four different types of precipitation regimes were parametrized based on climatic data from Rwanda. Means were built between the project districts of Bugesera (slightly dryer) and Rulindo (slightly wetter) based on data from Meteo Rwanda (2020) and the World Meteorological Organization (2021). The four resulting precipitation types were: the mean wet season during February, March and April, named “rain”; an event of extreme precipitation where the precipitation of a mean rainy day from the wet season gets concentrated into one hour, named “heavy rain”; the typical dry season lasting from June to August, named “drought”; and a precipitation type named “extreme drought”, where the mean amount of rain during the dry season is divided by ten to account for the 20 % chance of not having any rain at all during the entire dry period (see Table 5).

**Table 5** Parametrization of precipitation types with intensity and interval according to the method of Sarrazin et al. (2018), as well as respective evaporation and transpiration according to data from Martens et al. (2017).

| Type of precipitation | Intensity [mm/day] | Interval [days] | Evaporation [mm] | Transpiration [mm] |
|-----------------------|--------------------|-----------------|------------------|--------------------|
| rain                  | 8.0                | 1               | 0.7500           | 2.2500             |
| heavy rain            | 192.0              | 1               | 0.1075           | 0.3225             |
| drought               | 9.0                | 14              | 0.7500           | 2.2500             |
| extreme drought       | 0.9                | 14              | 1.1500           | 3.4500             |

Potential evaporation and potential transpiration were calculated according to local means (Martens et al., 2017). As data was only available for evapotranspiration,  $\frac{3}{4}$  of the value was attributed to transpiration and  $\frac{1}{4}$  to evaporation. Although exact partitioning varies according to factors such as vegetation cover and point in the vegetation period, transpiration water comes from the whole root depth of 15 cm whereas evaporation takes place roughly in the upper 5 cm (Sutanto et al., 2012; Wei et al., 2015). A 1:3 relation can therefore be assumed. For all precipitation types, means from the two project areas Bugesera and Rulindo were used since the difference in their respective means was negligible. For the drought and rain precipitation regimes, the mean of a PET time series was calculated. For heavy rain, very low PET values were assumed and thus the fifth percentile of the time series was used for further calculations. Extreme drought was parametrized with the 95<sup>th</sup> percentile to account for PET values above normal (Martens et al., 2017).

Rainfall, potential evaporation and potential transpiration were thus combined in a way to create two normal and two extreme meteorological conditions (see Table 5).

The length of a cycle of atmospheric boundary conditions was chosen to be 30 days long. This length was defined in order to account for different precipitation intervals (e.g. in 30 days, intervals of 2, 14, etc. days can be fitted to create precipitation patterns that are 3, 15, etc. days long).

This cycle of 30 days was repeated until a steady state was reached, which meant in this case, a repetition of five times to assure stationary behavior over the last 30 days of the 150 days simulation period (Herzog, 2018; Sarrazin et al., 2018). SWB data observed during this 30-day period of steady state were defined as simulation outputs. This allowed leaving initial conditions out of consideration.

### Automation of model runs

In a next step, variable and semi-variable H1D inputs were replaced by dummies in the template files in H1D input 2, which in turn permitted input information to be added for each model run.

To conduct a set of model runs, a Python script was developed that extracts for every sample ID inputs from H1D input 1 and writes them in the place of the respective dummies in the H1D input 2 files (see Appendix 8 for the complete code). The script further contains functions on how to run H1D using the given inputs and what outputs to extract from generated output files. Commands defined in the script are marked in orange in Figure 10. The H1D input 2 folder not only contains inputs but also output files that are modified during model execution. Output files required for subsequent data processing in R were also specified in the Python script.

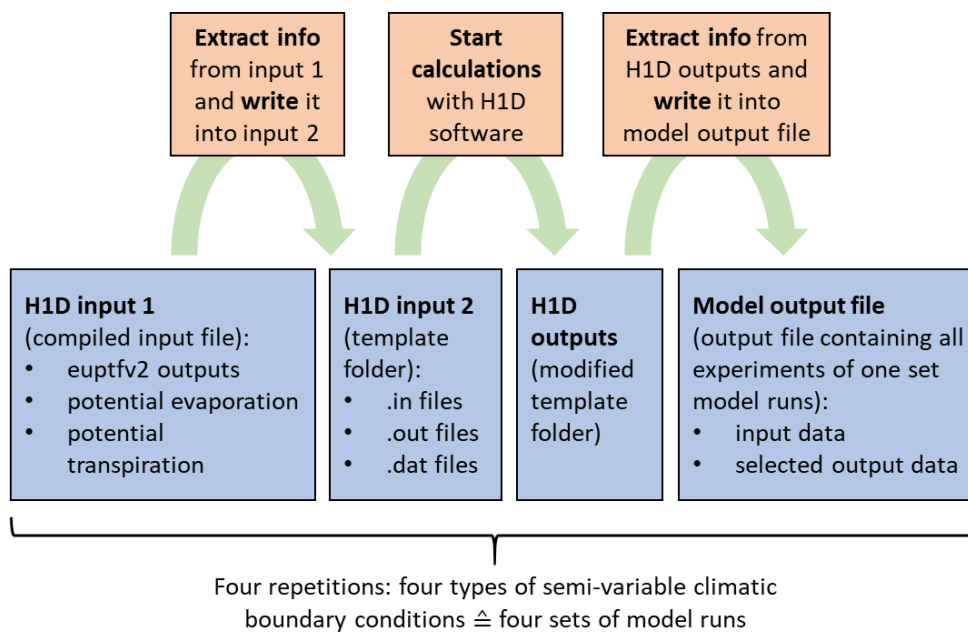


**Figure 10** Set of model runs with in- and outputs of H1D (blue), as well as the processing steps automated with a Python script (orange).

Within the steady state observation period of 30 days, the behavior of SWB components was analyzed. In H1D, the output file “obs\_node.out” contains actual water contents (“theta”), in a specific depth, over time. As defined above, this depth was of -7.5 cm. The mean value of the water content at this depth over the observation period was of interest, as well as its minima and maxima. Further, the output file “T\_level.out” was considered, which contains time dependent information on runoff (“RunOff”), actual surface flux (“vTop”, evaporation/infiltration  $\triangleq$  +/-), actual transpiration rate (“vRoot”) and actual bottom flux (“vBot”, here taken as a proxy for deep percolation). For these outputs, means, minima and maxima over the stationary state observation period were extracted.

### **Extraction and processing of outputs**

The output values from the last 30 days of simulation were thus extracted from the respective H1D output files, means, minima and maxima calculated and written into experiment output files (one file per set of model runs). An output file contained one experiment per line with information on inputs and respective modeling approach outputs (SHPs and SWB parameters).

Since it was not possible within the scope of this thesis to analyze the SWB specificities for every single USDA soil type, six out of 12 soils were extracted for analysis. The choice was based on the following criteria: Presence of the texture under tropical climates and more specifically in the regions of interest in Rwanda; model convergence for the soil type; and representation of broad spans of the SHPs Ks, Qr and Qs.

The soils resulting from this consideration were sandy clay, clay, clay loam, loam, loamy sand and sandy clay loam. See Figure 2 for the respective contents in clay, silt and sand.

In a next step, every experiment output file was imported to R (Version 1.3.959) to create plots and conduct statistical analyses. In order to analyze the correlation between SOC contents and soil hydrology, various correlation coefficients were available. Pearsons correlation coefficient (parametric correlation test) is most known, however it assumes linearity and homoscedasticity, which were not present in the data of this thesis (Dormann, 2017). Since only monotonic relationships could be observed in most plots, a non-parametric correlation coefficient was required. Kendall’s tau was chosen (instead of Spearman’s rho) due to its suitability for small samples (Dormann, 2017).

### **3.2.2 Modeling the Rwanda carbon project**

For the Rwanda carbon project, soil data was partly available from project records and partly extracted from the Food and Agriculture Organization’s harmonized world soil database (HWSD, Nachtergaele et al., 2008).

The HWSD contains a worldwide soil map with information on topsoil (0-30 cm) and subsoil (30-100 cm) properties.

In order to obtain topsoil textures for the project areas in Rwanda project area shape-files, as well as the HWSD soil map, were imported to the geographical information system QGIS (version 3.16). The HWSD raster was subsequently clipped to the shapes of the project areas and information on soil textures and their distribution extracted from the result.

Topsoil SOC contents were also taken from HWSD for the baseline and were calculated for projected developments after the 20-year project period. Project carbon calculations were based on results from a large carbon project in Kenya. Conservative calculations for OC inputs without the additional influence of trees yielded an increase per year of 1.6 t CO<sub>2</sub>/ha in the Kenyan project (VERRA, 2021d). With the help of the atomic weight of CO<sub>2</sub>, this value was converted to a yearly increase of 0.44 t SOC/ha. It was further transformed to a percentage of SOC, using the following formula by the Government of Western Australia - Department of Primary Industries and Regional Development (2021):

$$stock\ SOC = \frac{\% SOC}{100} \cdot BD \cdot 3000 \cdot \left(1 - \frac{gravel\ content}{100}\right) \quad (4)$$

$\leftrightarrow$

$$\% SOC = \frac{100 \cdot stock\ SOC}{BD \cdot 3000 \cdot \left(1 - \frac{gravel\ content}{100}\right)} \quad (5)$$

In the equation SOC is the amount of SOC per ha and the gravel content is the percentage of gravel in the topsoil, as extracted from HWSD. Subsequently, the increase per year in % SOC was multiplied by 20 for a 20-year project period and added to the percentages of SOC as indicated in the HWSD (for a complete overview see Appendix 6).

Extracted soil texture information together with calculated SOC contents and the above-described procedure of data generation through virtual experiments permitted result generation for the Rwanda carbon project's soil hydrology under conditions of drought, rain, extreme drought and heavy rain.

## 4 Results

This chapter describes the results obtained from applying the above-described methodology. The first part addresses the RQ of how the effect of SOC on the SWB can be predicted with a physically-based soil hydrology model. The structure of the proposed modeling approach resulting from the development step is depicted in Figure 8 in chapter 3.2.

The second part of this chapter provides information on the question of whether intentionally enhanced SOC in carbon projects is beneficial to the SWB. To answer the sub-question on the controlling factors within this relation, various aspects of the presented results needed to be compiled and set in relation to existing knowledge. This is presented in the discussion (chapter 5.2).

### 4.1 Evaluation of the modeling approach

This first part of the results chapter describes the steps that were undertaken to develop, test and justify the modeling approach. It refers to the preselection of PTFs, the final selection and testing of euptfv2, as well as to the evaluation of H1D and its interplay with euptfv2.

#### 4.1.1 Preselection of pedotransfer functions

Over the course of the literature review a great variety of PTFs were considered (see Appendix 7). However, applying the obligatory criteria as defined in Table 1 reduced the range of PTFs massively. Many PTFs were exempted from further consideration due to their development before the year 2000 (e.g. Wösten et al., 1999 and Rawls et al., 1982). The criterion of SOC or OM as an input further excluded many popular PTFs such as Rosetta (Schaap et al., 2001) or the tropical PTF by Ottoni et al. (2019). Additionally, the criterion of a broad applicability due to large geographical areas and overarching datasets led to the exclusion of further two PTFs: the tropical PTFs by Oliveira et al. (2002) since it was calibrated only in few Brazilian regions; and the one by Hodnett and Tomasella (2002) due to its small soil dataset. Applying this criterion of geographical generalizability highlighted the inevitable decision between broadly applicable, highly cited PTFs and PTFs that were designed specifically for tropical soils.

After applying these three obligatory criteria, two PTFs remained: euptfv2 by Szabó et al. (2020) and SPAW by Saxton et al. (2005) described in Singh and Frevert (2006).

Concerning the optional criteria, both PTFs had a published GUI and neither of them were developed specifically for the tropics. They differed however in their provision of error margins, which can be included in the results of euptfv2 which is not the case for SPAW. Euptfv2 additionally provides a GUI that makes it easy to process multiple samples simultaneously due to the possibility of uploading an input CSV-file that is automatically populated with results.

#### 4.1.2 Scenarios for testing and justifying pedotransfer functions

To choose the better performing PTF, the two preselected ones were compared to each other with the help of scenarios from the literature. For seven experiments from the literature, control and amended scenarios were extracted. The changes between both scenarios in terms of soil hydrology were subsequently compared with changes in respective modeling results. From the experiments, differences in SOC content between control and amended scenario ranged between 0.42 and 6.98 mass % (from here on referred to only as %). Soil textures considered were loamy sand, silty clay loam, silty clay, sandy clay loam, clay loam and sandy loam. Very few studies on tropical soils could be identified and only one among them (Mbagwu, 1989) contained the information required to be included in the scenarios.

The color-coding method yielded satisfactory results for both PTFs, as only three (euptfv2) and one (SPAW) PTF results pointed to the opposite impact direction when compared to the original (e.g. positive impact of SOC in the paper and negative in the PTF results). For euptfv2, sixteen out of 19 results (84.2 %) pointed in the correct direction while for SPAW, 18 out of 19 results (94.7 %) had the correct direction. Although SPAW thus seemed to be the more accurate PTF, when counting the color-coded steps of deviation from the original impact size, euptfv2 turned out to be the overall better performing PTF with 20 steps of deviation against 23 steps for SPAW (see Table 2).

Furthermore, considering how the two PTFs generally react to increases in SOC content, it could be observed that SPAW yields ever-increasing values for  $K_s$ ,  $Q_r$  and  $Q_s$  for any given soil. Such simple relationships were not reflected in the literature. As this thesis aims for conservative and solid instead of overly optimistic results, these findings were a further argument against SPAW and favored the use of the more differentiated euptfv2. The results from the literature scenarios color-coding method were further supported by general observations and resulted in the PTF choice falling on euptfv2.

In a next step, absolute paper results were compared to the 5<sup>th</sup> and 95<sup>th</sup> euptfv2 simulation quantiles to verify whether the simulated range between these quantiles comprises the paper results (see Table 4). For  $K_s$ , this was the case for all 14 simulations.  $Q_r$  was underestimated by euptfv2 in three out of 12 values (paper values marked in red) while for  $Q_s$ , a tendency could be observed towards overestimation for four out of 12 results (marked in blue).

Overall, this leads to results outside the quantile range in seven out of 38 predictions, which makes a share of correct results of 81.6 %. This is slightly above the threshold of 80 % as defined in chapter 3.1.3.

Considering these two steps, of color-coding and paper results comparison to predicted quantiles, the reliability of euptfv2 for predicting results of the impact of SOC on  $K_s$ ,  $Q_r$  and  $Q_s$  could be confirmed.



### 4.1.3 Evaluating the use of Hydrus-1D

In order to evaluate the use of the combination of H1D with euptfv2, the same literature scenarios method was applied. It must however be noted that barely any studies containing H1D outputs together with required inputs exist. Most studies focus on MVG outputs and do not process these outputs further to calculate the resulting SWB components. As stated above, this issue could be compensated by the fact that H1D is a well-known model that had already previously been proven to be adequate for the purposes of this thesis.

The interaction between euptfv2 and H1D remained to be tested. This was done with the help of the comparison of a literature scenario extracted from Whelan et al. (2013). The scenarios “Clay loam” and “Field samples 750 t/ha” were used as their results on H1D outputs were available. As stated in the paper, meteorological information was taken from a station near Cranfield University farm and used as H1D input (Met Office, 2021). PTF inputs were taken as calculated by euptfv2 based on inputs from the literature and remaining H1D inputs and parameters set as described in chapter 3.1.1.

Modeled results for all H1D outputs were qualitatively in line with paper results and the functioning of the interplay between euptfv2 and H1D could thus be confirmed. Water stored in the soil increased at higher levels of SOC contents, as well as water infiltrating the soil. This led to a reduction in runoff. The latter however could not be simulated with H1D at the precipitation levels found for Cranfield University farm (5 mm/ 3 days) (Met Office, 2021). Due to euptfv2 Ks output values of 80 and 99 cm/day for the given combination of PSD and SOC, modeled surface runoff occurred only at much higher precipitation levels of roughly 1000 mm/day. In the paper, it remains unclear how surface runoff could come about for both scenarios under such a low precipitation regime together with measured Ks values of eight and 122 cm/day.

## 4.2 Application of the modeling approach

This second part of the results chapter describes the data generated by the application of the proposed modeling approach. As explained in chapter 3.2.1, only a subset of soil textures could be considered and the expression “all soils” thus refers to this studied subset. For simulated results, correlation significance was tested with the non-parametric Kendall rank correlation coefficient. All p-values therefore stem from this test and r-values indicate the results for Kendall’s tau (Dormann, 2017). Since the main interest lies in the relation between results, less attention is paid to absolute values, which can be taken from the graphs provided.

Chapters 4.2.1 to 4.2.3 present the results obtained from data generation (chapter 3.2.1), while chapter 4.2.4 expands more on the findings from Rwanda and thereby relates to the methodological chapter 3.2.2.

#### 4.2.1 Water retention

In order to describe the behavior of water retention with increasing SOC contents, mean values of the actual water content ( $\theta$ , its averages over the 30-day output period, as described in chapter 3.2.1) were analyzed for the four precipitation types. Euptfv2 outputs for  $Q_s$  and  $Q_r$  were also taken into consideration for this chapter due to their crucial function for  $\theta$ .

For all soils,  $Q_s$  was found to increase significantly ( $p < 0.001$ ) with increasing SOC content.  $Q_r$  was much less affected, with most soils showing no significant in- or decrease; a minor significant increase for loamy sand and a minor significant decrease for sandy clay could be observed.

The difference between  $Q_r$  and  $Q_s$  indicates the amount of water available to plants and was thus of special interest. Significantly increasing plant available water contents ( $p < 0.001$ ,  $r = 0.883$  to  $0.946$ ) were found for all soils from the difference of  $Q_s$  minus  $Q_r$  as can be seen in Figure 11. Especially steep increases were observed between 0 and 5.5 % SOC, while with a SOC above 5 % the curves flattened for all soils.

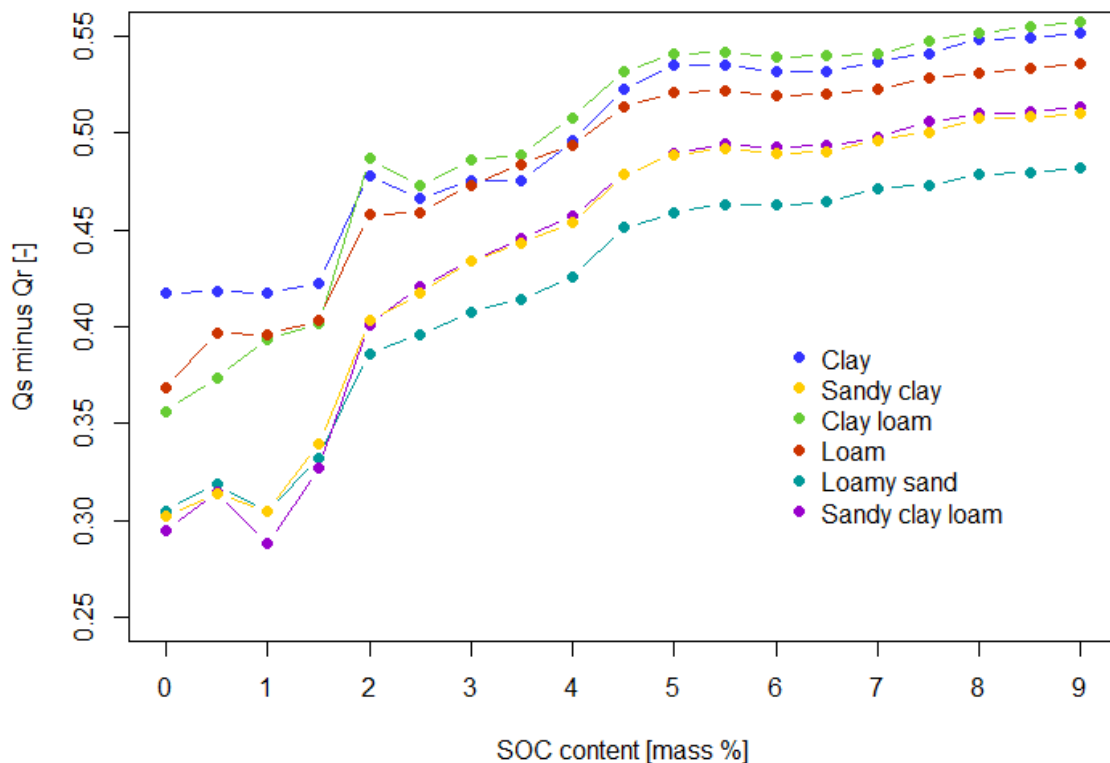


**Figure 11** Difference of  $Q_s$  and  $Q_r$  as influenced by the SOC content. Water between  $Q_s$  and  $Q_r$  is plant available and therefore of particular interest for this thesis. Significant increases for all soils:  $p < 0.001$ ,  $r = 0.883$  to  $0.946$ .

Theta, lying between  $Q_r$  and  $Q_s$ , was found to increase significantly ( $p < 0.001$ ,  $r = 0.871$  to  $0.953$ ) with SOC for all soils under wet conditions (precipitation types “rain” and “heavy rain”). Figure 12 illustrates the increase of theta with SOC content, for all soils, under a mean rain season precipitation regime. This behavior was less pronounced the more theta approached  $Q_r$  (due to dryer conditions) and ceased to be significant for all soils except for loam under extreme drought.

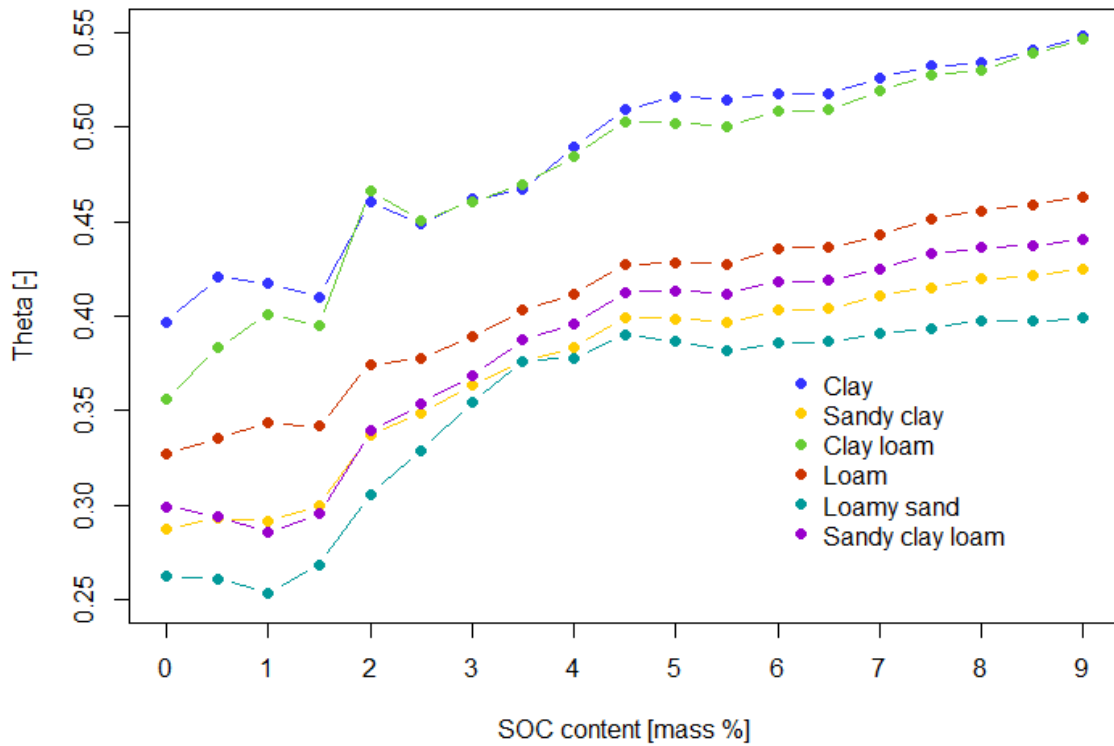


**Figure 12** Theta under rain conditions as influenced by SOC. Significant increases for all soils:  $p < 0.001$ ,  $r = 0.871$  to  $0.953$ .

Figure 13 shows the example of theta in sandy clay under rain conditions together with its limits of  $Q_s$  and  $Q_r$ . It can be seen that under rain conditions theta increased together with  $Q_s$  while  $Q_r$  remained relatively unaffected by additional SOC.  $Q_r$  and the increase of theta can be seen as exemplary for all considered soils under rain conditions with deviating absolute values.

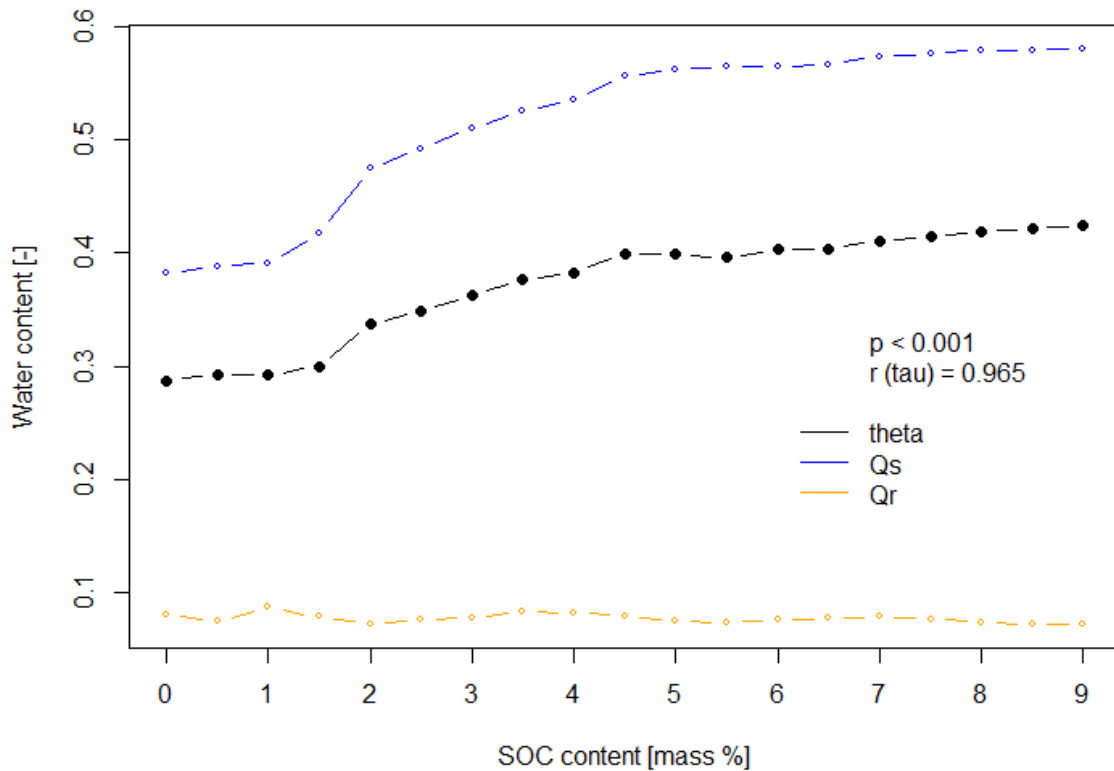


**Figure 13** Theta, Qs and Qr in sandy clay under rain conditions. R and p values for theta are indicated in the graph.

In order to understand how theta behaves under very wet and very dry conditions, and with what implications, theta values under extreme drought were compared to Qr and theta under heavy rain to Qs.

It resulted that under extreme drought, the difference between theta and Qr decreased to below 0.17. It differed largely between soil types, with clay and clay loam holding most plant available water, as can be seen in Figure 14. The difference between Qr and theta still increased significantly ( $p < 0.05$ ,  $r = 0.590$  to  $0.906$ ) with SOC for all soils which shows that, on average, more water was still available to plants under extreme drought conditions when more SOC was contained in soils.

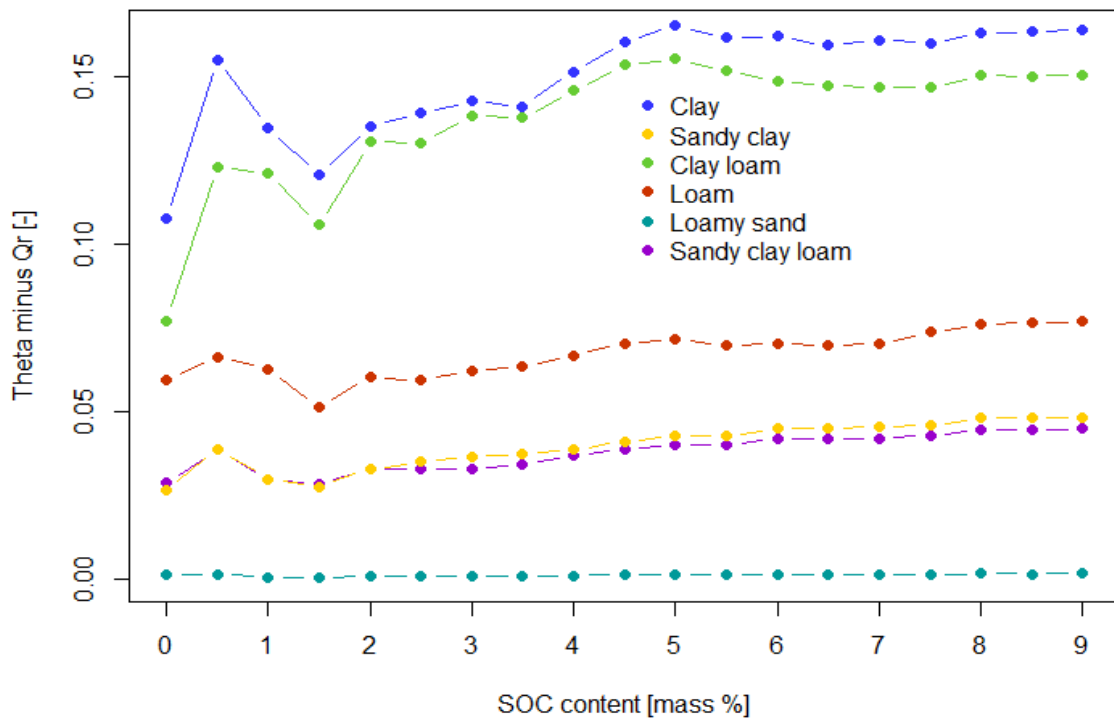


**Figure 14** Difference of theta and Qr as influenced by SOC content under conditions of extreme drought. Significant increases for all soils:  $p < 0.05$ ,  $r = 0.590$  to  $0.906$ .

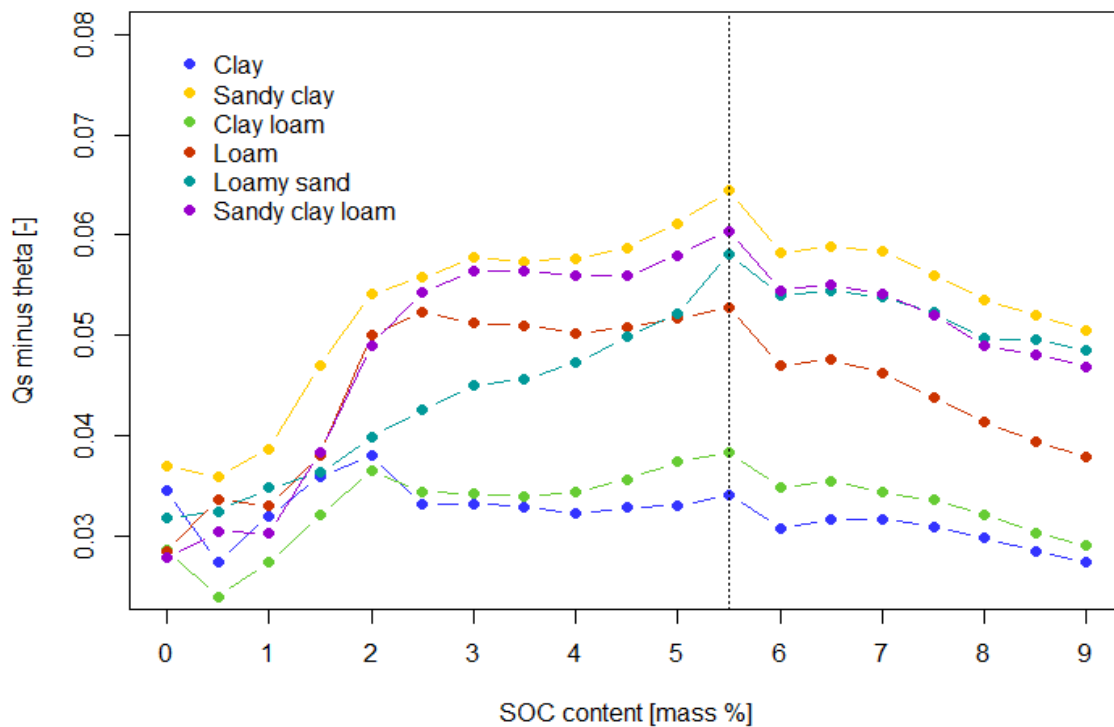


**Figure 15** Difference of Qs and theta as influenced by SOC content under conditions of heavy rain. The reaction to increasing SOC contents can be distinguished between the SOC percentages below and above 5.5 % (dashed line). Significant increases below 5.5 % SOC for all soils except for clay:  $p < 0.05$ ,  $r = 0.556$  to 1.

Figure 15 shows the difference between  $Q_s$  and  $\theta$  under conditions of heavy rain. Results were not significant when the whole range of SOC contents was considered since the difference first increased up to a maximum under SOC equal to 5.5 % and dropped beyond that threshold. Interestingly, increases were found to be significant with  $p < 0.05$  ( $r = 0.556$  to  $1$ ), for all soils except for clay, when only the range from zero to 5.5 % SOC was considered. This means that up to this point, an increase in SOC led to a greater share of soil pores still being unsaturated under heavy rain.

Generally, when analyzing the behavior of water contents under wet conditions, with increasing SOC contents, three main sections could be recognized in the graphs. They could be distinguished in all soils, however, with different degrees of expression: First, a steep increase of water contents could be observed under SOC values of up to 2 %. This was followed by slightly flattened increases up to 4.5-5.5 % SOC. Beyond this point, further flattening followed or a decrease of water contents could be observed as in Figure 15.

#### 4.2.2 Saturated hydraulic conductivity and runoff

It was observed that the occurrence of runoff was mainly determined by the amount of precipitation and the size of  $K_s$ : when saturation is reached, infiltration rates are limited by  $K_s$  and excess rainfall runs off superficially, potentially causing erosion.

Euptfv2 results for  $K_s$  did overall not show clear patterns, as can be seen in Figure 16. Highest values of up to 200 cm/day were found for soils with high percentages in clay and low percentages in sand. Lowest  $K_s$  values were found for loamy sand, which contains the highest share of sand among the soils under consideration (see Figure 2). Soil textures reacted very differently up to a SOC content of 5.5 %. Beyond that point,  $K_s$  decreased first sharply and above 6.5 % steadily for all soil textures.

For all soils, it was found that no (0 %) and very high (above 5.5 %) SOC contents were generally suboptimal for  $K_s$  (see Figure 16). A tendency for higher sand contents requiring higher rates of OC to reach an optimum could be observed.

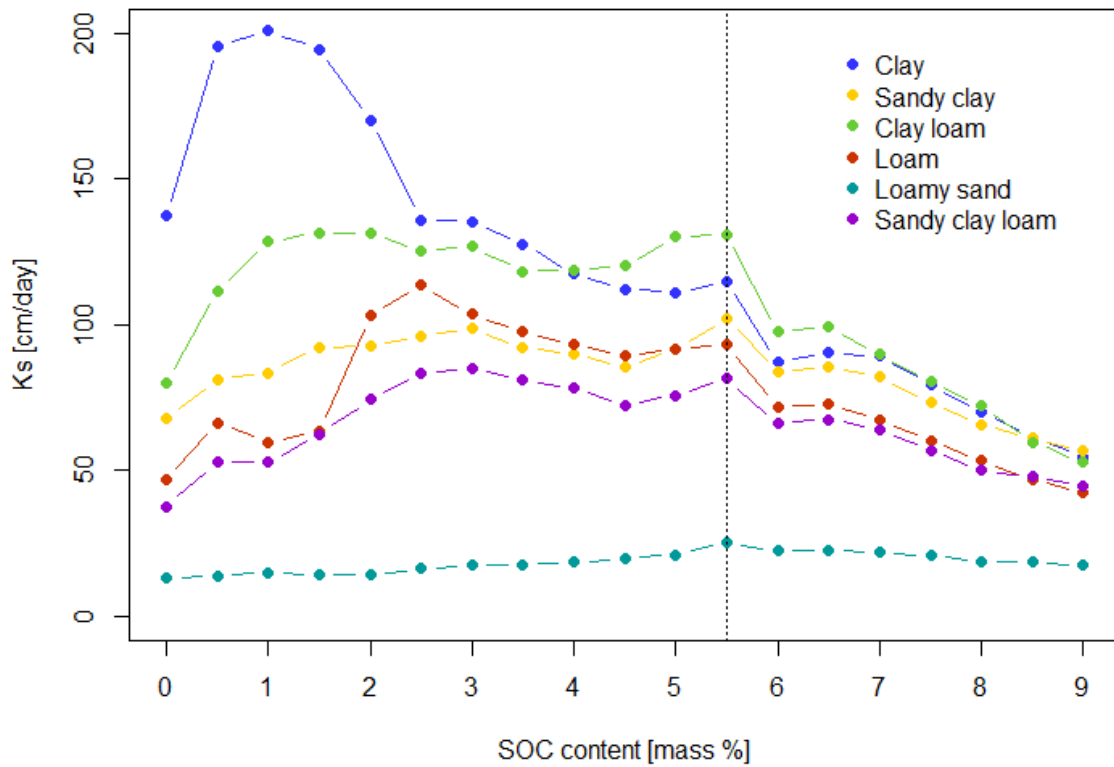


**Figure 16** Ks of analyzed soils and its dependence on SOC content. A steep decrease can be observed above 5.5 % SOC (dashed line) for all soils.

From Figure 16 it can further be deduced that under the precipitation regime defined as heavy rain, with intensities of 192 mm/day, no surface runoff could potentially occur for any soils except for loamy sand. As all other data points for Ks ranged above that threshold, infiltration was never limited by Ks and thus all simulated rainwater could infiltrate into the soil.

For loamy sand however, precipitation exceeded Ks and caused surface runoff. Runoff peaks reached intensities of up to 60 mm/day in soils without OC. Figure 17 illustrates the opposite behavior of runoff and Ks, with high runoff at low Ks values and vice versa. It can be seen that, for loamy sand, Ks increased with the SOC content up to an optimum under SOC equal to 5.5 %. Runoff dropped down to zero in the course of that increase and only slightly increased again on going beyond a SOC content of 7.7 %.

This behavior also translated to altered bottom flow, where mean values varied only marginally with SOC for all soils except for loamy sand. For loamy sand, an important share was found to flow off superficially for certain SOC contents. This water leaving the system superficially could be observed in decreased rates of bottom flow, thereby decreasing the potential groundwater recharge.

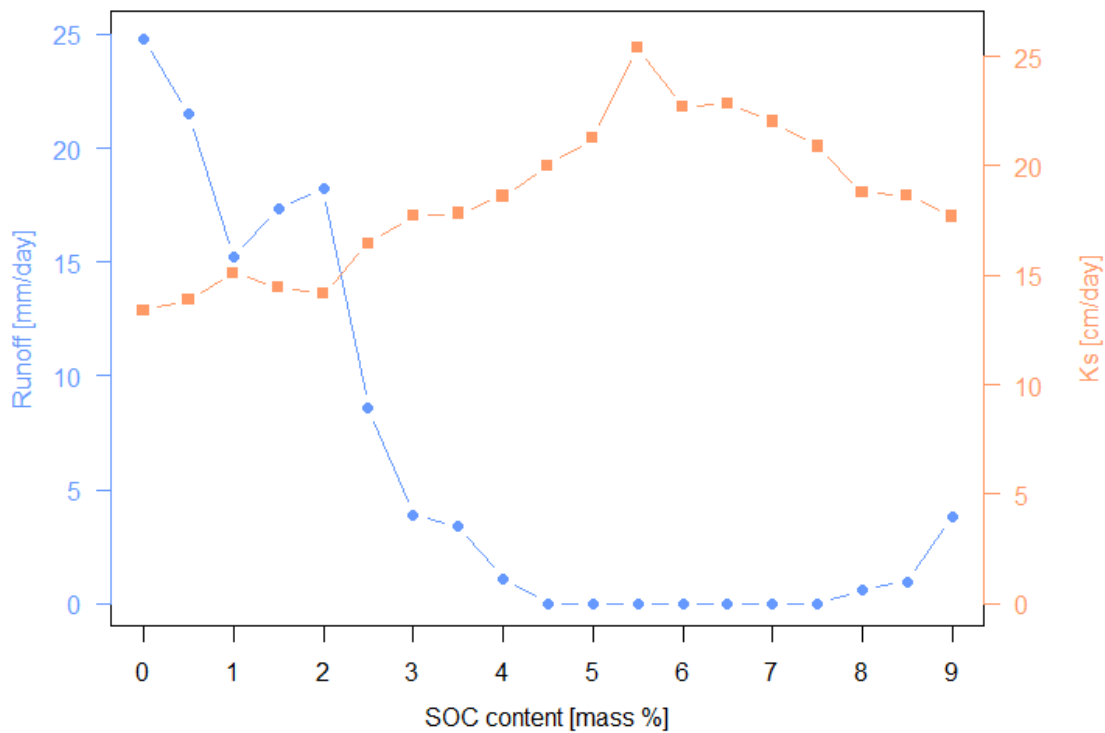


**Figure 17** Runoff and Ks in loamy sand as influenced by SOC content under conditions of heavy rain. The opposite behavior of runoff and Ks can be observed.

For Ks and the resulting runoff behavior it could be concluded that enhanced SOC contents had the capacity to increase Ks and thereby avoid potentially occurring surface runoff. The optimal amount of SOC was, however, found to be strongly dependent on soil texture.

#### 4.2.3 Actual transpiration

Actual transpiration (hereafter only referred to as transpiration) was found to be dependent on soil texture, and in its reaction to increased SOC contents depended on the type of modeled precipitation regime. As can be seen in Figure 18, under heavy rain, transpiration had a tendency to decrease at higher SOC contents for most soils. For all soils, except for loamy sand and sandy clay, this effect was found to be significant with  $p < 0.05$  ( $r = -0.509$  to  $-0.918$ ).

For extreme drought conditions however, modeling results showed opposite tendencies with transpiration rates increasing at higher SOC contents, as Figure 19 suggests. For all soils, except for loam and clay loam, transpiration increases with SOC were found to be significant with  $p < 0.05$  ( $r = 0.556$  to  $0.895$ ).



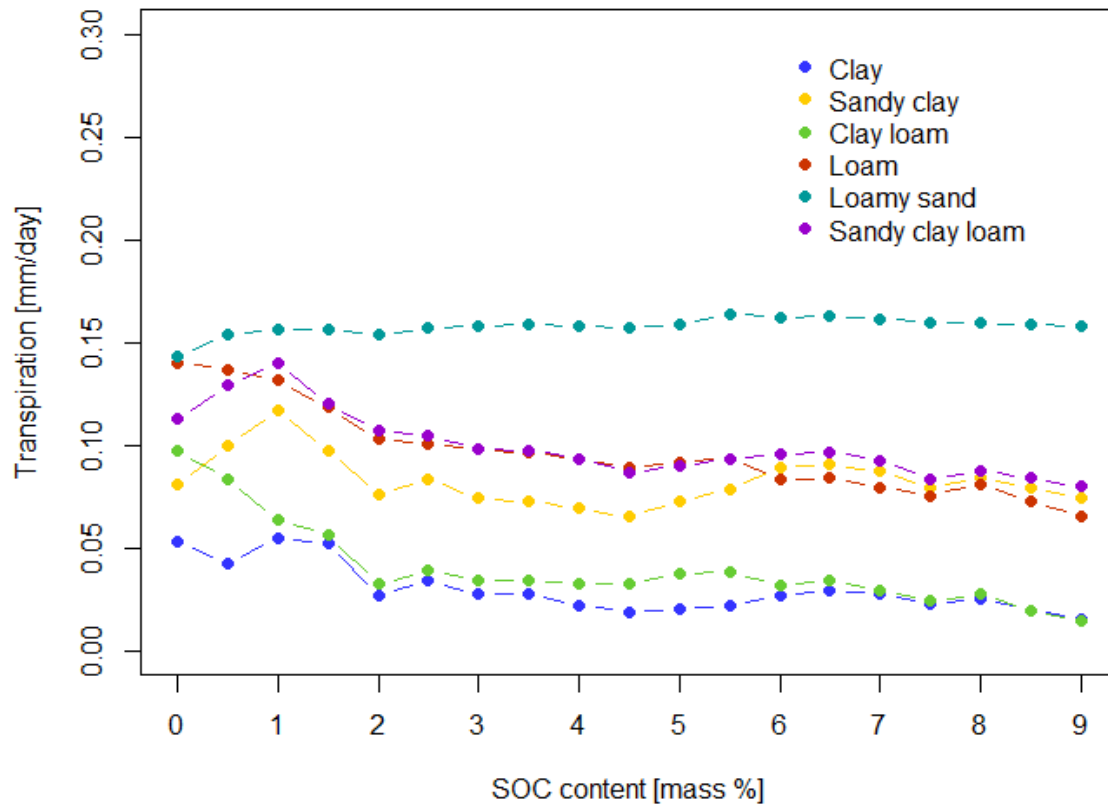


**Figure 18** Actual plant transpiration as influenced by SOC content under heavy rain. Significant decreases for soils except for loamy sand and sandy clay:  $p < 0.05$ ,  $r = -0.509$  to  $-0.918$ .

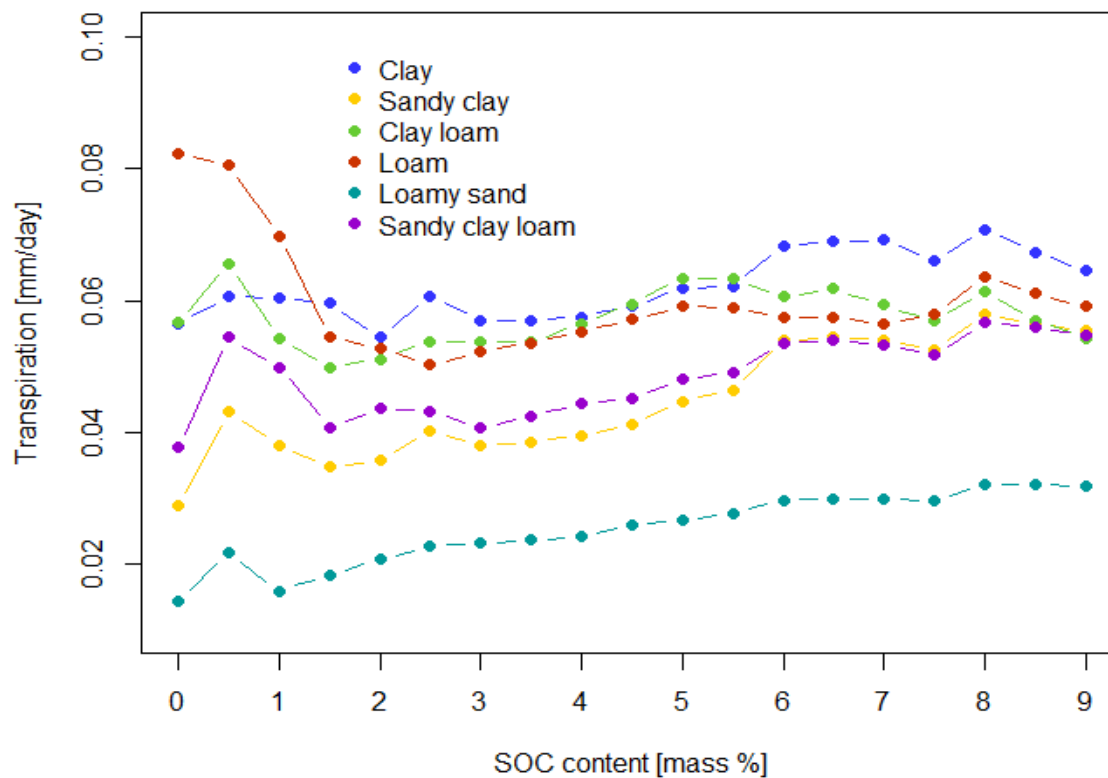


**Figure 19** Actual plant transpiration as influenced by SOC content under extreme drought. Significant increase for soil except for loam and clay loam:  $p < 0.05$ ,  $r = 0.556$  to  $0.895$ .

#### 4.2.4 The Rwanda carbon project

The increase in SOC over the projected 20-year project period of the Rwanda carbon project was found to be 0.87 % for clay, and ranging between 0.21 and 0.26 % for the other soils. A table presenting all SOC percentages for the baseline (in percentages and t per year and ha), the annual increments and the SOC contents after 20 years can be found in Appendix 6. These project-induced changes in SOC translated into soil hydrology characteristics as shown in Table 6. Ks was considered as a proxy for potentially occurring runoff since actual runoff was not present in the Rwanda results under the modeled precipitation regimes. The distribution of soils in the project area is shown in Figure 20 and can be assigned to the soil hydrology results by the colors used.

Overall, it resulted that due to the absolute increases in SOC ranging (far) below 1 %, effects on soil hydrology were in most cases positive (as can be seen in Table 6), but not large.

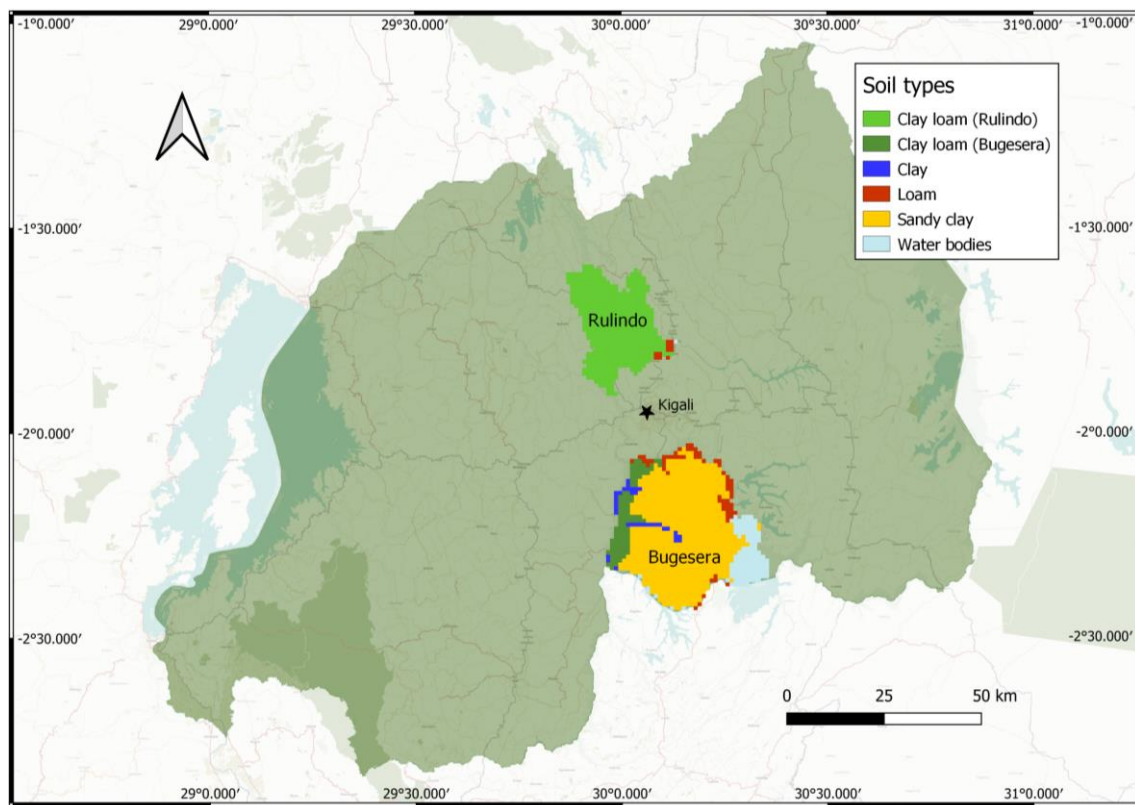


**Figure 20** Map of Rwanda showing all soil types present in the project areas Rulindo and Bugesera. Colors are the same as in Table 6 to relate table contents to the respective areas.

**Table 6** Soil types in the project regions and their soil hydrology before and after the 20-year project period.

| Soil type              | OC<br>[mass %] | Ks<br>[cm/day] | Theta<br>ED [-] | Theta<br>D [-] | Theta<br>R [-] | Theta<br>HR [-] | Transpiration<br>ED [mm/day] | Transpiration<br>HR [mm/day] |
|------------------------|----------------|----------------|-----------------|----------------|----------------|-----------------|------------------------------|------------------------------|
| sandy clay A           | 0.74           | 82.737         | 0.115           | 0.129          | 0.284          | 0.341           | 0.0426                       | 0.1174                       |
| sandy clay B           | 0.98           | 83.661         | 0.115           | 0.129          | 0.287          | 0.347           | 0.0388                       | 0.1198                       |
| clay loam (Bugesera) A | 3.88           | 117.952        | 0.207           | 0.208          | 0.469          | 0.524           | 0.0541                       | 0.0346                       |
| clay loam (Bugesera) B | 4.14           | 122.524        | 0.213           | 0.214          | 0.483          | 0.541           | 0.0581                       | 0.0357                       |
| clay A                 | 27.15          | 21.486         | 0.223           | 0.223          | 0.578          | NA              | 0.0480                       | NA                           |
| clay B                 | 28.02          | 21.486         | 0.223           | 0.223          | 0.578          | NA              | 0.0480                       | NA                           |
| loam A                 | 5.2            | 93.240         | 0.125           | 0.125          | 0.427          | 0.522           | 0.0588                       | 0.0940                       |
| loam B                 | 5.44           | 94.226         | 0.124           | 0.124          | 0.427          | 0.523           | 0.0592                       | 0.0943                       |
| clay loam (Rulindo) A  | 3.21           | 124.299        | 0.206           | 0.207          | 0.467          | 0.523           | 0.0551                       | 0.0363                       |
| clay loam (Rulindo) B  | 3.42           | 119.130        | 0.207           | 0.208          | 0.469          | 0.524           | 0.0539                       | 0.0343                       |

increasing  
decreasing  
indifferent

ED = extreme drought

D = drought

R = rain

HR = heavy rain

A = baseline

B = after 20 years

## 5 Discussion

### 5.1 Extent of model applicability and reliability

This sub-chapter discusses the extent to which the modeling approach, its components and related modeling assumptions yielded reliable results. It analyzes limitations and sources of uncertainty of the approach to classify results. In a first subsection, the general functionality and assumptions of the proposed modeling approach are discussed. In a second subsection, the PTF of choice, euptfv2, is reviewed with respect to its limitations and application uncertainties pertaining to tropical soils.

#### 5.1.1 The modeling approach: functionality and assumptions

As a main observation, it can be stated that the proposed modeling approach was functional. It was for most calculations possible to substitute the H1D internal PTF Rosetta with euptfv2 and thereby include SOC as a predictor. Since Rosetta is based on a smaller and older number of soil samples than euptfv2, the substitution could possibly even have improved the prediction accuracy of final SWB results.

#### **Issues of non-convergence**

However, while applying the proposed modeling approach, serious issues of model convergence occurred in H1D. The occurrence of these issues was mainly determined by the soil type, in combination with certain precipitation regimes: heavy rain was an issue for silty soils and drought for sand. It must therefore be assumed that the combination of parameter inputs from euptfv2 is possibly not fully appropriate for further processing in H1D. Better functionality with H1D internal Rosetta-parametrized soils speaks in favor of this assumption; nonetheless, some cases of non-convergence also occurred with these soils. The convergence issue can therefore not fully be attributed to euptfv2 outputs. The extent to which the combination of euptfv2 and H1D is indeed the reason for the numerical instability remained unclear and needs further investigation in future studies.

For the purpose of data generation in this thesis, the number of convergence issues could substantially be reduced by adapting the minimum time step in the H1D time discretization. When the minimum time step was too large ( $dt_{\min} \geq 10^{-3}$ ), calculations did in some cases not converge for steep gradients in atmospheric boundary conditions. In case where it was too small ( $dt_{\min} < 10^{-4}$ ), the system did not converge either. The latter is presumably due to very small time steps, that in some cases, forced the system to deal with numbers that are smaller than the computer error. This leads to random results and thereby also to non-convergence. With  $dt_{\min} = 10^{-4}$  the convergence problems under the heavy rain precipitation type could be reduced to occur only in silty soils. As silty soils are barely found in the

tropics and subtropics, the exclusion of silty soils from the analysis was not an issue to this thesis' data output generation. It is however worth noting that for heavy rain on silty soils, no results could be generated for most SOC contents. The same applies to many SOC contents in sand under drought conditions.

In chapter 3.2.1 the reasons for automated model runs were briefly outlined with one of them being "probing the data". The automation actually made this possible, permitting easy testing with different parameter combinations. Although automation thereby greatly helped in finding parameter combinations that avoided non-convergence, persisting convergence issues were also the hindrance to further "probing the data". More rain than the heavy rain precipitation scenario, for instance, would have been an interesting model input to find out more on the reaction of the soils that did not produce surface runoff under any of the modeled scenarios. Due to convergence issues, however, H1D input parameters could be varied only to a limited extent. This issue would need to be addressed and amended in the proposed modeling approach to generate further knowledge in the future.

Concerning the general interplay between euptfv2 and H1D, no further problems were detected and the results obtained from the modeling approach were thus considered numerically valid.

### **General model simplifications and assumptions**

The data generation was, however, subject to a number of modeling simplifications and assumptions, which limited the informative value of the outcomes to the respective conditions. The most important limitations are outlined in the following section.

Firstly, it was assumed that the soil is not compacted, that no damming layers exist at any depth and that water can freely drain to the groundwater below the lower end of the soil. It is however possible that, due to geological characteristics, tillage practices or other land use practices, only the top layer is well permeable (Amelung et al., 2018). Such characteristics could possibly further be enhanced by increased SOC contents in the topsoil, since, according to the results of this thesis, up to 5.5 % SOC content further improves Ks in the amended soil layers. Compaction, damming layers or at least rapidly decreasing Ks values with depth could have been the case in the scenario taken from Whelan et al. (2013) which served for the testing of the modeling approach in chapter 3.1.3. Such soil characteristics could have been the reason for runoff occurring at normal precipitation in the field study, while the proposed modeling approach required approximately 200 times higher precipitation intensities to yield runoff.

The modeled soils were additionally assumed to not exhibit significant inclination, and the possible occurrence of ponding depths was neglected. Non-infiltrated water was thus assumed to run off directly instead of ponding up while not exhibiting fast flow rates that exceed infiltration rates, as would the case in steep terrain. For the modeling of a specific

project, respective relief-related information could be included in the future. However, corresponding data must be collected directly in the field since topographic information on the micro level is necessary to assess the actual inclination or potential ponding depths of fields.

Further, it was assumed that no maximum storage capacity existed in the modeled soils. Since an infinite storage capacity cannot be exhausted at any point, the results suggest that  $K_s$  is always the more important parameter under heavy rain. It has the capacity to avoid surface runoff and thereby erosion. However, in actual soils in a carbon project, the water storage capacity could be exhausted after a period of heavy rainfall. Surface runoff would thus not (only) occur due to low  $K_s$ , but also be due to fully saturated storages. In case of an inclined terrain and high  $K_s$  lateral sub-surface flow, in the direction of the next receiving water, would additionally take place in such a scenario. Lateral subsurface flow and fast drainage towards the receiving waters such as rivers could thereby cause flooding, although surface runoff is reduced due to high  $K_s$  values. This is the case in Rwanda for example, where the carbon project regions Rulindo and Bugesera are medium to highly prone to river flood. It remains unclear from the sources, however, whether surface runoff or subsurface flow is the main contributor (Global Facility for Disaster Reduction and Recovery, 2020). Modeling results must therefore also be considered from this point of view, which makes good water storage capacities a valuable parameter not only under drought but also under rainy conditions.

While considering the above outlined model limitations, it must be noted that the main purpose of this thesis was to analyze the effect of intentionally added SOC on the SWB. More importance must thus be attributed to the relative results than to absolute values. It can therefore be stated that, for the purposes of this thesis defined in chapter 2, simplifications were valid and expedient since comparable results could be obtained. Nevertheless, if in the future, changes in the modeling approach are to be made, based on refined knowledge of soil conditions, they can be easily incorporated into the proposed modeling approach.

### **The assumption of a stable SOC baseline in the Rwanda carbon project**

For the modeling of the Rwanda carbon project, an additional assumption must be clarified and discussed. It was assumed that the SOC baseline remains constant and that all additionally sequestered OC is added without loss. However, depending on factors, such as how long the area had been deforested, it could be more appropriate to assume a declining baseline (Amelung et al., 2018). In the verification process of carbon projects, only the increase in sequestered  $\text{CO}_2$  is monitored (VERRA, 2021b). No information is available on absolute SOC contents in the project records. It seems therefore justified to assume a constant baseline for the purposes of this thesis and add a shrinking factor to the calculation in case respective information becomes available in field measurements.

The Rwanda modeling results are therefore valid only for the ideal state of stable SOC baseline contents or for very depleted soils where a shrinking factor would only have minor consequences for the baseline.

### 5.1.2 The pedotransfer function of choice and tropical soils

This sub-chapter analyzes the causes of uncertainty stemming from euptfv2 and the implications for the results of this thesis.

It shall be highlighted that all PTFs are cause of uncertainties since they are based on inter- and extrapolations of data measured in the field and reduce complex soil processes to simplified equations. X. Zhang et al. (2019) found available PTFs yield overall unsatisfactory results and that this is, according to the authors, mainly due to systematic underestimation of macropores and soil structure. It seems therefore wise to be cautious when using PTFs and analyzing their results. Trends of over- or underestimation will be discussed below in order to classify modeling results.

#### **The prediction of $K_s$**

A primary factor of uncertainty is the prediction of  $K_s$ . As reported by various authors,  $K_s$  is very difficult to model and therefore tied to the highest RMSEs (Filipović et al., 2020; Lilly et al., 2008; Tóth et al., 2015; Y. Zhang & Schaap, 2017). This is also the case for euptfv2 where among all output parameters,  $K_s$  is the one with the least accurate prediction (Szabó et al., 2020). In this thesis, the uncertainty tied to  $K_s$  can, among others, be attributed to the fact that  $K_0$  (used instead of  $K_s$  as described in chapter 3.2.1) is influenced by a variety of different factors. Other parameters rather have one to three predictors standing out with special importance like BD for  $Q_s$  and  $Q_r$ , as can be seen in Figure 21 (Szabó et al., 2020).

Yet, as stated above, absolute results were not the focus of this thesis and much more attention was paid to the relative influence of SOC. In the further processing of the euptfv2 results in H1D, absolute results gain in importance: Since the quantity of rainwater is the counterpart of  $K_s$  in the production of surface runoff, systematically over- or underestimated  $K_s$  could lead to a total absence of surface runoff or an excessive importance attributed to it. This must be kept in mind in the further analysis of results and when weighing the benefits of improved storage capacity against decreasing  $K_s$  at high SOC contents.

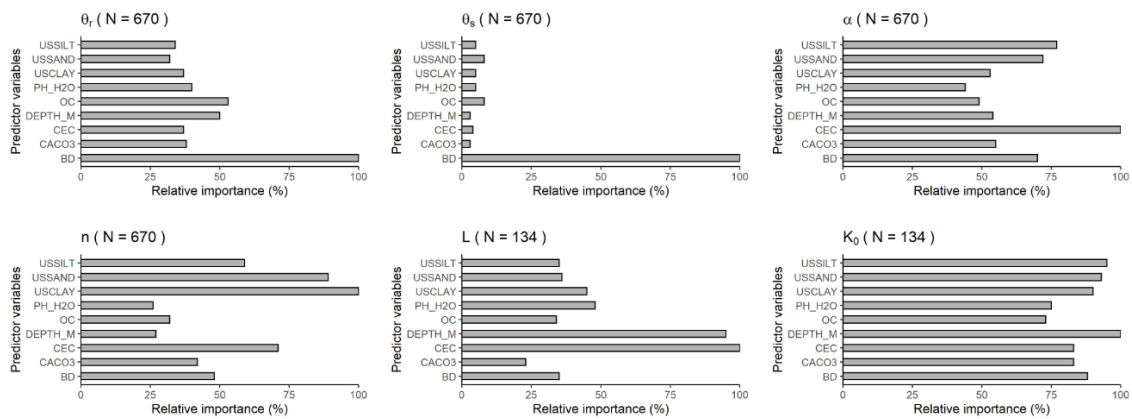


**Figure 21** Relative importance of predictors for MVG parameters predicted by PTF32 of the euptfv2 set in Szabó et al. (2020).

$\theta_s$  [-] = saturated water content (Qs);  $\theta_r$  [-] = residual water content (Qr);  $K_0$  [cm/day] = saturated hydraulic conductivity (in the original: “hydraulic conductivity acting as a matching point at saturation”);  $\alpha$  [1/cm] = reciprocal of the air entrance value for MVG;  $n$  [-] = shape parameter for MVG; USSILT [mass %] = silt content; USCLAY [mass %] = clay content; USSAND [mass %] = sand content; PH\_H2O [-] = pH in water; DEPTH\_M [cm] = mean soil depth; CEC [cmol/kg] = cation exchange capacity; CACO3 [mass %] = calcium carbonate content.

### Tropical and subtropical soils and their chemistry, clay content and macroporosity

The location of carbon projects represents a further factor of uncertainty. Although Rwanda is an example of a typical carbon project being executed in the tropics and subtropics, a temperate PTF was used in this thesis. The reasons for the PTF choice described in chapter 3.1.2. Nonetheless, the chosen PTF type produces further sources of uncertainty that need to be considered for the classification of this thesis’ results. The location related uncertainties can mainly be attributed to different soil chemistry, higher clay contents and different characteristics of macroporosity, as expounded in the following paragraph.

According to Szabó et al. (2020), soil chemistry plays an important role for various MVG parameters. The authors’ proposed PTF euptfv2 only has a limited applicability in the typically more weathered and acidic soils of the tropics and subtropics. Ottoni et al. (2018) compared the performance of their Brazilian PTF and euptfv2 using Brazilian soil data and concluded that especially for weathered, very fine textured soils, the Brazilian PTF performed better. According to their findings, weathered clays that can frequently be found in the tropics are important for the distinction between the hydraulic behavior of tropical and temperate soils.

Tropical soils are additionally harder to predict due to their statistically higher percentages in clay contents as shown in Figure 22. Although only minor areas in Rwanda presented clay contents above 40 % (see Figure 22), high tropical clay contents are a general problem for SWB predictions in carbon projects. High clay contents generally pose difficulties in SWB prediction and temperate PTFs are in addition not calibrated to reflect very clay-rich soils



(Hodnett & Tomasella, 2002; Ottoni et al., 2019). According to Ottoni et al. (2018), a greater soil structure complexity can be expected with increasing clay fractions due to the more heterogenic structural properties. Although calibrated in the tropics and subtropics, the authors found that their PTFs were less accurate for clay-rich soils due to the associated prediction uncertainties.

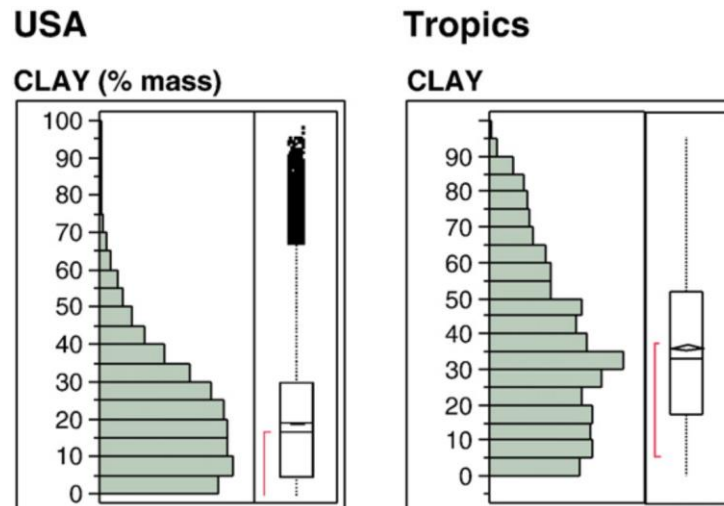


**Figure 22** Clay contents in temperate soils (USA) and in tropical soils as contrasted by Minasny and Hartemink (2011).

The results of this thesis must be considered against this background. When following the recommendations deduced from the results, SOC contents above circa 1.5 % should be avoided in clay soils where runoff is the a major issue due to climatic conditions. This does not, however, go in line with the related literature where organic amendments were found to have positive effects on Ks, infiltration rates and water stable aggregates specifically in fine-textured soils (Brown & Cotton, 2011; Chawade et al., 2006; Taye et al., 2018; Whelan et al., 2013). Modeling results of clay-rich soils should therefore be viewed critically.

Equally influenced by the location of the studied soils are the characteristics and occurrence of macroporosity with macroporosity depending mainly on PSD, climate and SOC (Nemes et al., 2005).

The influence of PSD on macroporosity is related to the special structure building characteristics of clay. Nemes et al. (2001) found overall decreasing values of Ks with increasing clay content, but at the same time a significant increase in the spread of the values. They attribute this wider spread to a more pronounced effect of soil structure, which also increases spatial heterogeneity. A heterogeneous pore structure in clay-rich soils was also found by Condappa et al. (2008). A bi-modal PSD is described as being the result of this heterogeneous structure, with two maxima weight percentage for sand (mostly made of aggregated clay particles) and for clay (Condappa et al., 2008; Ries et al., 2015). This bi-modal

PSD present in tropical soils could lead to hydraulic properties also being bi-modally distributed (Condappa et al., 2008). Yet, such soil physical characteristics were not respected in the proposed modeling approach since clay-sized particles were exclusively modeled as clay fraction. In the prediction of soil hydraulic properties in carbon projects, the influence of these special characteristics must be kept in mind.

In addition to high clay contents, tropical and subtropical climates dominate most carbon projects and further influence the expression of macroporosity. While dryer and warmer climates promote the development of macropores in the surface-layer, more humid and cooler climates restrict the expression of the latter (Hirmas et al., 2018). In addition, SOC promotes the formation of aggregates that play an important role in macroporosity (Nemes et al., 2001). Due to biotic processes of aggregate formation, this process is equally enhanced by warmer climates (Hirmas et al., 2018).

These various factors influencing macroporosity together form a basis on which it is difficult to predict  $K_s$ . It is additionally crucial to note that macroporosity, and related effects of concentrated infiltration and preferential flow, are not represented in the  $K_s$  value as calculated in this thesis. Thus, it is essential to keep in mind a possible shift towards (partially) higher  $K_s$  under real conditions, compared to the modeling results presented in this thesis.

### **Trends of over- and underestimation**

It can thus be stated that common PTFs are problematic to a certain extent, mainly in terms of  $K_s$  prediction and when applied to the tropics and subtropics. With regard to the modeling results of this thesis, the question remains, if a trend of over- or underestimation can be determined.

Contradictory results from the literature make such a statement complex. On the one hand, findings from the literature speak in favor of substantial deviations from the modeled results. Results on the overall underestimation of macropores by established PTFs, statistically higher  $K_s$  and higher  $Q_r$  in tropical soils, as well as the importance of soil chemistry, are examples of such findings (Minasny & Hartemink, 2011; Ries et al., 2015; X. Zhang et al., 2019). On the other hand, Ottoni et al. (2019) found in their best performing PTF that pedogenetic origin is not a relevant factor in the estimation of  $K_s$ . Furthermore, most tropical PTFs use the same predictors as in temperate regions, with calibration that also does not show large differences (Minasny & Hartemink, 2011). Especially for coarse textured soils, temperate PTFs were shown to yield accurate results, also in tropical and subtropical soils (Ottoni et al., 2018).

From these considerations, together with own findings from the comparison of euptfv2 modeling results and measurements provided in Ottoni et al. (2018), the following tendencies result:

Q<sub>r</sub> is likely to be indeed underestimated by euptfv2 as also described in Minasny and Hartemink (2011). In their study, it is stated that due to measurements based on disturbed samples, their results might actually be systematic overestimations. However, similar results were found in the comparison of euptfv2 and undisturbed results from the HYBRAS database in Ottoni et al. (2018). Underestimation ranged between 0 and 0.25 cm/day with absolute values showing an increasing tendency at higher clay contents (see Appendix 5).

Q<sub>s</sub> was not found, in the literature, to deviate greatly and was well estimated by euptfv2, with deviations from HYBRAS ranging between +0.04 and -0.07 cm/day (see Appendix 5). Although increased volumes of tropical macropores might have an effect on this parameter, related results in this thesis are therefore considered accurate.

For K<sub>s</sub>, based on the information available, it was not possible to deduce a range of deviation. The comparison with tropical soils from HYBRAS yielded important underestimations for coarse textured and overestimations for fine textured soils, but with half of the values missing due to data gaps in the HYBRAS database, this is a weak conclusion (see Appendix 5). In determining the reliability of K<sub>s</sub> results, this thesis therefore follows the advice by Ottoni et al. (2018) and classifies K<sub>s</sub> results from weathered clay soils as rather non-reliable. Results from coarse textured soils can however be considered reliable (Ottoni et al., 2018).

## 5.2 The controlling factors of the benefits of soil organic carbon

The key outcomes concerning controlling factors of SOC benefits are discussed in this subchapter. After the preceding, more general chapter on the plausibility of modeling results, actual outcomes are analyzed and, grouped into four categories, related to their implications, with information being further complemented by the literature findings.

### 5.2.1 The quantity of sequestered organic carbon

The results of this thesis found that SOC content has a positive influence on several parameters in most of the considered soils. However, for various parameters, 5 to 5.5 % SOC represented an important threshold beyond which benefits started to flatten or decrease more or less sharply. These results align with findings from Reynolds et al. (2015). In their study, SOC contents were found to be optimal in a range between 3 and 5 % for physical soil quality (see Appendix 1). Critical limits were stated to be especially important for fine textured soils with SOC contents below 2.3 % potentially causing loss of soil structure and above 6 % making soils susceptible to compaction. A comparable “tipping point behavior” was also described by Brown and Cotton (2011).

Due to the different behavior of parameters below and above 5.5 % SOC, this threshold is also important in weighing improved storage (Q<sub>s</sub> or theta) against enhanced K<sub>s</sub> or

reduced runoff. While  $\theta$  exclusively increased with SOC under most precipitation scenarios,  $K_s$  decreased sharply above 5.5 %. From a hydrological point of view, and according to results from this thesis, SOC contents higher than 5.5 % should therefore only be aimed at if runoff does not represent an issue in the area under consideration.

For Rwanda, according to the modeling results, this lack of runoff would be the case. However, it is known that in the past Rwanda has struggled repeatedly with heavy rains and associated surface runoff causing erosion and flooding in the project regions (Nkurunziza, 2021a, 2021b). Due to the uncertainties related to the modeling of  $K_s$ , it would thus be wise not to rush decisions regarding the risk of surface runoff and rather keep SOC contents as close as possible to the optimal range.

In the Rwanda Carbon Project, however, the projected increase in SOC over the 20-year period was calculated to be less than total 0.3 % for all soils except clay soils, with corresponding marginal effects on soil hydrology. For clay soils, SOC contents are already very high before the project and, although they were modeled to increase more strongly over the 20-year period than in other soils, the increase did not have any effect at all on the modeled hydrological parameters. In addition, as described in chapter 5.1.1, all modeling results are based on the assumption of a stable SOC baseline since the percentage of decline can vary widely and is not known from project records. It is however likely that some kind of SOC decline takes place in most carbon project baselines. SOC contents below the optimal range, throughout the whole project period, are therefore much more likely to occur than excessive sequestration rates which could actually cause additional surface runoff due to decreasing  $K_s$ . Results like those in Reynolds et al. (2015) rather show that very high OC applications (in their case: a single application of 300 dry t/ha) are required to lead to significant positive influences on SHPs.

### 5.2.2 Soil texture

Soil texture has an important influence on all SHPs (Filipović et al., 2020). However, based on the modeling results of this thesis it cannot be stated with certainty to what extent PSD is a controlling factor for the benefits of SOC on SHPs. This is the case mainly because the prediction of clayey soils is very error prone as outlined in chapter 5.1.2. The comparison of clayed soils with the remaining sandy soils is therefore not expedient.

It can however more generally be stated that some soils already dispose of favorable hydrological properties at low SOC contents while other PSDs need the addition of OC to develop good properties. For example, according to this thesis' results,  $K_s$  values for all soils, except for loamy sand, ranged between 43.2 and 432 cm/day which was found to be the optimal range by Reynolds et al. (2015).  $K_s$  of loamy sand, however, was modeled to range below that limit and got close to the critical lower limit of water logging (8.64 cm/day according to Reynolds et al., 2015) with heavy rain therefore producing runoff in the modeling

results. Here, additional SOC had a strong beneficial effect by increasing  $K_s$  and reducing runoff to zero in the range between 4.5 and 7.5 % SOC.

Regarding the role of soil texture, the following can thus be stated: The proposed modeling approach did not yield clear results on the role of PSD as a controlling factor for the beneficial effect of SOC on SHPs. However, it was found that some soils benefit more from additional SOC than others do. Although soil texture can hardly be changed on a field, this knowledge is valuable to the process of prioritization when designing carbon projects.

### 5.2.3 The role of precipitation regimes

Depending on whether drought or heavy rain is the bigger problem, improvements in available water content ( $Q_s$  minus  $Q_r$ ) or  $K_s$  tend to lead to the higher benefit. The modeling results showed that up to a certain texture dependent SOC content, both parameters increase. Beyond this soil specific point, and especially over 5.5 % SOC,  $K_s$  decreased while the available water content further increased with additional SOC. From the point on where  $K_s$  and available water content start to react differently to a further increase in SOC percentages, the type of precipitation regime thus becomes important by determining whether SOC should further be increased or not.

As discussed in chapter 5.1.1, however,  $Q_s$  also plays an important role in flood prevention. Additionally, due to difficulties in  $K_s$  prediction, especially in clayey soils, not too much weight should be attributed to potentially decreasing  $K_s$  values above 5.5 % SOC. Keeping this in mind, it can be recommended also in this context to aim for the upper optimal range of SOC without attributing too much weight to potentially occurring runoff under heavy rain.

Based on the results obtained in this thesis, the role of precipitation regimes rather consists of prioritized OC sequestration. Prioritized areas should be those where return rates of extreme events are short and corresponding improvements in SHPs can be made by sequestering additional OC.

### 5.2.4 Factors controlling plant water availability, transpiration and crop yield

In the modeling results it was found that, for all soils, within the modeled range, the difference between  $Q_s$  and  $Q_r$  increased significantly with additional SOC. This means that under higher SOC levels, more water is potentially available to plants. In tropical soils, the absolute value of the plant available water is however likely to be reduced by up to 0.25 cm/day compared to what resulted from the modeling approach. This is due to the systematic underestimation of  $Q_r$  in the tropics and subtropics, as discussed in chapter 5.1.2. Nonetheless, the increase of this important soil quality indicator with SOC remains significantly positive.

Along with plant available water, also actual plant transpiration increased significantly with SOC for most soils, but only under extreme drought. Under heavy rain, the contrary

occurred, however, with fewer soils showing significant trends than under extreme drought conditions. Since plant transpiration rates and dry matter production are proportional, such SOC-related trends imply increases or decreases in plant productivity, respectively (Arkley, 1963). Regarding the relevance of these transpiration effects, the length of the respective effect plays an important role: While drought is by definition an event of potentially very long durations (various days to months), heavy rain typically occurs in time scales of minutes to hours (Panagos et al., 2015). It can thus be stated, that in climates where both extremes occur, more importance should be attributed to maximizing plant productivity during periods of drought than during heavy rain. A periodic change between dry and wet seasons applies to many tropical and subtropical climates. According to the modeling results, it seems thus reasonable to favor higher SOC contents in order to increase overall plant productivity in carbon projects.

However, findings related to significant effects of SOC on transpiration could not be identified in the literature. Since most papers focused on soil biological properties rather than on soil physical or hydrological properties, effects of increased productivity through SOC were often attributed to increased nutrient availability instead of better soil structure. Diacono and Montemurro (2011) for example, found the crop yield to increase by 250 %, and the crop quality to be improved, under long term application of high rates of municipal solid waste compost in a semi-arid Mediterranean region. They made, however, no statement about the SOC effect to which these benefits were attributable.

In order to gain a deeper understanding of the different effects of SOC on actual plant transpiration and crop yield, field studies need to be conducted in the future. They could help disentangle the beneficial effects of SOC and thereby prove or refute the findings regarding the effect of SOC on plant transpiration presented in this thesis.

### 5.3 Temporal and spatial transferability

The modeling approach proposed in this thesis, as well as its results, can to some extent be transferred to other temporal and spatial contexts. This transfer will be discussed in the present sub-chapter.

Temporal transferability describes, in this context, the possibility of using the results for the same project location, but under changed climatic conditions. The discussion of temporal transferability thus provides an overview of climatic changes in Rwanda and the extent to which the results from this thesis are useful under such changing conditions.

The paragraph on spatial transferability analyzes to what extent the results can be used in locally different agricultural carbon projects.

### 5.3.1 Temporal transferability

Climate change is already manifesting itself in various forms in Rwanda but forecasts are not very reliable due to a rather poor data situation, as outlined in chapters 1.2.3 and 1.2.4. In available weather records, there are however indications for weather events and seasonality becoming more extreme. Partially significant trends indicating a decreasing number of rainy days and increasing amounts of rain per rainy day were found for the whole country (Muhire & Ahmed, 2015). Additionally, temperatures seem to rise faster than the global mean with related effects on weather and soils (Strategic Foresight Group, 2013). The Rwanda Environment Management Authority reported already in 2009 more concentrated rain events and at the same time an overall warmer and dryer climate. Concentrated rain resulted in, among others, flash floods, erosion and major destruction of crops, as reported by a Rwandan daily for the last two main rainy seasons (Nkurunziza, 2021a, 2021b).

Under current climatic and geological conditions, 47 % of Rulindo was found to be prone to flash floods and erosion due to high elevations, while 100 % of the Bugesera area is threatened by high to moderate risks of extended drought (Global Facility for Disaster Reduction and Recovery, 2020; MIDIMAR, 2015). These risks might further be enhanced by climatic developments towards the extremes (Global Facility for Disaster Reduction and Recovery, 2020). Especially before the background of erosion reacting unproportionately stronger to increases in rainfall intensity than runoff (as described in chapter 1.2.4) risks of erosion should be minimized (Nearing et al., 2005).

Adaptation to a changing climate is of uppermost importance for these rural households, whose livelihoods entirely depend on crop yields, as outlined in chapter 1.2.3. Also from a more general point of view, especially the maximization of water storage in soils is a very important measure in attenuating the impacts of measured and projected Rwandan climatic extremes. Under climatic shifts towards the extremes, it becomes even more crucial to infiltrate and store water, on the one hand, in soils that are exposed to heavy rain, since this can help in reducing destructive erosion, triggered landslides and flash floods. It also becomes important, on the other hand, in soils that are increasingly prone to droughts, such as those in Bugesera, where improved capacities of soils to store plant available water is an important step in climate adaptation.

Regarding aspects of strategic climate adaptation in the Rwanda agricultural carbon project, a temporal transfer of thesis results can be of use. So far, in the project area, from the modeled climatic scenarios, no excessively low (at or below  $Q_r$ ) or high (full saturation and surface runoff) soil water contents were found. However, the more general results from chapter 4.2 can be used in various beneficial ways: Given the likely shift towards more frequent and more concentrated rain events, modeling results can, for example, be used to identify those soils where  $K_s$  is low and runoff is most likely to occur. Among the project soils, these would be the clay soils. However, it was found, albeit with a high degree of uncertainty, that further increases in SOC would not change the hydrology in these specific

soils. It would therefore be wise, based on the modeling results, to concentrate on the second smallest  $K_s$  in sandy clay soils. Given the very low SOC values here, it can be seen in the modeling results that further sequestration would additionally contribute to make important improvements in plant available water contents.

The temporal transfer of modeling results thus helps in strategic adaptation to a changing climate by facilitating specific provision for its effects.

### 5.3.2 Spatial transferability

The proposed modelling approach is especially of use for the transfer to a different locality. Since its results are specific to Rwandan climate, new results must be generated in a spatial transfer. Due to the possibility of automated model runs, this can easily be done by adapting climatic boundary conditions to a different climate.

For other tropical and subtropical climates however (e.g. a new carbon project locality), special attention should be paid to the presented limitations and uncertainties related to tropical soils (see chapter 5.1.2). Under the regime of even more rainy climates, with higher rainfall intensities than the Rwanda heavy rain scenario, an increase in the number of non-convergence cases in H1D could occur. Depending on the extent to which this hinders the calculations, it is imperative to find a solution to these problems before applying the modeling approach to a corresponding new locality. This is also the case for the transfer to temperate conditions. Since temperate soils contain higher percentages of silt, the modeling of this texture class needs to be included in respective calculations (Nachtergaele et al., 2008).

However, as discussed in chapter 5.1.2, MVG parameters are so far calculated by the temperate PTF *eupfv2*. The reliability of results generated with the modeling approach could therefore possibly be improved by a transfer of the approach to temperate soils. Additionally, uncertainties related to tropical soils as described in chapter 5.1.2 do not apply here, which further improves model reliability.

Spatial transferability is thus only limited by the possible occurrence of additional convergence issues and by the availability of meteorological data necessary to apply the modeling approach to a new region. If these limitations do not pose a problem, spatial and temporal transferability can also be combined to use the benefits of a temporal transfer in a different location. This could be especially interesting for regions that are likely to be heavily influenced by macroclimatic shifts and related floods and droughts, as described in chapters 1.2.3 and 1.2.4.



## 6 Conclusion and outlook

Intentionally enhanced SOC was found to be mostly beneficial to the SWB in the context of carbon projects. The effects were determined by controlling factors, most importantly by the soil texture, baseline SOC content and sequestration rate, as well as by the local precipitation regime defining whether drought or erosion is likely to be the major issue.

The effect size could be predicted, with some limitations, with the help of the proposed modeling approach, since general reliability of the approach was confirmed. The systematic generation of insights into the effect of SOC on the SWB was thus made possible. However, under specific conditions, SWB outcomes could not be generated, either due to convergence issues, or due to the limited reliability of modeling results. Limitations in reliability were mainly due to generalized modeling assumptions and shortcomings of euptfv2. Both of these causes could potentially be addressed in future studies by adjusting the modeling approach through the use of more informed and project-specific assumptions and implementing a PTF that is better tailored to the specific climatic conditions.

The data that could be generated indicated that the intentionally increased SOC significantly increases water retention and plant available water. Additional SOC further significantly increased plant transpiration (and thereby yield), under extreme drought, as well as  $K_s$ , up to a certain SOC content. In carbon projects, the possibility of targeted maximization of these benefits can help give weight to climate adaptation through more resilient soil hydrology.

For the case of Rwanda, the project increases in SOC showed only very slight positive impacts on modeled SWB results. However, since the general results for SOC between zero and nine percent were generated based on the climate and textures of the Rwanda carbon project, resulting trends could in the future be useful to prioritize specific sites in the Rwanda carbon project.

The possibility for the informed prioritization of areas, with respect to OC sequestration within a carbon project, is a key outcome of this thesis. By systematically adapting the modeling approach to project specific conditions, the approach could be spatially transferred to another project location. Based on knowledge regarding controlling factors of the positive effect of SOC, informed decisions can be taken on where OC sequestration efforts should be concentrated. With the additional inclusion of climate change predictions, carbon projects can thereby be designed proactively, prioritizing areas where climate adaptation is most needed. Since the main strength of the proposed modeling approach is the comparison of areas, rather than the prediction of absolute values, the model can thereby be used to maximize SWB benefits of OC sequestration.

This maximization of positive effects can generally be beneficial in the targeted design and on-the-ground implementation of development cooperation programs, as well as climate projects. Based on the results of this thesis, economically viable approaches can be

combined with other environmental benefits to embed natural drought prevention and improve traditional, as well as modern agricultural practices.

More research is advisable, however, in order to improve estimations on absolute values and thereby give impetus to the attention to the SWB as influenced by SOC, as well as to its economic importance.

Firstly, a PTF is required that yields more reliable results for tropical and subtropical conditions. The inclusion of soil chemistry, clay content, and associated effects on macroporosity and aggregate formation appear to be crucial here. A first step in this direction would be to further clarify how SOC affects effective porosity. Corresponding insights could allow the implementation of the promising but effective porosity-based tropical PTF proposed by Ottoni et al. (2019) in the modeling approach to replace euptfv2.

Secondly, field studies are needed to verify whether the modeling results of growing transpiration and plant yield with increasing SOC under conditions of extreme drought are confirmed. This would further increase awareness for the importance of SOC in agricultural regions with recurrent droughts or projected drought risk.

Thirdly, once a modeling approach with a higher level of reliability has been attained, it would be interesting to implement the approach in a geographical information system environment. Pixel-based calculations could simplify spatial planning and the prioritization of specific project areas. Based on a revised approach, surrogate models could additionally be developed. Surrogate models mimic the behavior of a complex model in a simplified way and could thereby permit the development of a decision tool. These technical additions could provide quick and easy estimates of SWB benefits and help incorporate appropriate considerations into carbon project design.

Finally, given the great potential of OC sequestration for climate mitigation and adaptation, more research should be conducted to increase the amount of sequestered OC in carbon projects. In this regard, one promising area appears to be the recently emerging research on biochar. If the production and application of biochar proves to be a viable method that can also be integrated into carbon projects, its targeted use could increase the positive effects of intentionally increased SOC on the SWB.

In order to integrate this thesis into the broader research field, it shall conclude with an amended citation by Muhire and Ahmed (2015), that, complemented with the findings from this thesis, reads as follows: "Water is life. For this reason, it is paramount that no effort be spared in trying to understand rainfall trends [as well as the benefits from targeted sequestration of SOC] for effective and efficient water management".

## 7 References

- Abbott, L. K., & Murphy, D. V. (2007). *Soil biological fertility*. Springer.
- Amelung, W., Blume, H.-P., Fleige, H., Horn, R., Kandeler, E., Kögel-Knabner, I., Kretzschmar, R., Stahr, K., & Wilke, B.-M. (2018). *Scheffer/Schachtschabel Lehrbuch der Bodenkunde*. Springer Berlin Heidelberg. <https://doi.org/10.1007/978-3-662-55871-3>
- Amelung, W., Bossio, D., Vries, W. de, Kögel-Knabner, I., Lehmann, J., Amundson, R., Bol, R., Collins, C., Lal, R., Leifeld, J., Minasny, B., Pan, G., Paustian, K., Rumpel, C., Sanderman, J., van Groenigen, J. W., Mooney, S., van Wesemael, B., Wander, M., & Chabbi, A. (2020). Towards a global-scale soil climate mitigation strategy. *Nature Communications*, 11(1), 5427. <https://doi.org/10.1038/s41467-020-18887-7>
- ARCOS network. (2021, April 22). *30,000 Small Holder Farmers in Rulindo and Bugesera Districts are Partnering with ARCOS to improve their Livelihoods through Agroforestry — Albertine Rift Conservation Society*. <http://www.arcosnetwork.org/en/article/30000-small-holder-farmers-in-rulindo-and-bugesera-districts-are-partnering-with-arcos-to-improve-their-livelihoods-through-agroforestry>
- Arkley, R. J. (1963). Relationships between plant growth and transpiration. *Hilgardia*, 34(13), 559–584. <https://doi.org/10.3733/hilg.v34n13p559>
- Asumadu-Sarkodie, S., Rufangura, P., Jayaweera, H. M., & Asantewaa Owusu, P. (2015). Situational analysis of flood and drought in Rwanda. *International Journal of Scientific and Engineering Research*, 6(8).
- Bass, A. M., Bird, M. I., Kay, G., & Muirhead, B. (2016). Soil properties, greenhouse gas emissions and crop yield under compost, biochar and co-composted biochar in two tropical agronomic systems. *The Science of the Total Environment*, 550, 459–470. <https://doi.org/10.1016/j.scitotenv.2016.01.143>
- Børgesen, C. D., & Schaap, M. G. (2005). Point and parameter pedotransfer functions for water retention predictions for Danish soils. *Geoderma*, 127(1-2), 154–167. <https://doi.org/10.1016/j.geoderma.2004.11.025>
- Botula, Y.-D., Cornelis, W. M., Baert, G., & van Ranst, E. (2012). Evaluation of pedotransfer functions for predicting water retention of soils in Lower Congo (D.R. Congo). *Agricultural Water Management*, 111, 1–10. <https://doi.org/10.1016/j.agwat.2012.04.006>
- Brando, P. M., Paolucci, L., Ummenhofer, C. C., Ordway, E. M., Hartmann, H., Cattau, M. E., Rattis, L., Medjibe, V., Coe, M. T., & Balch, J. (2019). Droughts, Wildfires, and Forest Carbon Cycling: A Pantropical Synthesis. *Annual Review of Earth and Planetary Sciences*, 47(1), 555–581. <https://doi.org/10.1146/annurev-earth-082517-010235>
- Brown, S., & Cotton, M. (2011). Changes in Soil Properties and Carbon Content Following Compost Application: Results of On-farm Sampling. *Compost Science & Utilization*, 19(2), 87–96. <https://doi.org/10.1080/1065657X.2011.10736983>

- Cai, W., Santoso, A., Wang, G., Weller, E., Wu, L., Ashok, K., & Yamagata, T. (2014). Increased frequency of extreme Indian Ocean Dipole events due to greenhouse warming. *Nature*, 510, 254–258. <https://doi.org/10.1038/nature13327>
- Caiqiong, Y., & Jun, F. (2016). Application of HYDRUS-1D model to provide antecedent soil water contents for analysis of runoff and soil erosion from a slope on the Loess Plateau. *CATENA*, 139, 1–8. <https://doi.org/10.1016/j.catena.2015.11.017>
- Chalwade, P. B., Kulkarni, V. K., & Lakade, M. B. (2006). Effect of inorganic and organic fertilization on physical properties of vertisol. *Journal of Soils and Crops*, 16(1), 148–152.
- Chen, Y., Day, S. D., Wick, A. F., & McGuire, K. J. (2014). Influence of urban land development and subsequent soil rehabilitation on soil aggregates, carbon, and hydraulic conductivity. *The Science of the Total Environment*, 329–336. <https://doi.org/10.1016/j.scitotenv.2014.06.099>
- Cherobim, V. F., Favaretto, N., Freitas Melo, V. de, Barth, G., & Huang, C.-H. (2018). Soil surface sealing by liquid dairy manure affects saturated hydraulic conductivity of Brazilian Oxisols. *Agricultural Water Management*, 203, 193–196. <https://doi.org/10.1016/j.agwat.2018.03.016>
- Condappa, D. de, Galle, S., Dewandel, B., & Haverkamp, R. (2008). Bimodal Zone of the Soil Textural Triangle: Common in Tropical and Subtropical Regions. *Soil Science Society of America Journal*, 72(1), 33–40. <https://doi.org/10.2136/sssaj2006.0343>
- Da Pinho, R. E. C. d., & Miranda, J. H. de (2014). Avaliação do modelo HYDRUS-1D na simulação do transporte de água e potássio em colunas preenchidas com solos tropicais. *Engenharia Agrícola*, 34(5), 899–911. <https://doi.org/10.1590/S0100-69162014000500009>
- Di Gregorio, M., Nurrochmat, D. R., Paavola, J., Sari, I. M., Fatorelli, L., Pramova, E., Locatelli, B., Brockhaus, M., & Kusumadewi, S. D. (2017). Climate policy integration in the land use sector: Mitigation, adaptation and sustainable development linkages. *Environmental Science & Policy*, 67, 35–43. <https://doi.org/10.1016/j.envsci.2016.11.004>
- Diacono, M., & Montemurro, F. (2011). Long-Term Effects of Organic Amendments on Soil Fertility. In E. Lichtfouse (Ed.), *EDP sciences: Vol. 2. Sustainable agriculture* (pp. 761–786). Springer. [https://doi.org/10.1007/978-94-007-0394-0\\_34](https://doi.org/10.1007/978-94-007-0394-0_34)
- Dormann, C. F. (2017). *Parametrische Statistik*. Springer Berlin Heidelberg. <https://doi.org/10.1007/978-3-662-54684-0>
- European Union Council. (2007). *Council Regulation N. 834 on organic production and labelling of organic products and repealing regulation (EEC)*. <https://eur-lex.europa.eu/legal-content/EN/TXT/?uri=celex%3A32007R0834>
- Fan, J., McConkey, B., Wang, H., & Janzen, H. (2016). Root distribution by depth for temperate agricultural crops. *Field Crops Research*, 189, 68–74. <https://doi.org/10.1016/j.fcr.2016.02.013>

- Farrick, K. K., Akweli, Z., & Wuddivira, M. N. (2018). Influence of manure, compost additions and temperature on the water repellency of tropical soils. *Soil Research*, 56(7), 685. <https://doi.org/10.1071/SR17303>
- Ferré, T., & Warrick, A. W. (2005). Infiltration. In D. Hillel (Ed.), *Encyclopedia of soils in the environment* (pp. 254–260). Elsevier. <https://doi.org/10.1016/B0-12-348530-4/00382-9>
- Filipović, V., Černe, M., Šimůnek, J., Filipović, L., Romić, M., Ondrašek, G., Bogunović, I., Mustać, I., Krevh, V., Ferenčević, A., Robinson, D., Palčić, I., Pasković, I., Goreta Ban, S., Užila, Z., & Ban, D. (2020). Modeling Water Flow and Phosphorus Sorption in a Soil Amended with Sewage Sludge and Olive Pomace as Compost or Biochar. *Agronomy*, 10(8), 1163. <https://doi.org/10.3390/agronomy10081163>
- Fuss, S., Flachsland, C., Koch, N., Kornek, U., Knopf, B., & Edenhofer, O. (2018). A Framework for Assessing the Performance of Cap-and-Trade Systems: Insights from the European Union Emissions Trading System. *Review of Environmental Economics and Policy*, 12(2), 220–241. <https://doi.org/10.1093/reep/rey010>
- Glaser, R., Hauter, C., Faust, D., Glawion, R., Saurer, H., Schulte, A., & Sudhaus, D. (2016). *Physische Geographie kompakt*. Springer Berlin Heidelberg. <https://doi.org/10.1007/978-3-662-50461-1>
- Global Facility for Disaster Reduction and Recovery. (2020, June 30). *Think Hazard - Rwanda*. <https://thinkhazard.org/en/report/205-rwanda>
- Government of Western Australia - Department of Primary Industries and Regional Development. (2021, April 21). *Measuring and reporting soil organic carbon | Agriculture and Food*. <https://www.agric.wa.gov.au/soil-carbon/measuring-and-reporting-soil-organic-carbon>
- Gülser, C., & Candemir, F. (2015). Effects of agricultural wastes on the hydraulic properties of a loamy sand cropland in Turkey. *Soil Science and Plant Nutrition*, 61(3), 384–391. <https://doi.org/10.1080/00380768.2014.992042>
- Herzog, A. (2018). *Revealing West African hard rock properties to foster hydrological modeling of the full critical zone: The example of Benin* [Master Thesis]. Karlsruhe Institute of Technology, Karlsruhe.
- Hirmas, D. R., Giménez, D., Nemes, A., Kerry, R., Brunsell, N. A., & Wilson, C. J. (2018). Climate-induced changes in continental-scale soil macroporosity may intensify water cycle. *Nature*, 561(7721), 100–103. <https://doi.org/10.1038/s41586-018-0463-x>
- Hodnett, M. G., & Tomasella, J. (2002). Marked differences between van Genuchten soil water-retention parameters for temperate and tropical soils: a new water-retention pedo-transfer function developed for tropical soils, 108, 155–180. [https://doi.org/10.1016/S0016-7061\(02\)00105-2](https://doi.org/10.1016/S0016-7061(02)00105-2)

- Intergovernmental Panel on Climate Change. (2014). Climate Phenomena and their Relevance for Future Regional Climate Change. In I. P. o. C. Change (Ed.), *Climate Change 2013: The Physical Science Basis* (pp. 1217–1308). Cambridge University Press. <https://doi.org/10.1017/CBO9781107415324.028>
- Intergovernmental Panel on Climate Change. (2019). *Climate Change and Land: an IPCC special report on climate change, desertification, land degradation, sustainable land management, food security, and greenhouse gas fluxes in terrestrial ecosystems*. <https://www.ipcc.ch/srccl/>
- Kranz, C. N., McLaughlin, R. A., Johnson, A., Miller, G., & Heitman, J. L. (2020). The effects of compost incorporation on soil physical properties in urban soils - A concise review. *Journal of Environmental Management*, 261, 110209. <https://doi.org/10.1016/j.jenvman.2020.110209>
- Lal, R. (2003). Global Potential of Soil Carbon Sequestration to Mitigate the Greenhouse Effect. *Critical Reviews in Plant Sciences*, 22(2), 151–184. <https://doi.org/10.1080/713610854>
- Lal, R. (2006). Enhancing crop yields in the developing countries through restoration of the soil organic carbon pool in agricultural lands. *Land Degradation & Development*, 17(2), 197–209. <https://doi.org/10.1002/ldr.696>
- Lal, R., Smith, P., Jungkunst, H. F., Mitsch, W. J., Lehmann, J., Nair, P. R., McBratney, A. B., Moraes Sá, J. C. de, Schneider, J., Zinn, Y. L., Skorupa, A. L., Zhang, H.-L., Minasny, B., Srinivasrao, C., & Ravindranath, N. H. (2018). The carbon sequestration potential of terrestrial ecosystems. *Journal of Soil and Water Conservation*, 73(6), 145A-152A. <https://doi.org/10.2489/jswc.73.6.145A>
- Larney, F. J., & Angers, D. A. (2012). The role of organic amendments in soil reclamation: A review. *Canadian Journal of Soil Science*, 92(1), 19–38. <https://doi.org/10.4141/cjss2010-064>
- Lehtinen, T., Dersch, G., Söllinger, J., Baumgarten, A., Schlatter, N., Aichberger, K., & Spiegel, H. (2017). Long-term amendment of four different compost types on a loamy silt Cambisol: impact on soil organic matter, nutrients and yields. *Archives of Agronomy and Soil Science*, 63(5), 663–673. <https://doi.org/10.1080/03650340.2016.1235264>
- Lilly, A., Nemes, A., Rawls, W. J., & Pachepsky, Y. A. (2008). Probabilistic Approach to the Identification of Input Variables to Estimate Hydraulic Conductivity. *Soil Science Society of America Journal*, 72(1), 16–24. <https://doi.org/10.2136/sssaj2006.0391>
- Livelihoods Funds. (2021, April 21). *RWANDA: agroforestry at scale for soil, water and food*. <https://livelihoods.eu/portfolio/rwanda-agroforestry-at-scale-for-soil-water-and-food/>
- Mandal, P., Chaturvedi, M. K., Bassin, J. K., Vaidya, A. N., & Gupta, R. K. (2014). Qualitative assessment of municipal solid waste compost by indexing method. *International Journal of*

- Recycling of Organic Waste in Agriculture*, 3(4), 133–139. <https://doi.org/10.1007/s40093-014-0075-x>
- Martens, B., Miralles, D. G., Lievens, H., van der Schalie, R., Jeu, R. A. M. de, Fernández-Prieto, D., Beck, H. E., Dorigo, W. A., & Verhoest, N. E. C. (2017). GLEAM v3: satellite-based land evaporation and root-zone soil moisture. *Geoscientific Model Development*, 10(5), 1903–1925. <https://doi.org/10.5194/gmd-10-1903-2017>
- Mbagwu, J. (1989). Effects of organic amendments on some physical properties of a tropical ultisol. *Biological Wastes*, 28(1), 1–13. [https://doi.org/10.1016/0269-7483\(89\)90044-X](https://doi.org/10.1016/0269-7483(89)90044-X)
- Melillo, E. D. (2012). The First Green Revolution: Debt Peonage and the Making of the Nitrogen Fertilizer Trade, 1840–1930. *The American Historical Review*, 117(4), 1028–1060. <https://doi.org/10.1093/ahr/117.4.1028>
- Met Office. (2021, March 17). *UK climate averages*. <https://www.metoffice.gov.uk/research/climate/maps-and-data/uk-climate-averages>
- Meteo Rwanda. (2020, March 19). *Daily Precipitation Analysis*. <http://maproom.meteorwanda.gov.rw/maproom/>
- MIDIMAR. (2015, June 1). *The national risk atlas of Rwanda*. <https://www.gfdrr.org/en/publication/rwanda-national-risk-atlas>
- Minasny, B., & Hartemink, A. E. (2011). Predicting soil properties in the tropics. *Earth-Science Reviews*, 106(1-2), 52–62. <https://doi.org/10.1016/j.earscirev.2011.01.005>
- Mualem, Y. (1976). A new model for predicting the hydraulic conductivity of unsaturated porous media. *Water Resources Research*, 12(3), 513–522. <https://doi.org/10.1029/WR012i003p00513>
- Muhire, I., & Ahmed, F. (2015). Spatio-temporal trend analysis of precipitation data over Rwanda. *South African Geographical Journal*, 97(1), 50–68. <https://doi.org/10.1080/03736245.2014.924869>
- Nachtergaele, F. O., van Velthuisen, H., Verelst, L., Batjes, N. H., Dijkshoorn, J. A., van Engelen, V. W. P., Fischer, G., Jones, A., Montanarella, L., Petri, M., Prieler, S., Teixeira, E., Wilberg, D., & Shi, X. (2008). *Harmonized World Soil Database (version 1.0)*. <https://edepot.wur.nl/30776>
- Nearing, M. A., Jetten, V., Baffaut, C., Cerdan, O., Couturier, A., Hernandez, M., Le Bissonnais, Y., Nichols, M. H., Nunes, J. P., Renschler, C. S., Souchère, V., & van Oost, K. (2005). Modeling response of soil erosion and runoff to changes in precipitation and cover. *CATENA*, 61(2-3), 131–154. <https://doi.org/10.1016/j.catena.2005.03.007>
- Nemes, A., Rawls, W. J., & Pachepsky, Y. A. (2005). Influence of Organic Matter on the Estimation of Saturated Hydraulic Conductivity. *Soil Science Society of America Journal*, 69(4), 1330–1337. <https://doi.org/10.2136/sssaj2004.0055>

- Nemes, A., Schaap, M., Leij, F., & Wösten, J. (2001). Description of the unsaturated soil hydraulic database UNSODA version 2.0. *Journal of Hydrology*, 251(3-4), 151–162. [https://doi.org/10.1016/S0022-1694\(01\)00465-6](https://doi.org/10.1016/S0022-1694(01)00465-6)
- Nkurunziza, M. (2021a, May 1). Economic impact of disasters in 2020. <https://www.newtimes.co.rw/business/economic-impact-disasters-2020>
- Nkurunziza, M. (2021b, September 1). Heavy rains damage crops, injure seven across Rwanda. <https://www.newtimes.co.rw/news/heavy-rains-damage-crops-injure-seven-across-rwanda>
- Noack, F., Riekhof, M.-C., & Di Falco, S. (2019). Droughts, Biodiversity, and Rural Incomes in the Tropics. *Journal of the Association of Environmental and Resource Economists*, 6(4), 823–852. <https://doi.org/10.1086/703487>
- Oliveira, L. B., Ribeiro, M. R., Jacomine, P. K. T., Rodrigues, J. J. V., & Marques, F. A. (2002). Funções de pedotransferência para predição da umidade retida a potenciais específicos em solos do estado de Pernambuco. *Revista Brasileira De Ciência Do Solo*, 26(2), 315–323. <https://doi.org/10.1590/S0100-06832002000200004>
- Olson, K. R., Al-Kaisi, M. M., Lal, R., & Lowery, B. (2014). Experimental Consideration, Treatments, and Methods in Determining Soil Organic Carbon Sequestration Rates. *Soil Science Society of America Journal*, 78(2), 348–360. <https://doi.org/10.2136/sssaj2013.09.0412>
- Otoni, M. V., Otoni Filho, T. B., Lopes-Assad, M. L. R., & Rotunno Filho, O. C. (2019). Pedotransfer functions for saturated hydraulic conductivity using a database with temperate and tropical climate soils. *Journal of Hydrology*, 575, 1345–1358. <https://doi.org/10.1016/j.jhydrol.2019.05.050>
- Otoni, M. V., Otoni Filho, T. B., Schaap, M. G., Lopes-Assad, M. L. R., & Rotunno Filho, O. C. (2018). Hydrophysical Database for Brazilian Soils (HYBRAS) and Pedotransfer Functions for Water Retention. *Vadose Zone Journal*, 17(1), 170095. <https://doi.org/10.2136/vzj2017.05.0095>
- Panagos, P., Ballabio, C., Borrelli, P., Meusburger, K., Klik, A., Rousseva, S., Tadić, M. P., Michaelides, S., Hrabalíková, M., Olsen, P., Aalto, J., Lakatos, M., Rymaszewicz, A., Dumitrescu, A., Beguería, S., & Alewell, C. (2015). Rainfall erosivity in Europe. *The Science of the Total Environment*, 511, 801–814. <https://doi.org/10.1016/j.scitotenv.2015.01.008>
- Rawls, W. J., Brakensiek, D. L., & Saxton, K. E. (1982). Estimation of Soil Water Properties. *Transactions of the ASAE*, 25(5), 1316–1320. <https://doi.org/10.13031/2013.33720>
- Razzaghi, F., Obour, P. B., & Arthur, E. (2020). Does biochar improve soil water retention? A systematic review and meta-analysis. *Geoderma*, 361, 114055. <https://doi.org/10.1016/j.geoderma.2019.114055>
- Reichert, J. M., Albuquerque, J. A., Solano Peraza, J. E., & da Costa, A. (2020). Estimating water retention and availability in cultivated soils of southern Brazil. *Geoderma Regional*, 21, e00277. <https://doi.org/10.1016/j.geodrs.2020.e00277>



- Reynolds, W. D., Drury, C. F., Tan, C. S., & Yang, X. M. (2015). Temporal effects of food waste compost on soil physical quality and productivity. *Canadian Journal of Soil Science*, 95(3), 251–268. <https://doi.org/10.4141/cjss-2014-114>
- Ries, F., Lange, J., Schmidt, S., Puhlmann, H., & Sauter, M. (2015). Recharge estimation and soil moisture dynamics in a Mediterranean, semi-arid karst region. *Hydrology and Earth System Sciences*, 19(3), 1439–1456. <https://doi.org/10.5194/hess-19-1439-2015>
- Rwanda Environment Management Authority. (2009, October 1). *Rwanda state of environment and outlook*. <https://www.rema.gov.rw/soe/chap9.php>
- Sarrazin, F., Hartmann, A., Pianosi, F., Rosolem, R., & Wagener, T. (2018). V2Karst V1.1: a parsimonious large-scale integrated vegetation–recharge model to simulate the impact of climate and land cover change in karst regions. *Geoscientific Model Development*, 11(12), 4933–4964. <https://doi.org/10.5194/gmd-11-4933-2018>
- Schaap, M. G., Leij, F. J., & van Genuchten, M. T. (2001). Rosetta: a computer program for estimating soil hydraulic parameters with hierarchical pedotransfer functions. *Journal of Hydrology*, 251(3–4), 163–176. [https://doi.org/10.1016/S0022-1694\(01\)00466-8](https://doi.org/10.1016/S0022-1694(01)00466-8)
- Sciubba, L., Cavani, L., Negroni, A., Zanaroli, G., Fava, F., Ciavatta, C., & Marzadori, C. (2014). Changes in the functional properties of a sandy loam soil amended with biosolids at different application rates. *Geoderma*, 221–222, 40–49. <https://doi.org/10.1016/j.geoderma.2014.01.018>
- Shanahan, T. M., Overpeck, J. T., Anchukaitis, K. J., Beck, J. W., Cole, J. E., Dettman, D. L., Peck, J. A., Scholz, C. A., & King, J. W. (2009). Atlantic forcing of persistent drought in West Africa. *Science (New York, N.Y.)*, 324(5925), 377–380. <https://doi.org/10.1126/science.1166352>
- Šimůnek, J., Sejna, M., Saito, H., Sakai, M., & van Genuchten, M. T. (2013). *The hydrus1d software package for simulating the one-dimensional movement of water, heat, and multiple solutes in variably-saturated media* (Version 4.08) [Computer software].
- Šimůnek, J., van Genuchten, M. T., & Sejna, M. (2005). The HYDRUS-1D software package for simulating the one-dimensional movement of water, heat, and multiple solutes in variably-saturated media. *University of California-Riverside Research Reports*, 3, 1–240.
- Singh, V., & Frevert, D. (2006). *Watershed models*. Taylor & Francis. <http://site.ebrary.com/lib/alltitles/docDetail.action?docID=10144191>
- Stockmann, U., Adams, M. A., Crawford, J. W., Field, D. J., Henakaarchchi, N., Jenkins, M., Minasny, B., McBratney, A. B., Courcelles, V. R. de, Singh, K., Wheeler, I., Abbott, L., Angers, D. A., Baldock, J., Bird, M., Brookes, P. C., Chenu, C., Jastrow, J. D., Lal, R., . . . Zimmermann, M. (2013). The knowns, known unknowns and unknowns of sequestration of soil organic carbon. *Agriculture, Ecosystems & Environment*, 164, 80–99. <https://doi.org/10.1016/j.agee.2012.10.001>
- Strategic Foresight Group. (2013). *Blue peace for the Nile*. Mail Order Solutions India.

- Sutanto, S. J., Wenninger, J., Coenders-Gerrits, A. M. J., & Uhlenbrook, S. (2012). Partitioning of evaporation into transpiration, soil evaporation and interception: a comparison between isotope measurements and a HYDRUS-1D model. *Hydrology and Earth System Sciences*, 16(8), 2605–2616. <https://doi.org/10.5194/hess-16-2605-2012>
- Szabó, B., Gyurkó, D., Weynants, M., & Weber, T. K. D. (2019). *Web interface for European hydraulic pedotransfer functions (euptfv2)*. <https://doi.org/10.34977/EUPTFV2.01>
- Szabó, B., Weynants, M., & Weber, T. K. D. (2020). Updated European Hydraulic Pedotransfer Functions with Communicated Uncertainties in the Predicted Variables (euptfv2). <https://doi.org/10.5194/gmd-14-151-2021>
- Taheri Soudejani, H., Shayannejad, M., Kazemian, H., Heidarpour, M., & Rutherford, M. (2020). Effect of co-composting municipal solid waste with Mg-modified zeolite on soil water balance components using HYDRUS-1D. *Computers and Electronics in Agriculture*, 176, 105637. <https://doi.org/10.1016/j.compag.2020.105637>
- Tallaksen, L. M., & van Lanen, H. A. Hydrological drought: processes and estimation methods for streamflow and groundwater. In *Developments in Water Science* (Vol. 48).
- Taye, M., Simane, B., Selssie, Y. G., Zaitchik, B., & Setegn, S. (2018). Analysis of the Spatial Variability of Soil Texture in a Tropical Highland: The Case of the Jema Watershed, Northwestern Highlands of Ethiopia. *International Journal of Environmental Research and Public Health*, 15(9). <https://doi.org/10.3390/ijerph15091903>
- Toková, L., Igaz, D., Horák, J., & Aydin, E. (2020). Effect of Biochar Application and Re-Appliation on Soil Bulk Density, Porosity, Saturated Hydraulic Conductivity, Water Content and Soil Water Availability in a Silty Loam Haplic Luvisol. *Agronomy*, 10(7), 1005. <https://doi.org/10.3390/agronomy10071005>
- Tóth, B., Weynants, M., Nemes, A., Makó, A., Bilas, G., & Tóth, G. (2015). New generation of hydraulic pedotransfer functions for Europe. *European Journal of Soil Science*, 66(1), 226–238. <https://doi.org/10.1111/ejss.12192>
- UNIQUE forestry and land use. (2021, April 21). *Showcase – Smallholder carbon credits in Rwanda*. <https://digital.unique-landuse.de/showcases/showcase-building-resilience-to-climate-change-and-sustainable-livelihoods-in-rwandas-agro-ecosystems/>
- United Nations. (2015). *Paris agreement*. <https://unfccc.int/process-and-meetings/the-paris-agreement/the-paris-agreement>
- van Camp, L., Bujarrabal, B., Gentile, A. R., Jones, R. J., Montanarella, L., Olazabal, C., & Selvaradjou, S. K. (2004). *Reports of the technical working groups established under the thematic strategy for soil protection*. <http://citeseerx.ist.psu.edu/viewdoc/download?doi=10.1.1.400.5923&rep=rep1&type=pdf>
- van Genuchten, M. T. (1980). A Closed-form Equation for Predicting the Hydraulic Conductivity of Unsaturated Soils. *Soil Science Society of America Journal*, 44(5), 892–898. <https://doi.org/10.2136/sssaj1980.03615995004400050002x>

- van Loon, A. F. (2015). Hydrological drought explained. *Wiley Interdisciplinary Reviews: Water*, 2(4), 359–392. <https://doi.org/10.1002/wat2.1085>
- van Looy, K., Bouma, J., Herbst, M., Koestel, J., Minasny, B., Mishra, U., Montzka, C., Nemes, A., Pachepsky, Y. A., Padarian, J., Schaap, M. G., Tóth, B., Verhoef, A., Vanderborght, J., Ploeg, M. J., Weihermüller, L., Zacharias, S., Zhang, Y., & Vereecken, H. (2017). Pedotransfer Functions in Earth System Science: Challenges and Perspectives. *Reviews of Geophysics*, 55(4), 1199–1256. <https://doi.org/10.1002/2017RG000581>
- Ventrella, D., Castellini, M., Di Prima, S., Garofalo, P., & Lassabatère, L. (2019). Assessment of the Physically-Based Hydrus-1D Model for Simulating the Water Fluxes of a Mediterranean Cropping System. *Water*, 11(8), 1657. <https://doi.org/10.3390/w11081657>
- Vereecken, H., Huisman, J. A., Hendricks Franssen, H. J., Brüggemann, N., Bogaen, H. R., Kollet, S., Javaux, M., van der Kruk, J., & Vanderborght, J. (2015). Soil hydrology: Recent methodological advances, challenges, and perspectives. *Water Resources Research*, 51(4), 2616–2633. <https://doi.org/10.1002/2014WR016852>
- Vereecken, H., Maes, J., Feyen, J., & Darius, P. (1989). Estimating the soil moisture retention characteristic from texture, bulk density, and carbon content, 148, 1-12.
- Vereecken, H., Weynants, M., Javaux, M., Pachepsky, Y., Schaap, M. G., & van Genuchten, M. (2010). Using Pedotransfer Functions to Estimate the van Genuchten-Mualem Soil Hydraulic Properties: A Review. *Vadose Zone Journal*, 9(4), 795–820. <https://doi.org/10.2136/vzj2010.0045>
- VERRA. (2021a, March 9). *Verra Search Page*. <https://registry.verra.org/app/search/VCS/All%20Projects>
- VERRA. (2021b, April 22). *Approved VCS Methodology VM0017: Adoption of Sustainable Agricultural Land Management* [Version 1, Sectoral Scope 14]. <https://verra.org/wp-content/uploads/2018/03/VM0017-SALM-Methodolgy-v1.0.pdf>
- VERRA. (2021c, April 22). *New Methodology: VM0017 Sustainable Agricultural Land Management*. [https://verra.org/SALM\\_methodology\\_approved/](https://verra.org/SALM_methodology_approved/)
- VERRA. (2021d, April 30). *Verra Search Page - Project 1225*. <https://registry.verra.org/app/projectDetail/VCS/1225>
- Villagra-Mendoza, K., & Horn, R. (2018). Effect of biochar addition on hydraulic functions of two textural soils. *Geoderma*, 326, 88–95. <https://doi.org/10.1016/j.geoderma.2018.03.021>
- Wang, X., Li, Y., Wang, Y., & Liu, C. (2018). Performance of HYDRUS-1D for simulating water movement in water-repellent soils. *Canadian Journal of Soil Science*, 98(3), 407–420. <https://doi.org/10.1139/cjss-2017-0116>
- Weber, T. K., Durner, W., Streck, T., & Diamantopoulos, E. (2019). A modular framework for modelling unsaturated soil hydraulic properties over the full moisture range. *Water Resources Research*. Advance online publication. <https://doi.org/10.1029/2018WR024584>

- Wei, Z., Paredes, P., Liu, Y., Chi, W. W., & Pereira, L. S. (2015). Modelling transpiration, soil evaporation and yield prediction of soybean in North China Plain. *Agricultural Water Management*, 147, 43–53. <https://doi.org/10.1016/j.agwat.2014.05.004>
- Weynants, M., Vereecken, H., & Javaux, M. (2009). Revisiting Vereecken Pedotransfer Functions: Introducing a Closed-Form Hydraulic Model. *Vadose Zone Journal*, 8(1), 86–95. <https://doi.org/10.2136/vzj2008.0062>
- Whelan, A., Kechavarzi, C., Coulon, F., Sakrabani, R., & Lord, R. (2013). Influence of compost amendments on the hydraulic functioning of brownfield soils. *Soil Use and Management*, 29(2), 260–270. <https://doi.org/10.1111/sum.12028>
- World Meteorological Organization. (2021, February 25). *World Weather Information Service / WMO*. <https://worldweather.wmo.int/en/city.html?cityId=254>
- Wösten, J., Lilly, A., Nemes, A., & Le Bas, C. (1999). Development and use of a database of hydraulic properties of European soils. *Geoderma*, 90(3-4), 169–185. [https://doi.org/10.1016/S0016-7061\(98\)00132-3](https://doi.org/10.1016/S0016-7061(98)00132-3)
- Yu, H., Zou, W., Chen, J., Chen, H., Yu, Z., Huang, J., Tang, H., Wei, X., & Gao, B. (2019). Biochar amendment improves crop production in problem soils: A review. *Journal of Environmental Management*, 232, 8–21. <https://doi.org/10.1016/j.jenvman.2018.10.117>
- Zdruli, P., Lal, R., Cherlet, M., & Kapur, S. (2016). New World Atlas of Desertification and Issues of Carbon Sequestration, Organic Carbon Stocks, Nutrient Depletion and Implications for Food Security. In S. Erşahin, S. Kapur, E. Akça, A. Namlı, & H. E. Erdoğan (Eds.), *The Anthropocene: Politik-Economics-Society-Science. Carbon Management, Technologies, and Trends in Mediterranean Ecosystems* (1st ed., Vol. 15, pp. 13–25). Springer International Publishing AG. [https://doi.org/10.1007/978-3-319-45035-3\\_2](https://doi.org/10.1007/978-3-319-45035-3_2)
- Zhang, X., Zhu, J., Wendroth, O., Matocha, C., & Edwards, D. (2019). Effect of Macroporosity on Pedotransfer Function Estimates at the Field Scale. *Vadose Zone Journal*, 18(1), 1–15. <https://doi.org/10.2136/vzj2018.08.0151>
- Zhang, Y., & Schaap, M. G. (2017). Weighted recalibration of the Rosetta pedotransfer model with improved estimates of hydraulic parameter distributions and summary statistics (Rosetta3). *Journal of Hydrology*, 547, 39–53. <https://doi.org/10.1016/j.jhydrol.2017.01.004>

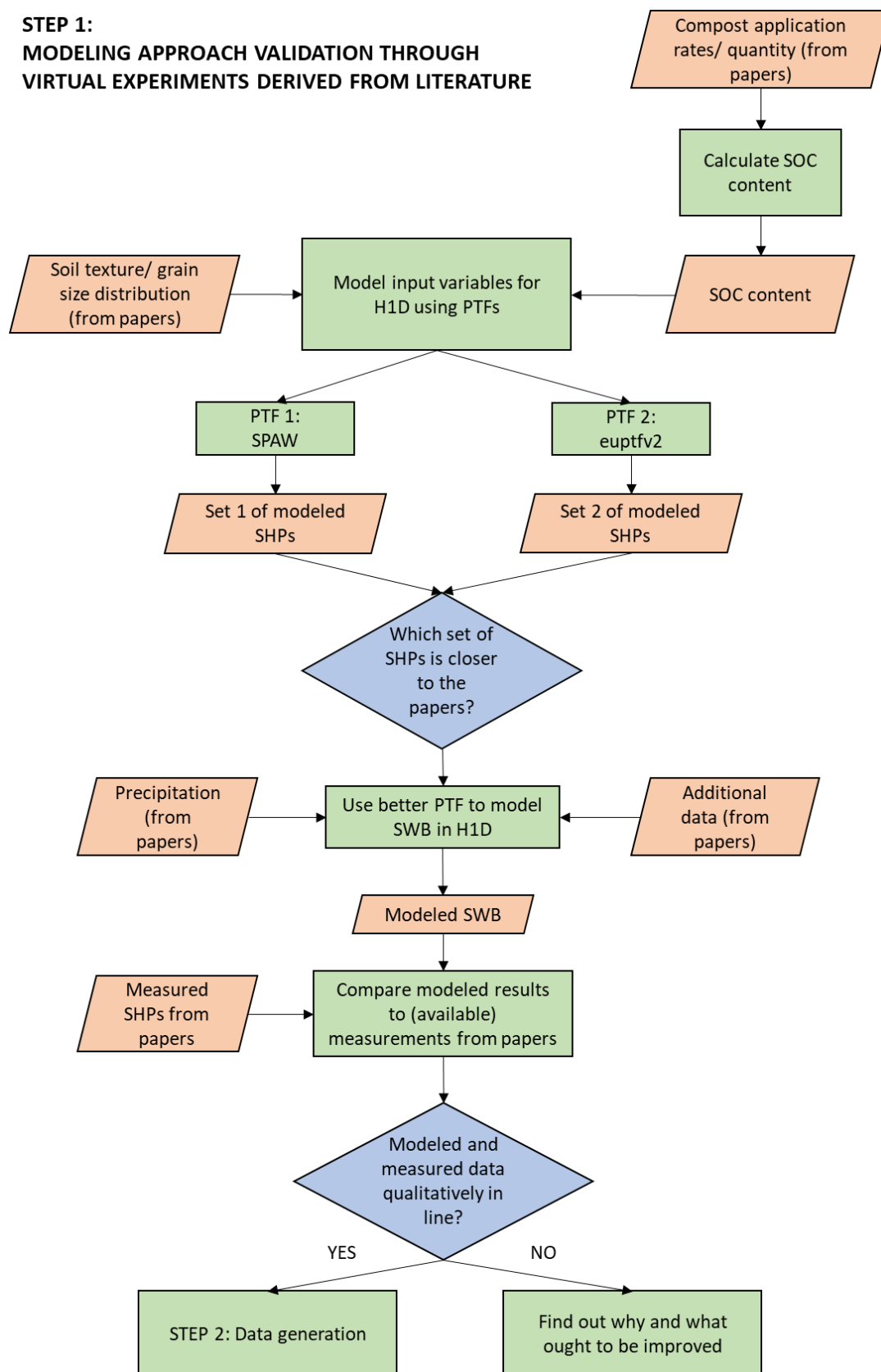


# Appendix

**Appendix 1** Soil physical quality parameters and their optimal ranges, as well as critical limits as indicated by Reynolds et al. (2015).

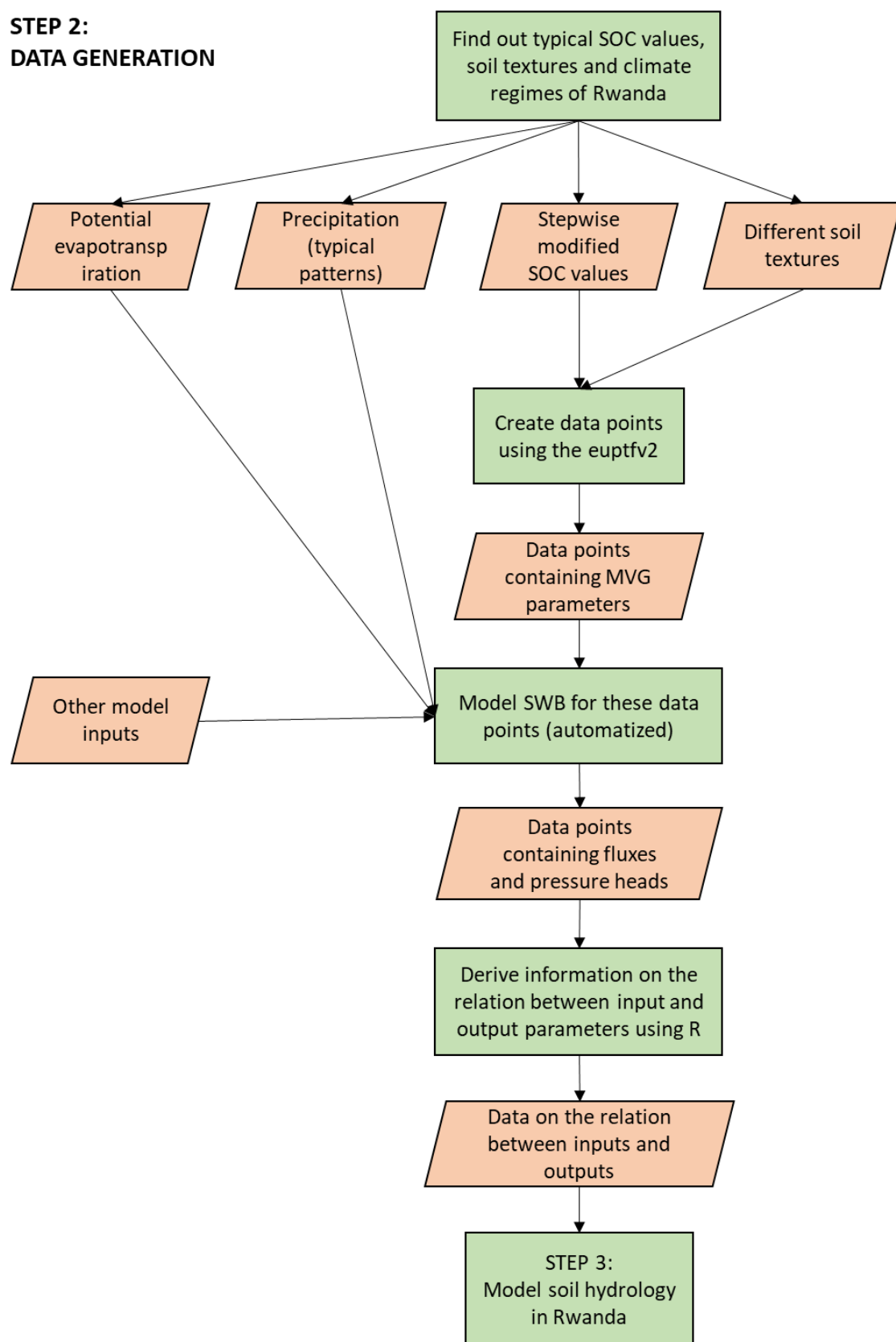
| Soil physical quality parameter                                      | Working definition or function  | Optimal ranges and/or critical limits   |
|--|---|---|
| Dry bulk density, BD ( $\text{Mg m}^{-3}$ )                          | Indicator of mechanical resistance to root growth.  | Optimal range for most soil textures: $0.9 \leq \text{BD} \leq 1.2 \text{ Mg m}^{-3}$ ;<br>Upper critical limit for Brookston clay loam where root growth effectively stops: $\text{BD} \approx 1.47 \text{ Mg m}^{-3}$   |
| Soil organic carbon content, OC ( $\text{g kg}^{-1}$ )               | Influences virtually all aspects of soil physical quality including soil hardness, and storage and transmission of soil air and soil water. | Optimal range for plant production: $30 \leq \text{OC} \leq 50 \text{ g kg}^{-1}$ ;<br>Upper critical limit where fine-textured soil becomes susceptible to compaction: $\text{OC} \approx 60 \text{ g kg}^{-1}$<br>Lower critical limit where tillage can cause loss of soil structure in fine-textured soils: $\text{OC} \approx 23 \text{ g kg}^{-1}$  |
| Air capacity, AC ( $\text{m}^3 \text{ m}^{-3}$ )                     | Indicator of soil's ability to store root-zone air (degree of soil aeration).   | Ideal for maintaining atmospheric concentrations of $\text{O}_2$ and $\text{CO}_2$ in fine-textured soil: $\text{AC} \geq 0.20 \text{ m}^3 \text{ m}^{-3}$<br>Lower optimal limit for adequate aeration of fine-textured soil: $\text{AC} \approx 0.14 \text{ m}^3 \text{ m}^{-3}$ ;<br>Lower critical limit where fine-textured soil becomes susceptible to periodic anaerobiosis: $\text{AC} \approx 0.09 \text{ m}^3 \text{ m}^{-3}$ |
| Plant-available water capacity, PAWC ( $\text{m}^3 \text{ m}^{-3}$ ) | Indicator of soil's ability to store plant-available water.   | For sufficient root growth/function and drought resilience in medium to fine textured soils:<br>Ideal: $\text{PAWC} > 0.20 \text{ m}^3 \text{ m}^{-3}$ ;<br>Good: $0.15 \leq \text{PAWC} \leq 0.20 \text{ m}^3 \text{ m}^{-3}$ ;<br>Limited: $0.10 \leq \text{PAWC} \leq 0.15 \text{ m}^3 \text{ m}^{-3}$ ;<br>Poor: $\text{PAWC} < 0.10 \text{ m}^3 \text{ m}^{-3}$  |
| Relative field capacity, RFC (—)                                     | Indicates the soil's primary limitation with respect to water and air storage.  | Optimal range: $0.6 \leq \text{RFC} \leq 0.7$ ;<br>Primary limitation is air storage (poor aeration): $\text{RFC} > 0.7$ ;<br>Primary limitation is water storage (droughtiness): $\text{RFC} < 0.6$  |
| Saturated hydraulic conductivity, $K_s$ ( $\text{cm s}^{-1}$ )       | Indicator of soil's ability to imbibe crop-essential water and drain excess water.  | Optimal range in humid climates: $5 \times 10^{-4} \leq K_s \leq 5 \times 10^{-3} \text{ cm s}^{-1}$ ;<br>Upper critical limit where soil becomes susceptible to droughtiness and excessive nutrient leaching: $K_s \geq 10^{-2} \text{ cm s}^{-1}$ ;<br>Lower critical limit where soil becomes susceptible to water-logging, poor traffickability, runoff and erosion: $K_s \leq 10^{-4} \text{ cm s}^{-1}$                           |

**STEP 1:  
MODELING APPROACH VALIDATION THROUGH  
VIRTUAL EXPERIMENTS DERIVED FROM LITERATURE**



**Appendix 2** Step 1 of the detailed flow chart of methodological steps: Modeling approach validation through virtual experiments derived from the literature.

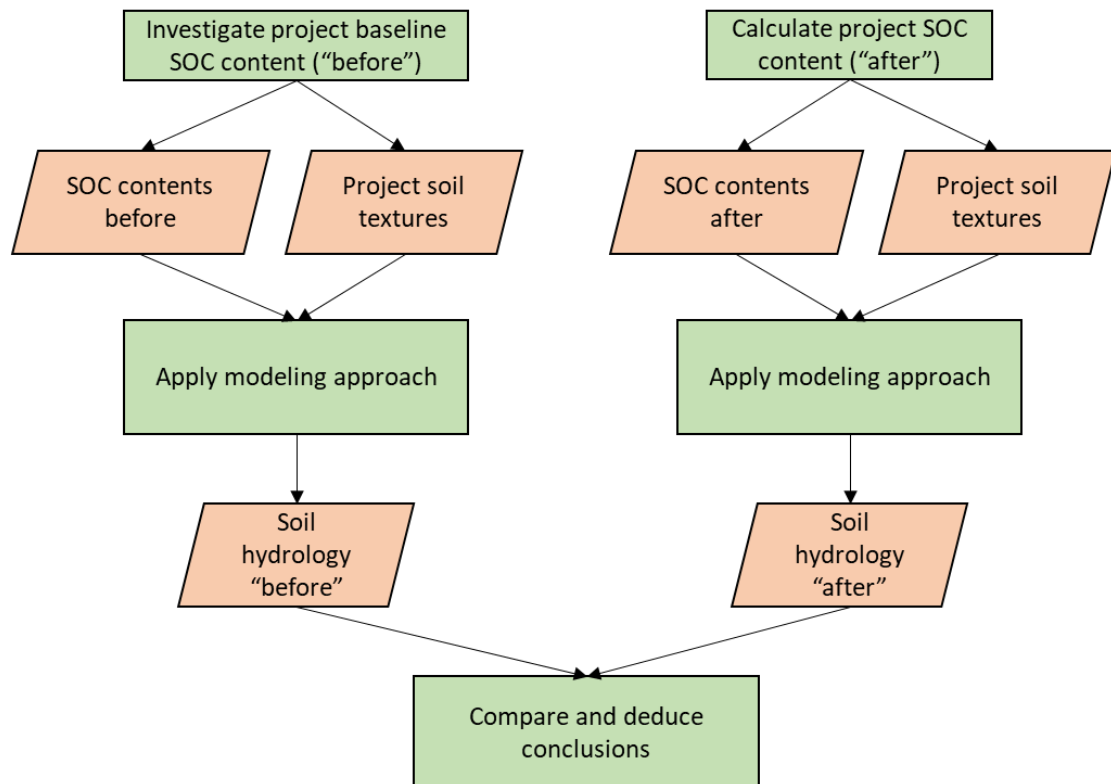
**STEP 2:  
DATA GENERATION**



**Appendix 3** Step 2 of the detailed flow chart of methodological steps: Data generation.



**STEP 3:  
MODEL SOIL HYDROLOGY IN THE  
RWANDA CARBON PROJECT**



**Appendix 4** Step 3 of the detailed flow chart of methodological steps: Modeling the soil hydrology in the Rwanda carbon project.

**Appendix 5** Tropical soils with sand, silt, clay and OC contents as described in Ottoni et al. (2018). K0, Qr and Qs are modeled for these soils by euptfv2 and measured by Ottoni et al. (2018). Deviations between eutpfv2 results and indications by Ottoni et al. (2018) are shown below.

| Sand [%] | Silt [%] | Clay [%] | OC [%] | K0 euptfv2 [cm/day] | Qr euptfv2 [-] | Qs euptfv2 [-] | Ks Ottoni [cm/day] | Qr Ottoni [-] | Qs Ottoni [-] |
|----------|----------|----------|--------|---------------------|----------------|----------------|--------------------|---------------|---------------|
| 92.8     | 2.8      | 4.4      | 1.02   | 17.41               | 0.05           | 0.38           | 184.00             | 0.05          | 0.40          |
| 85.1     | 5.0      | 9.9      | 1.31   | 8.51                | 0.07           | 0.37           |                    | 0.04          | 0.38          |
| 69.8     | 14.6     | 15.6     | 1.26   | 61.96               | 0.06           | 0.43           | 135.00             | 0.13          | 0.41          |
| 45.8     | 38.8     | 15.4     | 1.34   | 48.98               | 0.04           | 0.44           |                    | 0.19          | 0.41          |
| 62.1     | 11.6     | 26.2     | 1.02   | 37.53               | 0.09           | 0.35           | 66.00              | 0.16          | 0.42          |
| 34.8     | 32.6     | 32.6     | 2.67   | 95.79               | 0.06           | 0.51           | 56.00              | 0.27          | 0.52          |
| 12.2     | 54.6     | 33.3     | 3.88   | 48.06               | 0.04           | 0.65           |                    | 0.29          | 0.61          |
| 12.6     | 43.5     | 44.0     | 2.38   | 72.80               | 0.04           | 0.58           |                    | 0.29          | 0.57          |
| 50.0     | 9.7      | 40.3     | 1.01   | 81.83               | 0.09           | 0.44           | 52.00              | 0.20          | 0.47          |
| 24.2     | 18.8     | 57.0     | 1.51   | 98.61               | 0.06           | 0.51           | 65.00              | 0.29          | 0.56          |

| K0 euptfv2 - Ks Ottoni | Qr euptfv2 - Qr Ottoni | Qs euptfv2 - Qs Ottoni |
|------------------------|------------------------|------------------------|
| -166.59                | 0.00                   | -0.02                  |
| NA                     | 0.03                   | -0.01                  |
| -73.04                 | -0.07                  | 0.02                   |
| NA                     | -0.15                  | 0.03                   |
| -28.47                 | -0.07                  | -0.07                  |
| 39.79                  | -0.21                  | -0.01                  |
| NA                     | -0.25                  | 0.04                   |
| NA                     | -0.25                  | 0.01                   |
| 29.83                  | -0.11                  | -0.03                  |
| 33.61                  | -0.23                  | -0.05                  |

**Appendix 6** Soil types present in the Rwanda carbon project and their characteristics.

| Soil type      | Gravel [%] | Sand [%] | Silt [%] | Clay [%] | BD [g/cm <sup>3</sup> ] | SOC baseline [%] | C stocks [tC/ha] | Increase [tC/ha*year] | SOC increase [%/year] | SOC after 1 year [%] | SOC after 20 years [%] | SOC increase over 20 years [%] |
|----------------|------------|----------|----------|----------|-------------------------|------------------|------------------|-----------------------|-----------------------|----------------------|------------------------|--------------------------------|
| Sandy clay     | 0          | 52       | 6        | 42       | 1.22                    | 0.74             | 27.08            | 0.44                  | 0.012                 | 0.752                | 0.981                  | 0.241                          |
| Clay loam (B.) | 0          | 33       | 33       | 34       | 1.12                    | 3.88             | 130.37           | 0.44                  | 0.013                 | 3.893                | 4.143                  | 0.263                          |
| Clay           | 0          | 30       | 20       | 50       | 0.34                    | 27.15            | 276.93           | 0.44                  | 0.043                 | 27.193               | 28.016                 | 0.866                          |
| Loam           | 0          | 42       | 40       | 18       | 1.21                    | 5.2              | 188.76           | 0.44                  | 0.012                 | 5.212                | 5.443                  | 0.243                          |
| Clay loam (R.) | 0.01       | 33       | 33       | 34       | 1.37                    | 3.21             | 131.92           | 0.44                  | 0.011                 | 3.221                | 3.425                  | 0.215                          |

**Appendix 7** Non-exhaustive list of PTFs considered.

| <b>Author<br/>(name of the PTF)</b> | <b>Continuous/<br/>parametric</b> | <b>Input:<br/>texture</b> | <b>Input:<br/>only clay</b> | <b>Input:<br/>OC or OM</b> | <b>Output: MVG<br/>parameters</b> | <b>Broadly<br/>developed</b> | <b>GUI<br/>available</b> | <b>Developed<br/>for tropics</b> | <b>Error<br/>margins</b> |
|-------------------------------------|-----------------------------------|---------------------------|-----------------------------|----------------------------|-----------------------------------|------------------------------|--------------------------|----------------------------------|--------------------------|
| Bell and van Keulen, 1995           | -                                 |                           | only clay                   | x                          | x                                 | -                            | -                        | x                                | -                        |
| Costa et al., 2013                  | -                                 | x                         | x                           | x                          | x                                 | x                            | -                        | x                                | -                        |
| Hodnett and Tomasella, 2002         | x                                 | x                         | x                           | x                          | x                                 | -                            | -                        | x                                | -                        |
| Nemes et al., 2005                  | -                                 | x                         | x                           | x                          | -                                 | x                            | -                        | -                                | -                        |
| Oliveira et al., 2002               | x                                 | x                         | -                           | -                          | -                                 | -                            | -                        | x                                | -                        |
| Ottoni et al., 2019                 | x                                 | x                         | -                           | -                          | x                                 | x                            | -                        | x                                | -                        |
| Rawls et al., 1982                  | x                                 | x                         | x                           | x                          | x                                 | -                            | -                        | -                                | -                        |
| Reichert et al., 2009               | -                                 | x                         | x                           | x                          | x                                 | -                            | -                        | x                                | -                        |
| Saxton et al., 2005<br>(SPAW)       | x                                 | x                         | x                           | x                          | x                                 | x                            | x                        | -                                | -                        |
| Schaap et al., 2001<br>(Rosetta)    | x                                 | x                         | -                           | -                          | x                                 | x                            | x                        | -                                | -                        |
| Szabó et al., 2020<br>(eupthv2)     | x                                 | x                         | x                           | x                          | x                                 | x                            | x                        | -                                | x                        |
| Tóth et al., 2015<br>(eupthv1)      | x                                 | x                         | x                           | x                          | x                                 | x                            | -                        | -                                | -                        |
| Van den Berg et al., 1997           | x                                 | x                         | x                           | x                          | x                                 | -                            | only oxisols             | x                                | -                        |
| Vereecken et al., 1998              | x                                 | x                         | x                           | x                          | x                                 | -                            | -                        | -                                | -                        |
| Weynants et al., 2015               | x                                 | no silt                   | x                           | x                          | x                                 | -                            | -                        | -                                | -                        |
| Wösten et al., 1999                 | x                                 | x                         | -                           | -                          | x                                 | -                            | x                        | -                                | -                        |
| Zhang and Schaap, 2017              | x                                 | x                         | -                           | -                          | x                                 | x                            | -                        | -                                | -                        |

## Appendix 8 Python code to automate data generation in H1D.

```
1. '''
2. Hydrus window automated start with values from csv file
3.
4. install:
5.   use python3
6.   pip3 install -r pandas
7. usage:
8.   start powershell as admin:
9.   cd to python main file
10.  python main.py
11.  to start only one experiment: PS C:\Program Files (x86)\PC-Progress\Hydrus-1D
12.  4.xx> & ".\H1D_CALC.EXE"
13.  and change Level_01.dir to experiment of interest
14.  '''
15. import os.path as op # operating system path helper
16. import re # regular expression to search and edit strings
17. import pandas # to read and edit data (here: csv)
18. import shutil # helper for os file editing
19. import subprocess # start subprocesses (here: start hydrus)
20.
21. # path to hydrus exe
22. # windows always use raw prefix. r
23. BIN_PATH_HYDRUS = r"C:/Program Files (x86)/PC-Progress/Hydrus-1D 4.xx/"
24. HYDRUS_EXE = r"H1D_CALC.EXE"
25.
26. # hydrus output files
27. HYDRUS_OBS_FILE_NAME = 'Obs_Node.out'
28. HYDRUS_TLEVEL_FILE_NAME = 'T_Level.out'
29. #hydrus error file, which is created if model does not converge
30. HYDRUS_ERROR_FILE_NAME= "Error.msg"
31. # default time range: select the last values for an experiment based on the time
32.   range
33. DEFAULT_TIME_RANGE = 90 # last 30 days of interest for default time step
34. CSV_HYDRUS_INPUT = "hydrus_input_drought_0to9.csv"
35. HYDRUS_TEMPLATE_DIR = "./template_drought"
36. OUT_DIR = "./out_drought_test"
37.
38. # select values in csv to write in hydrus input files before the experiment
39. # mapping: keys are csv header, values are replacement names in the template files
40. # {csv_header:hydrus_input_replacment}
41. CSV_HYDRUS_TEMPLATE_MATCH =
42.   {"MVG_THR": "<MVG_THR>", "MVG_THS": "<MVG_THS>", "MVG_ALP": "<MVG_ALP>", \
43.    "MVG_N": "<MVG_N>", "MVG_K0": "<MVG_K0>", "MVG_L": "<MVG_L>", "Prec": "<Prec>",
44.    "Evap": "<Evap>", "Transp": "<Transp>"}
45.
46. def os_windows_run(cmd,cwd):
47.     ''' run window exe and suppress inputs and prints, cwd is the working dir'''
48.     # cwd must be changed for window to start .exe
49.     return subprocess.Popen(cmd, cwd=cwd, shell=True)
50.
51. def csv_read_excel(file_csv):
52.     ''' separator is ';' in windows excel '''
53.     df = pandas.read_csv(file_csv, sep=";")
54.     return df
55.
56. def run_hydrus(proj_path, hydrus_bin_path=BIN_PATH_HYDRUS,hydrus_exe=HYDRUS_EXE):
57.     ''' hydrus needs level_01.dir to set project path'''
58.     start_file = op.join(BIN_PATH_HYDRUS,'level_01.dir')
59.     with open(start_file, 'w') as f:
60.         f.seek(0)
61.         f.write(op.abspath(proj_path))
62.     hydrus_process = os_windows_run(hydrus_exe,cwd = hydrus_bin_path)
```

```

61.     hydrus_process.wait()
62.
63. def update_template(file_t, sub_dic):
64.     ''' replace template keys with values '''
65.     with open(file_t, 'r+') as f:
66.         text = f.read()
67.         for sub_name, val in sub_dic.items():
68.             # convert number to string
69.             if not isinstance(val, str):
70.                 val = str(val)
71.             text = re.sub(sub_name, val, text)
72.         # overwrite
73.         f.seek(0)
74.         f.write(text)
75.         f.truncate()
76.
77. def create_experiment_files(ex_path, template_dir):
78.     ''' rm existing and copy template files'''
79.     # python copy files https://datatofish.com/copy-file-python/
80.     if op.exists(ex_path):
81.         # remove if exists
82.         shutil.rmtree(ex_path)
83.     shutil.copytree(template_dir, ex_path)
84.
85. def get_input_values_from_csv(df, row_i, template_match):
86.     # example match_values = {"<MVG_THR>":df["MVG_THR"][row_i],...}
87.     # windows replace , by . to make compatible with hydrus
88.     return {hydrus_key : to_number(df[ csv_key ][row_i]) for csv_key, hydrus_key in
            template_match.items()}
89.
90. def to_number(csv_val):
91.     if isinstance(csv_val, str):
92.         csv_val = csv_val.replace(",",".")
93.     return float(csv_val)
94.
95. def read_hydrus_out_file(f, skiprows):
96.     ''' read common hydrus file format'''
97.     # engine='python' for warning supression for skipfooter
98.     return pandas.read_csv(f, sep=" ", header=0, skiprows=skiprows, comment='*', skipinitialspace=True, skipfooter=1, engine='python')
99.
100. def read_hydrus_error_file(f):
101.     ''' read the hydrus error msg file if exists'''
102.     # engine='python' for warning suppression for skipfooter
103.     try:
104.         with open(f, 'r') as file:
105.             return file.read().replace('\n', '').strip()
106.     except Exception as e:
107.         # not found, no error
108.         return
109.
110. def read_hydrus_t_level_file(f):
111.     header_line = 6
112.     skiprows = [i for i in range(8) if i !=header_line]
113.     df = read_hydrus_out_file(f, skiprows)
114.     return df
115.
116. def read_obs_node_file(f):
117.     header_line = 10
118.     skiprows = [i for i in range(10) if i !=header_line]
119.     df = read_hydrus_out_file(f, skiprows)
120.     return df
121.
122. def get_output_values(sample_id, out_dir, end_time_range=DEFAULT_TIME_RANGE):
123.     ''' read relevant infos from hydrus output files, get mean,max,min for the
        last time range '''

```

```

124.     ret_vals = {}
125.     # for windows use path.join, make path correct with "\\" and "/"
126.     #read hydrus error file if exists
127.     error = read_hydrus_error_file(op.join(out_dir, HYDRUS_ERROR_FILE_NAME))
128.     if error:
129.         print("ERROR hydrus for sample_id {} msg:\n {}".format(sample_id, error))
130.     return ret_vals
131.
132.     # read different hydrus output files
133.     # all files are in a different format
134.     df_t = read_hydrus_t_level_file(op.join(out_dir, HYDRUS_TLEVEL_FILE_NAME))
135.     # if no values are found return nothing
136.     if df_t is None:
137.         return ret_vals
138.
139.     # take mean of required values of n last steps
140.     n_steps = len(df_t)
141.     last_time = df_t["Time"][n_steps-1]
142.     start_time_data = last_time-end_time_range
143.
144.     time_idx = df_t["Time"]>=start_time_data
145.     # select time range from data
146.     df_t_time = df_t[time_idx]
147.     for k in ('vTop', 'vRoot', 'vBot', 'RunOff', 'Volume'):
148.         ret_vals[k+"_mean"] = df_t_time[k].mean()
149.         ret_vals[k+"_min"] = df_t_time[k].min()
150.         ret_vals[k+"_max"] = df_t_time[k].max()
151.     df = read_obs_node_file(op.join(out_dir, HYDRUS_OBS_FILE_NAME))
152.     # check for not a number values:
153.     time_idx = df["time"]>=start_time_data
154.
155.     # there are multiple thetas
156.     df_time = df[time_idx]
157.     for k in ["theta", "theta.1"]:
158.         ret_vals[k] = df_time[k].mean()
159.         ret_vals[k+"_min"] = df_time[k].min()
160.         ret_vals[k+"_max"] = df_time[k].max()
161.     return ret_vals
162.
163. def update_df_with_hydrus_outputs(df, out_dirs, id_key):
164.     ''' update pandas data frame with outputs from hydrus saved at "out_dirs" '''
165.     #read output files and update data frame
166.     outs = {}
167.     # loop over all output files and load values
168.     for id_s, d in out_dirs.items():
169.         out_vals = get_output_values(id_s, d)
170.         if out_vals:
171.             # map values to id_s if values are found
172.             for k, v in out_vals.items():
173.                 if k not in outs:
174.                     outs[k] = {}
175.                 outs[k][id_s] = v
176.
177.     # update df with mapping of values to experiment id
178.     # map output values to experiment row
179.     # see https://towardsdatascience.com/introduction-to-pandas-apply-applymap-
and-map-5d3e044e93ff
180.     for k, v in outs.items():
181.         df[k] = df[id_key].map(v)
182.     return df
183.
184. def main():
185.     ''' RUN hydrus simulation, with inputs for a csv file:
186.         for n rows in csv document take values and start hydrus with it
187.         hydrus needs files predefined in template folder
188.         values that should be changed in template file are marked with <...>

```

```

189.         hydrus is started and output for each experiment is saved to the output
190.         folder, experiments are named based on the csv id
191.     df = csv_read_excel(CSV_HYDRUS_INPUT)
192.
193.     # select a list of hydrus template files to change
194.     hydrus_input_files=['SELECTOR.IN','ATMOSPH.IN']
195.     n_ex = len(df) # rows of csv without header
196.
197.     # print csv data info to verify
198.     print('found n experiment in csv: {} keys: {}'.format(n_ex, df.keys()))
199.
200.     out_dirs = {} # id_sample:out_dirs
201.     # loop over all experiments and run the simulation
202.
203.     for i in range(n_ex):
204.         id_s = df["SAMPLE_ID"][i] # get id value from row i
205.         # get values from csv: mapping hydrus file key to value, e.g.
206.         {"<MVG_THR>":34.5}
207.         values_csv = get_input_values_from_csv(df, i, CSV_HYDRUS_TEMPLATE_MATCH)
208.         # create name of the exp. folder
209.         dir_ex = op.join(OUT_DIR, "sample_id_" + str(id_s)) # join operation sys-
210.         tem paths
211.         # copy experiment from template
212.         create_experiment_files(dir_ex, HYDRUS_TEMPLATE_DIR)
213.         out_dirs[id_s] = dir_ex
214.
215.         # change values in hydrus input files
216.         for f in hydrus_input_files:
217.             f = op.join(dir_ex,f)
218.             update_template(f, values_csv)
219.             # start the simulation
220.
221.             print('start sample id {} dir_ex: {}'.format(id_s, dir_ex))
222.             run_hydrus(dir_ex)
223.
224.         # get the simulation results
225.         df = update_df_with_hydrus_outputs(df, out_dirs, "SAMPLE_ID")
226.         update_csv_file = op.join(OUT_DIR, 'out.csv')
227.         # set encoding for correct format on windows
228.         df.to_csv(update_csv_file, encoding='utf-8', sep=';')
229.         print('updated csv saved to {}'.format(update_csv_file))
230.
231.
232. if __name__ == "__main__":
233.     main()
234.

```

## Declaration of honor

I hereby declare that I have written the submitted master thesis independently, that I have not used any sources or aids other than those indicated, and that I have marked all content taken verbatim or in spirit from other works as such.

The submitted master thesis is or was neither completely nor in essential parts subject of another assignment.

Hiermit versichere ich, dass ich die eingereichte Masterarbeit selbständig verfasst habe, keine anderen als die angegebenen Quellen und Hilfsmittel benutzt und alle wörtlich oder sinngemäß aus anderen Werken übernommenen Inhalte als solche kenntlich gemacht habe.

Die eingereichte Masterarbeit ist oder war weder vollständig noch in wesentlichen Teilen Gegenstand eines anderen Prüfungsverfahrens.

Place, date/ Ort, Datum

Signature/ Unterschrift